

17 **Abstract**

18 Trait-based approaches are of increasing concern in predicting vegetation changes and
19 linking ecosystem structures to functions at large scales. However, a critical challenge for such
20 approaches is acquiring spatially continuous plant functional trait maps. Here, six key plant
21 functional traits were selected as they can reflect plant resource acquisition strategies and
22 ecosystem functions, including specific leaf area (SLA), leaf dry matter content (LDMC), leaf N
23 concentration (LNC), leaf P concentration (LPC), leaf area (LA) and wood density (WD). A total
24 of 34589 in-situ trait measurements of 3447 seed plant species were collected from 1430 sampling
25 sites in China and were used to generate spatial plant functional trait maps (~1 km), together with
26 environmental variables and vegetation indices based on two machine learning models (random
27 forest and boosted regression trees). To obtain the optimal estimates, a weighted average
28 algorithm was further applied to merge the predictions of the two models to derive the final spatial
29 plant functional trait maps. The ~~two~~ models showed a good accuracy in estimating WD, LPC and
30 SLA, with average R² values ranging from 0.45-48 to 0.6668. In contrast, both the ~~two~~ models had
31 weak performance in estimating LDMC, with average R² values ~~below less than~~ 0.2530.
32 Meanwhile, LA showed considerable differences between two models in some regions. ~~To obtain~~
33 ~~the optimal estimates, a weighted average algorithm was further applied to merge the predictions~~
34 ~~of the two models to derive the final spatial plant functional trait maps.~~ Climatic effects were more
35 important than those of edaphic factors in predicting the spatial distribution of plant functional
36 traits. Estimates of plant functional traits in northeast China and the Qinghai-Tibet Plateau had
37 relatively high uncertainties due to sparse samplings, implying a need of more observations in
38 these regions in future. Our spatial trait maps could provide critical supports for trait-based
39 vegetation models and allow exploration into the relationships between vegetation characteristics
40 and ecosystem functions at large scales. The six plant functional traits maps for China with 1 km
41 spatial resolution are now available at <https://figshare.com/s/c527c12d310cb8156ed2> (An et al.,
42 [2023](#)).

43 **1 Introduction**

44 Climate change has been affecting vegetation distributions and biogeochemical cycling globally
45 and altering their feedbacks to ~~the~~-climate system (Kirilenko et al., 2000; Finzi et al., 2011;
46 Jónsdóttir et al., 2022). Dynamic global vegetation models (DGVMs) are powerful tools for
47 predicting changes in vegetation and ecosystem-atmosphere exchanges (e.g., water, carbon and
48 nutrient cycling) in a changing climate (Foley et al., 1996; Peng, 2000). However, conventional
49 DGVMs are still insufficient realistic, largely due to their dependence on the plant functional types
50 (PFTs) assumption (Sitch et al., 2008; Yurova and Volodin, 2011; Scheiter et al., 2013). PFTs in
51 conventional DGVMs commonly have fixed attributes (mostly trait values) (Van Bodegom et al.,
52 2012; Wullschleger et al., 2014) that do not reflect plant adaptation to environments, limiting the
53 quantification of carbon-water-nutrient feedback between terrestrial ecosystems and the
54 atmosphere (Zaehle and Friend, 2010; Liu and Yin, 2013). Trait-based approaches can provide
55 robust theoretical basis for developing the next generation of DGVMs (Van Bodegom et al., 2012;
56 Sakschewski et al., 2015; Matheny et al., 2017). Plant functional traits, which are closely
57 associated with ecosystem functions (Diaz et al., 2004; Yan et al., 2023), can effectively reflect
58 response and adaptation of plants to environmental conditions (Myers-Smith et al., 2019; Qiao et
59 al., 2023).

60 Attempts to predict spatially continuous trait maps have been conducted at regional to global
61 scales (Madani et al., 2018; Moreno-Martínez et al., 2018; Boonman et al., 2020; Loozen et al.,
62 2020; Dong et al., 2023). Webb et al. (2010) proposed that the environment creates a filtered trait
63 distribution along an environmental gradient, and such trait-environment relationships offer
64 fundamental supports to predict the spatial distribution of plant functional traits through
65 extrapolating local trait measurements. Boonman et al. (2020) mapped the global patterns of
66 specific leaf area (SLA), leaf N concentration (LNC) and wood density (WD) based on a set of
67 climate and soil variables. As the number of available regional and global trait databases increases
68 (Wang et al., 2018; Kattge et al., 2020), trait-environment relationships are becoming increasingly
69 quantitative and accurate (Bruehlheide et al., 2018; Myers-Smith et al., 2019). Alternatively, remote
70 sensing approaches, such as empirical methods and physical radiative transfer models (e.g., partial
71 least squares regression, and PROSPECT model), have been developed to estimate plant
72 physiological, morphological and chemical traits (e.g., leaf chlorophyll content, SLA, LNC and
73 leaf dry matter content (LDMC)) (Darvishzadeh et al., 2008; Romero et al., 2012; Ali et al., 2016).
74 Vegetation indices, such as ~~the~~-normalized difference vegetation index (NDVI) and ~~the~~-enhanced
75 vegetation index (EVI), have been successful in estimating plant functional traits of crops,
76 grasslands and forests (Clevers and Gitelson, 2013; Li et al., 2018; Loozen et al., 2018). Loozen et
77 al. (2020) demonstrated that EVI was the most important predictor for mapping the spatial pattern
78 of canopy nitrogen in European forests. Admittedly, a recent studies-study have-has suggested that
79 combining environmental variables and vegetation indices can improve the predictive accuracy of

80 canopy nitrogen compared to those based on vegetation indices alone (Loozen et al., 2020).

81 Although there have been reports on plant functional trait distribution in China in some
82 global or regional researches (Yang et al., 2016; Butler et al., 2017; Madani et al., 2018; Moreno-
83 Mart ínez et al., 2018; Boonman et al., 2020), they are still ~~of~~ large uncertainties in characterizing
84 the spatial distribution of plant functional traits in China. First, global studies generally have
85 relatively few, unevenly distributed sampling sites ~~in~~ across China (Butler et al., 2017; Madani et
86 al., 2018; Boonman et al., 2020), impeding our understanding of the true spatial characteristics of
87 trait variability. Second, the spatial pattern of traits among these studies are usually inconsistent.
88 For example, Moreno-Mart ínez et al. (2018) and Madani et al. (2018) demonstrated that SLA
89 values were low in the southeast areas but high in the southwest areas of China, whereas Boonman
90 et al. (2020) found the opposite. Third, most studies ~~mainly~~ focused on leaf traits (Yang et al.,
91 2016; Loozen et al., 2018; Moreno-Mart ínez et al., 2018), whereas traits associated with the
92 whole-plant strategies, such as WD, were ignored. Therefore, mapping and verifying the spatial
93 patterns of key functional traits that reflect the whole plant economics spectrum in China is a top
94 priority.

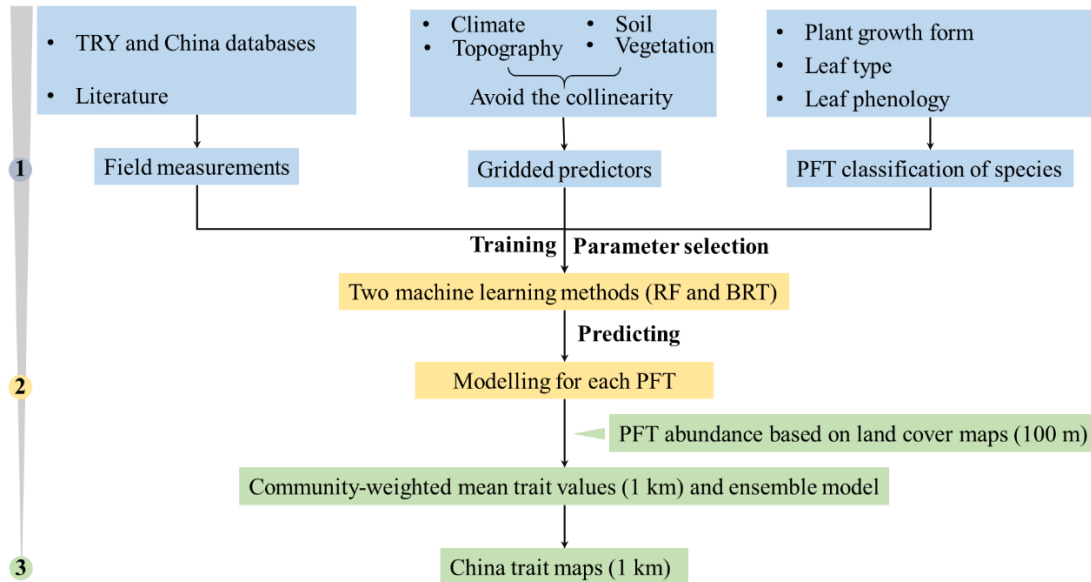
95 In this study, our main objective was to generate spatial maps for several key plant functional
96 traits, through combining field measurements, environmental variables and vegetation indices. We
97 selected six plant functional traits including SLA, LDMC, LNC, LPC, LA and WD. As key leaf
98 economics traits, SLA, LDMC, LNC and LPC were selected because they are closely linked to
99 plant growth rate, resource acquisition and ecosystem functions (Wright et al., 2004; Diaz et al.,
100 2016). LA is indicative of the trade-off between carbon assimilation and water-use efficiency
101 (Wright et al., 2017), and WD reflects the trade-off between plant growth rate and support cost,
102 with a higher WD linked to a lower growth rate, a higher survival rate and a higher biomass
103 support cost (King et al., 2006). For each plant functional trait, we predicted spatial patterns at a 1
104 km resolution using an ensemble modelling algorithm based on two machine learning methods
105 (i.e., random forest and boosted regression trees).

106 **2 Materials and Methods**

107 **2.1 Overview**

108 The spatial maps of plant functional traits in China were generated based on machine learning
109 ~~algorithms~~ methods trained by a large dataset of in-situ field measurements, environmental
110 variables and vegetation indices in three steps (Fig. 1). First, in-situ field measurements of six
111 plant functional traits were collected from TRY and China databases as well as published literature,
112 and the PFTs of plant species were classified based on plant growth form, leaf type and leaf
113 phenology. Multiple gridded predictors of climate, soil, topography and vegetation indices were
114 used after avoiding the collinearity among them. Second, random forest and boosted regression
115 trees were used to train the relationships between plant functional traits and predictors for each

116 PFT individually. Third, the spatial abundance of each PFT within 1 km grid cell was calculated
 117 using land cover map (100 m). Community-weighted trait values within 1 km grid cell were
 118 calculated based on these abundances of each PFT and their predicted trait values in Step 2. To
 119 reduce the variability of different single-models, we derived the final spatial maps of plant
 120 functional traits using ensemble model [algorithm](#) to merge the predictions of random forest and
 121 boosted regression trees according to their cross-validated R^2 values.



122
 123 **Figure 1.** Methodological workflow for spatial mapping of plant functional traits. Trait
 124 mapping is performed in three steps. Step 1: in-situ field measurement of plant functional traits,
 125 PFT classification of plant species and gridded predictors were collected. Step 2: two machine
 126 learning methods were used to predict trait values by training the field measurements and
 127 predictors for each PFT. Step 3: spatialization of trait maps by calculating the abundance of each
 128 PFT using 100 m land cover map and predicted trait values within 1 km grid cells. PFT, plant
 129 functional type; RF, random forest; BRT, boosted regression trees.

130 2.2 Plant functional trait collection and data processing

131 The information on the six plant functional traits and their ecological meanings are described in
 132 Table 1. Plant trait data was obtained and collected via two main sources. The first source was
 133 public trait databases, including the TRY database (Kattge et al., 2020) and the China Plant Trait
 134 Database (Wang et al., 2018). The second source was from literature (listed in Appendix A). To
 135 ensure data quality and comparability, we only included trait observations that met the following
 136 five criteria: 1) Measurements must be obtained from natural terrestrial fields in order to minimize
 137 the influences of management disturbance, and observations from cropland, aquatic habitat,
 138 control experiments ~~and or~~ gardens were excluded; 2) According to the mass ratio hypothesis, the
 139 effect of plant species on ecosystem functioning is determined to an overwhelming extent by the
 140 traits and functional diversity of the dominant species and is relatively insensitive to the richness

141 of subordinate species (Grime, 1998). Thus, we only included studies that measured plant trait
 142 observations from all species or dominant species within a community; 3) In order to consider the
 143 intraspecific trait variation, when the same species occurred in the same sampling site from
 144 different studies, we included all original observed data from different studies rather than
 145 averaging the values at the species level (Jung et al., 2010; Siefert et al., 2015); 4) Plant trait
 146 observations must be made on mature and healthy plant individuals, so some specific growth
 147 stages (e.g., seedling) and size classes (e.g., sapling) were excluded to reduce the confounding
 148 effect of ontogeny and seasonality (Thomas, 2010); 5) We only included studies with clear
 149 geographical coordinates to ~~ensure alignment with~~ match predictor variables. The sampling
 150 location and sampling time information were also included in the dataset. The sampling time
 151 mostly focused on the growing season of a year (i.e., May-October), which ensures the relative
 152 consistency of sampling time to minimize the effects of seasonality. Plant functional traits must be
 153 sampled and measured according to standardized measurement procedures (Perez-Harguindeguy
 154 et al., 2013) to reduce the variation and uncertainty among different data sources. In this study, we
 155 included SLA measurements on sun-leaves, and WD measurements on ~~both heartwood and~~
 156 sapwood main stem of ~~tree-woody~~ species.

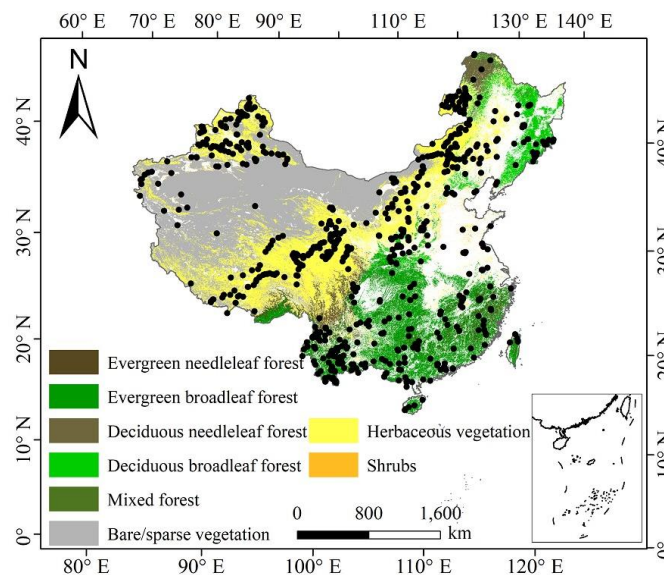
157 **Table 1** Description of plant functional traits selected in this study and their relevant
 158 ecosystem functions.

Trait	Abbreviation	Description	Relevant ecosystem functions
Specific leaf area	SLA	As a core leaf economics trait (Wright et al., 2004), it is related to trade-off between leaf lifespan and C acquisition as well as light competition (Reich et al., 1991)	Productivity, litter decomposition, competitive ability (Bakker et al., 2011; Smart et al., 2017)
Leaf dry matter content	LDMC	Strongly related to resource availability and potential growth rate (Hodgson et al., 2011)	Productivity, litter decomposition, herbivore resistance, and drought tolerance (Bakker et al., 2011; Smart et al., 2017; Blumenthal et al., 2020)
Leaf N concentration	LNC	As a core leaf economics trait, it is strongly related to photosynthetic capacity (Wright et al., 2004)	Productivity, nutrient cycling, litter decomposition (LeBauer and Treseder, 2008; Bakker et al., 2011)
Leaf P concentration	LPC	As a core leaf economics trait, it is strongly related to photosynthetic capacity (Wright et al., 2004)	Productivity, nutrient cycling, litter decomposition (LeBauer and Treseder, 2008; Bakker et al., 2011)
Leaf area	LA	Trade-off between C assimilation and water use efficiency, it is related to energy balance (Wright et al., 2017)	Productivity (Li et al., 2020)
Wood density	WD	A measure of carbon investment, representing the trade-off between growth and mechanical support (Mart ínez-Vilalta et al., 2010)	Drought tolerance, productivity (Hoeber et al., 2014; Liang et al., 2021)

159 The plant trait data was checked for possible errors and corrected in three steps as follows.
 160 First, species name and taxonomic nomenclature were corrected and standardized according to the

161 Plant List (<http://www.theplantlist.org/>) using the “plantlist” package. Second, illogical values,
 162 repeated values and outliers were removed, which were defined by observations exceeding 1.5
 163 standard deviations of the mean trait value for a given species (Kattge et al., 2011). Third, we
 164 appended information on plant growth form, leaf type and leaf phenology from the TRY
 165 categorical traits database (<https://www.try-db.org/TryWeb/Data.php#3>) and *Flora Reipublicae*
 166 *Popularis Sinicae* (<http://www.iplant.cn/frps>), which were used to match species names to PFTs.
 167 We associated each species with a corresponding PFT based on plant growth form (tree, shrub and
 168 grass), leaf type (broadleaf and needleleaf) and leaf phenology (evergreen and deciduous). For
 169 example, the information on *Salix matsudana* is: tree, deciduous and broadleaf, thus, we were able
 170 to associate the PFT of deciduous broadleaf forest (DBF) to this species. The species that did not
 171 correspond to any PFT were discarded. After these treatments, we collected a total of 34589 trait
 172 measurements from 1430 sampling sites for our database, representing 3447 species from 195
 173 families and 1066 genera (Fig. 2 and Fig. B1 in Appendix B). Information on the statistics for the
 174 six plant functional traits collected in this study is shown in Table B1 in Appendix B.

175



176

177

Figure 2. Location distribution and land cover map in China.

178

2.3 Preparing predictor variables

179

2.3.1 Climate data

180

Twenty-one climate variables were used in this study, including 19 bioclimate variables, solar radiation (RAD) and aridity index (AI) (Table B2 in Appendix B). The 19 bioclimate variables and RAD were obtained from the WorldClim version 2.1 for the period from 1970 to 2000 (<https://www.worldclim.org/data/worldclim21.html>). The AI data was extracted from the CGIAR Consortium of Spatial Information (CGIAR-CSI) website for the period from 1970 to 2000 (<http://www.csi.cgiar.org>) (Trabucco and Zomer, 2018). The spatial resolution of climate data is 1 km.

186

187

2.3.2 Soil data

188 Twelve soil variables were included in this study, representing the different aspects of soil
189 properties, i.e. soil texture, bulk density (BD), pH and soil nutrients (Table B2 in Appendix B). All
190 soil variables were extracted from the Soil Database of China for Land Surface Modeling
191 (<http://globalchange.bnu.edu.cn/research/soil2>) (Shangguan et al., 2013). Given the importance of
192 topsoil properties on community composition (Bohner, 2005), we averaged the first four layers to
193 represent the topsoil properties (~ 30 cm) in our study. The spatial resolution is 1 km.

194 2.3.3 Topography

195 The topographic variable was elevation. Elevation data was extracted from the STRM 90m dataset
196 in China, based on the SRTM V4.1 database (<https://www.resdc.cn/data.aspx?DATAID=123>). The
197 spatial resolution is 1 km.

198 Given the collinearity among climate and soil variables, we reduced the ~~number~~
199 ~~dimensionality~~ of ~~environmental~~ ~~these~~ predictors based on Pearson's correlation coefficient (r)
200 (Figs. ~~B2-B1~~ and ~~B3-B2~~ in Appendix B). Among a set of highly correlated variables ($r > 0.75$),
201 only one variable was retained in subsequent analysis to ensure a combination of different
202 environmental variables. The final selection of environment predictors included nineteen variables:
203 mean annual temperature (MAT), mean diurnal range (MDR), min temperature of coldest quarter
204 (Tmin), max temperature of warmest quarter (Tmax), temperature seasonality (TS), mean annual
205 precipitation (MAP), precipitation seasonality (PS), precipitation of wettest quarter (PEQ),
206 precipitation of driest quarter (PDQ), AI, RAD, elevation, soil sand content (SAND), pH, BD, soil
207 total N (STN), soil total P (STP), soil available P (SAP), soil alkali-hydrolysable N (SAN) and
208 cation exchange capacity (CEC).

209 2.3.4 Vegetation indices

210 Three categories of vegetation indices were included in this study (Table B2 in Appendix B). First,
211 EVI was extracted from the MOD13A3 V006 product
212 (<https://lpdaac.usgs.gov/products/mod13a3v006/>). This product is available as a monthly average
213 with spatial resolution of 1 km, ranging from January 2000 to December 2018. Second, MODIS
214 reflectance data was also extracted from the MOD13A3 V006 product, including MIR reflectance,
215 NIR reflectance, red reflectance and blue reflectance. Third, the MERIS terrestrial chlorophyll
216 index (MTCI) was extracted from the Natural Environment Research Council Earth Observation
217 Data Centre (NERC-NEODC, 2005) (<https://data.ceda.ac.uk/>). MTCI data is available globally as
218 a monthly average at 4.63 km spatial resolution, and ranges from June 2002 to December 2011. It
219 is noted that valid MTCI values should be greater than 1, so our study deleted any values less than
220 1.

221 To avoid collinearity, we also reduced the ~~dimensionality~~~~number~~ of vegetation indices based
222 on Pearson's correlation coefficient (r) (Fig. ~~B4-B3~~ in Appendix B). Most selected variables were
223 related to growing seasons due that plant functional traits were measured during the growing
224 season. Furthermore, based on the results of Pearson's correlation coefficient (r), MTCI, MIR,
225 NIR, red and blue in January showed low correlations with those in growing season, thus they

226 were included in subsequent analysis. The final selection included 36 variables: annual EVI, EVI
227 (May, June, July, August and September), MTCI, MIR, NIR, red and blue (all for January, June,
228 July, August and September).

229 Both environmental variables and vegetation indices variables were resampled to a consistent
230 spatial resolution of 1 km using the nearest neighborhood method.

231 PFT is also an important factor in influencing the variation of plant functional traits
232 (Verheijen et al., 2016; Loozen et al., 2020), thus the trait predictions were performed for each
233 PFT individually. We used the 2015 land cover map at a 100 m spatial resolution to calculate the
234 relative abundance of each PFT within 1 km grid cells, which was extracted from the Copernicus
235 Global Land Service (CGLS-LC100, Version 3) (<https://land.copernicus.eu/global/products/lc>)
236 (Buchhorn et al., 2020). We focused on natural terrestrial vegetation, so all artificial or crop areas
237 were thus eliminated in our dataset. Seven categories were included: evergreen needleleaf forest
238 (ENF), evergreen broadleaf forest (EBF), deciduous needleleaf forest (DNF), deciduous broadleaf
239 forest (DBF), shrubland (SHL), grassland (GRL) and bare/sparse vegetation.

240 **2.4 Model fitting and validation**

241 To predict spatial patterns of plant functional traits, we used two machine learning models, i.e.,
242 random forest and boosted regression trees.

243 Random forest is an ensemble machine learning method based on classification and
244 regression trees using collections of regression trees to classify observations according to a set of
245 predictive variables (Breiman, 2001). This method repeatedly constructs a set of trees from
246 random samples of training data, and the final prediction is produced by integrating the results of
247 all individual trees, which makes it a robust method. The model is controlled by two main
248 parameters: the number of sampled variables (mtry) and the number of trees (ntree). The mtry was
249 set to range from 1 to 57 (at an interval of 1), and the ntree was set as 500, 1000, 2000, 5000 and
250 10000 in subsequent runs. This analysis was performed using the 'randomForest' function in the
251 'randomForest' package (Liaw and Wiener, 2002).

252 Boosted regression trees are machine learning methods based on generalized boosted
253 regression models and using a boosting algorithm to combine many sample tree models to
254 optimize predictive performance (Elith et al., 2006). There is no need for prior data transformation
255 or the elimination of outliers, and this method can fit complex non-linear relationships while
256 automatically handling interaction effects between predictors (Elith et al., 2008). The four
257 parameters to optimize in these models are the number of trees, interaction depth, learning rate
258 and bag fractions. We varied the parameter settings to find the optimal parameter combination that
259 achieves minimum predictive error. The number of trees was set to 3000, the interaction depth
260 varied from 1 to 7 (at an interval of 1), the learning rate was set to 0.001, 0.01, 0.05 and 0.1, and
261 the bag fraction was set to 0.5, 0.6, 0.7 and 0.75. PFT was used as a dummy variable in the
262 boosted regression trees models. This analysis was conducted using the 'gbm' function in the

263 ‘gbm’ package (Ridgeway, 2006).

264 We built separate predictive model for each plant functional trait. To select the optimal
265 parameter combination and to evaluate the final model performance for each trait, we calibrated
266 the models 10 times using randomly selected 80% of the data for training the models and
267 validating against the remaining 20% based on cross-validation (Table B3 in Appendix B). The
268 predictive performance was evaluated by regressing the predicted and observed trait values from
269 all repetitions of the cross-validation. The fitting performances of the random forest and boosted
270 regression trees ~~methods~~ were evaluated using determinate coefficient (R^2), normalized root-
271 mean-square error (NRMSE) and mean ~~absolute~~ error (MAE). These scores are
272 calculated following Eq. (1), Eq. (2) and Eq. (3):

$$273 \quad R^2 = 1 - \frac{\sum_{i=1}^n (p_i - o_i)^2}{\sum_{i=1}^n (p_i - \hat{o}_i)^2} \quad (1)$$

$$274 \quad \text{NRMSE} = \frac{\sqrt{\frac{1}{n} \sum_{i=1}^n (p_i - o_i)^2}}{p_{\max} - p_{\min}} \quad (2)$$

$$275 \quad \text{MAE} = \frac{1}{n} \sum_{i=1}^n |o_i - p_i| \quad (3)$$

276 where p_i and o_i are the predictive values and observed values, respectively; \hat{o}_i is the mean of the
277 observed values.

278 To quantify the relative importance of each predictor across the two models consistently, we
279 used the method proposed by Thuiller et al. (2009). This method applies correlation between the
280 standard predictions fitted with the original data and predictions where the variable under
281 investigation has been randomly permuted. If the correlation is high, which indicates little
282 difference between the two predictions, the variable permuted is considered not important for the
283 model. This step was repeated multiple times for each predictor, and the mean correlation
284 coefficient over runs was recorded. Then the relative importance of each predictor was quantified
285 as one minus the Spearman rank correlation coefficient (see Boonman et al., 2020). In addition,
286 we used generalized additive models to fit the relationships between plant functional traits and the
287 most important variables using the ‘gam’ function in the ‘mgcv’ package.

288 2.5 Generation of plant functional trait maps and model performance

289 The generation of spatial maps of plant functional was performed in three steps. First, we
290 predicted trait values for each natural PFT (e.g., EBF, ENF, DBF, DNF, SHL and GRL) within 1
291 km grid cell separately. Second, the abundance of individual natural PFT within 1 km grid cell
292 was estimated using a land cover map with a spatial resolution of 100 m. Third, refer to the Eq. (4)
293 that has been widely applied in a community (Garnier et al., 2004), the final trait value in a given
294 1 km grid cell was calculated as the sum of the predicted trait values multiplying by corresponding
295 abundance of each natural PFT.

$$296 \quad \text{CWM} = \sum_{i=1}^n W_i X_i \quad (4)$$

297 where n is the total number of PFT in a given grid; W_i is the relative abundance of the i th natural

298 PFT; and X_i is the predicted trait value of the i th natural PFT.

299 To reduce the variability of different single-models and to construct a more stable and
300 accurate model, the ensemble model was further applied to merge the predictions of random forest
301 and boosted regression trees according to their cross-validated R^2 values. The predictive value of
302 ensemble model was calculated in a given grid cell as described by Eq. (5) (Marmion et al., 2009).
303 The model accuracy was calculated by regressing the predictive values of ensemble model against
304 the observed trait values.

$$305 \quad Pred_EM_t = \frac{\sum_{m=1}^2 (pred_{m,t} \times r_{m,t}^2)}{\sum_{m=1}^2 r_{m,t}^2} \quad (5)$$

306 where $Pred_EM_t$ is the predictive values of t trait in the ensemble model; $pred_{m,t}$ is the
307 predictive values of t trait in m model; $r_{m,t}^2$ is the cross-validated R^2 of t trait in m model.

308 To evaluate the model performance (i.e. the variability in the prediction across models), the
309 coefficient of variation (CV) was calculated as the difference between the predictions of random
310 forest and boosted regression trees methods and the ensemble prediction. CV is calculated as
311 following Eq. (6):

$$312 \quad CV_t = \frac{\sqrt{\sum_{m=1}^2 (pred_{m,t} - obs_t)^2 \times r_{m,t}^2}}{\sum_{m=1}^2 r_{m,t}^2} \quad (6)$$

313 where $pred_{m,t}$ is the predictive values of t trait in m model; obs_t is the values of t trait in the
314 ensemble model; $r_{m,t}^2$ is the cross-validated R^2 of t trait in m model.

315 2.6 Uncertainty assessments

316 Multivariate environmental similarity surface analysis (MESS) was used to identify the range of
317 the extrapolated predictor values across the locations in the plant trait dataset (Elith et al., 2010).
318 This method is often used to evaluate the extent of extrapolation and the applicability domain. If
319 the values are negative, this indicates that at a given grid cell, at least one predictor variable is
320 outside the extent of referenced predictor layer. This analysis was conducted using the ‘mess’
321 function in the ‘dismo’ package.

322 All analyses were performed in R 4.0.2 (R Core Team, 2020).

323 3 Results

324 3.1 Performances of prediction models

325 Cross-validation showed that the performance of the predictive models differed greatly among the
326 plant functional traits (Table 2, Tables C1 and C2 in Appendix C). WD had the best performance
327 in all three models, with R^2 values of 0.64, 0.68 and 0.67 for random forest, boosted regression
328 trees and ensemble model, respectively. SLA and LPC had R^2 values greater than 0.45, while
329 LDMC performed the worst, with R^2 values below 0.2530.

330 **Table 2** Results of plant functional traits for cross-validated R², NRMSE and MAE for
 331 random forest, boosted regression trees and ensemble model.

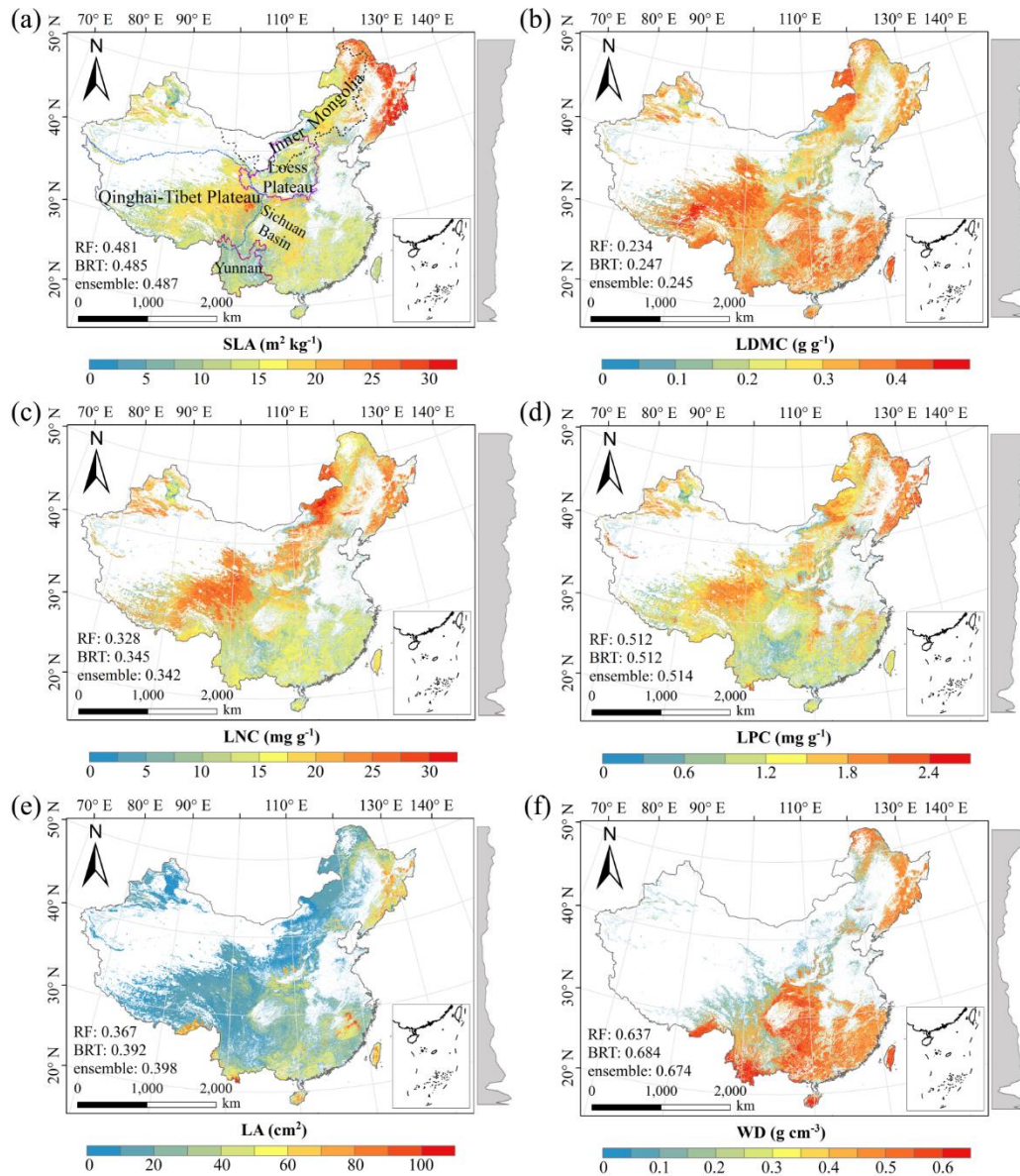
Traits	Random forest			Boosted regression trees			Ensemble model		
	R ²	NRMSE	MAE	R ²	NRMSE	MAE	R ²	NRMSE	MAE
SLA	0.48	0.22	5.10	0.48	0.20	5.08	0.49	0.21	5.07
LDMC	0.23	0.21	0.07	0.28	0.18	0.07	0.24	0.20	0.07
LNC	0.33	0.19	4.92	0.34	0.18	4.85	0.34	0.19	4.85
LPC	0.51	0.24	0.53	0.51	0.22	0.53	0.51	0.27	0.53
LA	0.37	0.45	26.76	0.39	0.51	27.47	0.40	0.58	26.59
WD	0.64	0.20	0.10	0.68	0.13	0.10	0.67	0.17	0.10

332 SLA, specific leaf area (m² kg⁻¹); LDMC, leaf dry matter content (g g⁻¹); LNC, leaf N concentration
 333 (mg g⁻¹); LPC, leaf P concentration (mg g⁻¹); LA, leaf area (cm²); WD, wood density (g cm⁻³); R²,
 334 determinate coefficient; NRMSE, normalized root-mean-square error; MAE, mean ~~absolute~~
 335 error.

336 3.2 Spatial patterns of predicted plant functional traits

337 There were relatively consistent spatial patterns for SLA, LNC and LPC, with high values in the
 338 northeastern and northwestern regions and the southeastern Qinghai-Tibet Plateau, and low values
 339 in southwestern China (Figs. 3a, 3c and 3d, Figs. ~~D1 and D2~~, ~~D3, D5 and D6~~ in Appendix D).
 340 SLA and LPC increased with latitude, while LNC did not vary significantly along the latitudinal
 341 gradient. For SLA, LNC and LPC, the variability was low among random forest, boosted
 342 regression trees and ensemble model, with an overall CV less than 0.3 (Figs. 4a, 4c and 4d).
 343 LDMC values were relatively high in most regions of China, and the low values were mainly
 344 located in eastern Yunnan and the Loess Plateau (Fig. 3b, Figs. ~~D1 and D2~~ and ~~D4~~ in Appendix
 345 D). LA showed high values in the northeastern and southern regions (except for the Sichuan
 346 Basin), and the southeastern Qinghai-Tibet Plateau (Fig. 3e, Figs. ~~D1 and D2~~ and ~~D7~~ in Appendix
 347 D). The strong latitudinal gradient was observed in LA, where ~~the~~ values decreased with latitude.

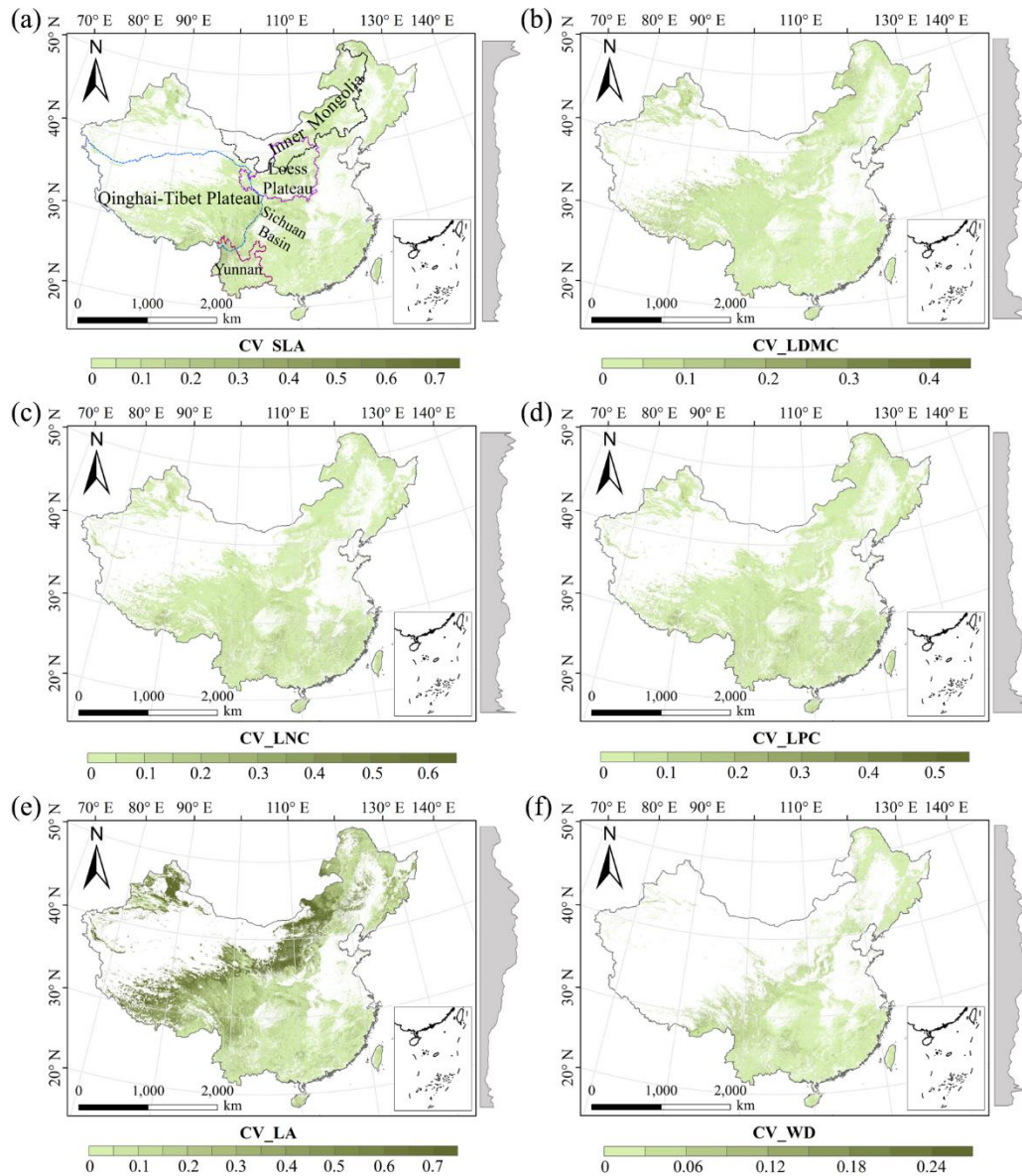
348 The CV values of LPC decreased with latitude, but other traits did not show latitudinal
 349 patterns (Fig. 4). The CV values of LA were relatively high, especially in the northwestern region
 350 and the Inner Mongolia-Loess Plateau region (Fig. 4e). WD had high values in the northeastern
 351 and southern regions (Fig. 2f, Figs. ~~D1 and D2~~ and ~~D8~~ in Appendix D), while CV values for WD
 352 in China were low throughout China (Fig. 4f).



353

354

Figure 3. Spatial patterns of predicted plant functional traits in China based on the ensemble
 355 model. The grey curves to the right of the maps display trait distribution along with latitude. The
 356 white areas represent artificial land cover types. RF, random forest; BRT, boosted regression trees;
 357 ensemble, ensemble model; SLA, specific leaf area; LDMC, leaf dry matter content; LNC, leaf N
 358 concentration; LPC, leaf P concentration; LA, leaf area; WD, wood density.



359

360

Figure 4. The variability in plant functional trait predictions among random forest, boosted regression trees and ensemble model. The grey curves to the right of the maps display coefficient of variation along with latitude. The white areas represent artificial land cover types. SLA, specific leaf area; LDMC, leaf dry matter content; LNC, leaf N concentration; LPC, leaf P concentration; LA, leaf area; WD, wood density.

365

3.3 Relative importance of predictive variables

366

The dominant factors explaining spatial variation differed greatly among plant functional traits (Table 3). Overall, climate variables were more important for predicting plant functional traits than were soil variables. Temperature variables (i.e., MAT, MDR and TS) showed close relationships with SLA, LDMC, LPC and WD, while precipitation variables (i.e., PS, PEQ, MAP and PDQ) were more important for predicting the spatial patterns of LNC, LPC and LA. RAD was

370

371 the fourth most dominant factor in predicting the spatial patterns of SLA and WD. Elevation also
 372 played an important role in the LDMC and LPC predictions. Within soil variables, soil nutrients
 373 (i.e., pH and SAP) showed close associations with SLA and LNC. In addition to the environmental
 374 variables, MTCI emerged as an important predictor for explaining SLA, LDMC and LA. Finally,
 375 EVI was the most important predictor for LA, and MIR in January and May were the primary
 376 predictors of WD. The relationships between plant functional traits and the most important
 377 variables were shown in Figs. E1 and E2 in Appendix E.

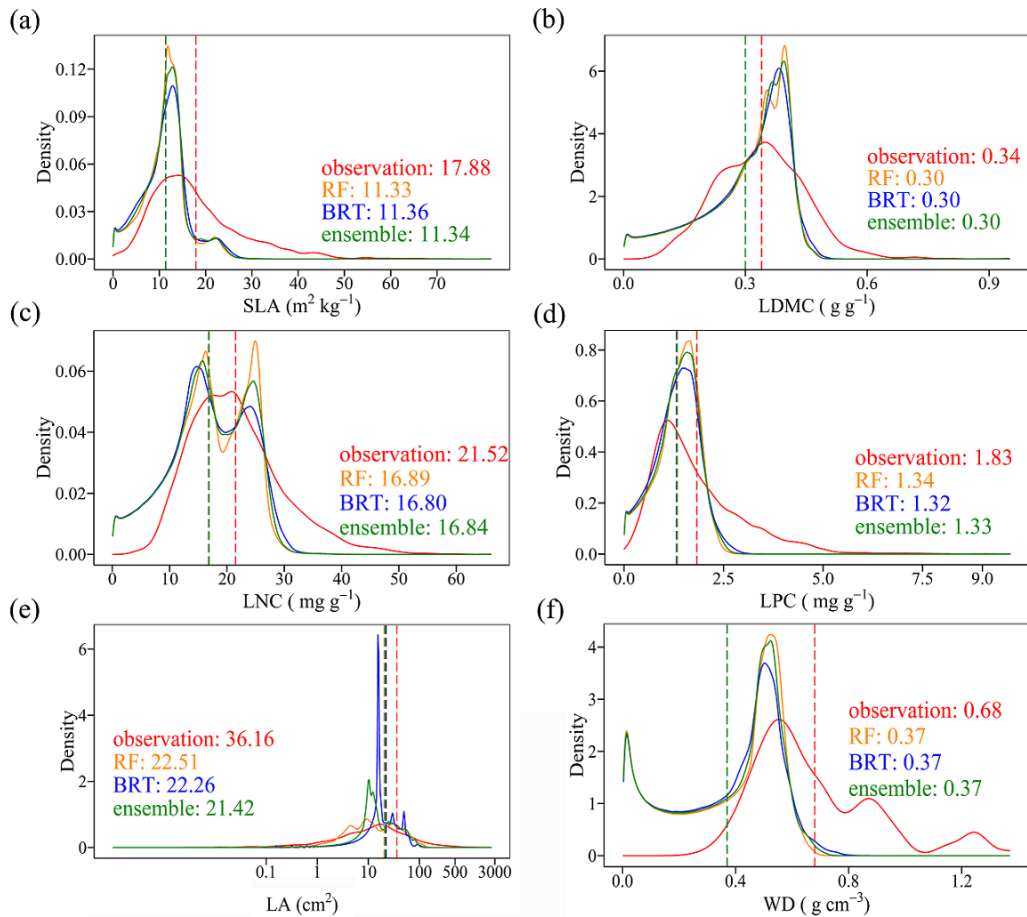
378 **Table 3** List of the eight most important variables for plant functional trait predictions.

Rank	SLA	LDMC	LNC	LPC	LA	WD
1	SAP	MAT	PS	MDR	EVI5	MIR1
2	TS	Elevation	SAP	PDQ	PEQ	TS
3	blue9	MTCI5	pH	Elevation	MTCI9	MIR5
4	RAD	blue8	MDR	MIR8	NIR9	RAD
5	MTCI4	MTCI4	MAP	Tmax	AI	MIR6
6	MTCI6	MTCI6	PEQ	MTCI6	MTCI6	pH
7	Elevation	NIR1	MIR1	MIR7	MAP	red5
8	MTCI7	CEC	Tmax	MIR9	red5	PS

379 SLA, specific leaf area ($\text{m}^2 \text{kg}^{-1}$); LDMC, leaf dry matter content (g g^{-1}); LNC, leaf N concentration
 380 (mg g^{-1}); LPC, leaf P concentration (mg g^{-1}); LA, leaf area (cm^2); WD, wood density (g cm^{-3}); SAP, soil
 381 available P; TS, temperature seasonality; blue, blue reflectance; RAD, solar radiation; MTCI, MERIS
 382 terrestrial chlorophyll index; MAT, mean annual temperature; NIR, near-infrared reflectance; CEC,
 383 cation exchange capacity; PS, precipitation seasonality; MDR, mean diurnal range; MAP, mean annual
 384 precipitation; PEQ, precipitation of wettest quarter of a year; MIR, middle infrared reflectance; Tmax,
 385 max temperature of warmest month of a year; PDQ, precipitation of driest quarter of a year; EVI,
 386 enhanced vegetation index; AI, aridity index; red, red reflectance.

387 3.4 Model performance

388 The distributions of the predictive trait values based on random forest, boosted regression trees,
 389 and ensemble model were consistent with the original trait observations, especially the peak
 390 values (Fig. 5). The mean values of trait observations were relatively higher than those of the
 391 predictive values.



392

393

Figure 5. Comparison of trait distribution between observations and predictive values in each of the different models. Each panel depicts the distribution of observations in solid red, of the random forest (RF) model in yellow, of the boosted regression trees (BRT) model in blue, and of the ensemble model in green. The dashed vertical lines indicate mean values. SLA, specific leaf area; LDMC, leaf dry matter content; LNC, leaf N concentration; LPC, leaf P concentration; LA, leaf area; WD, wood density.

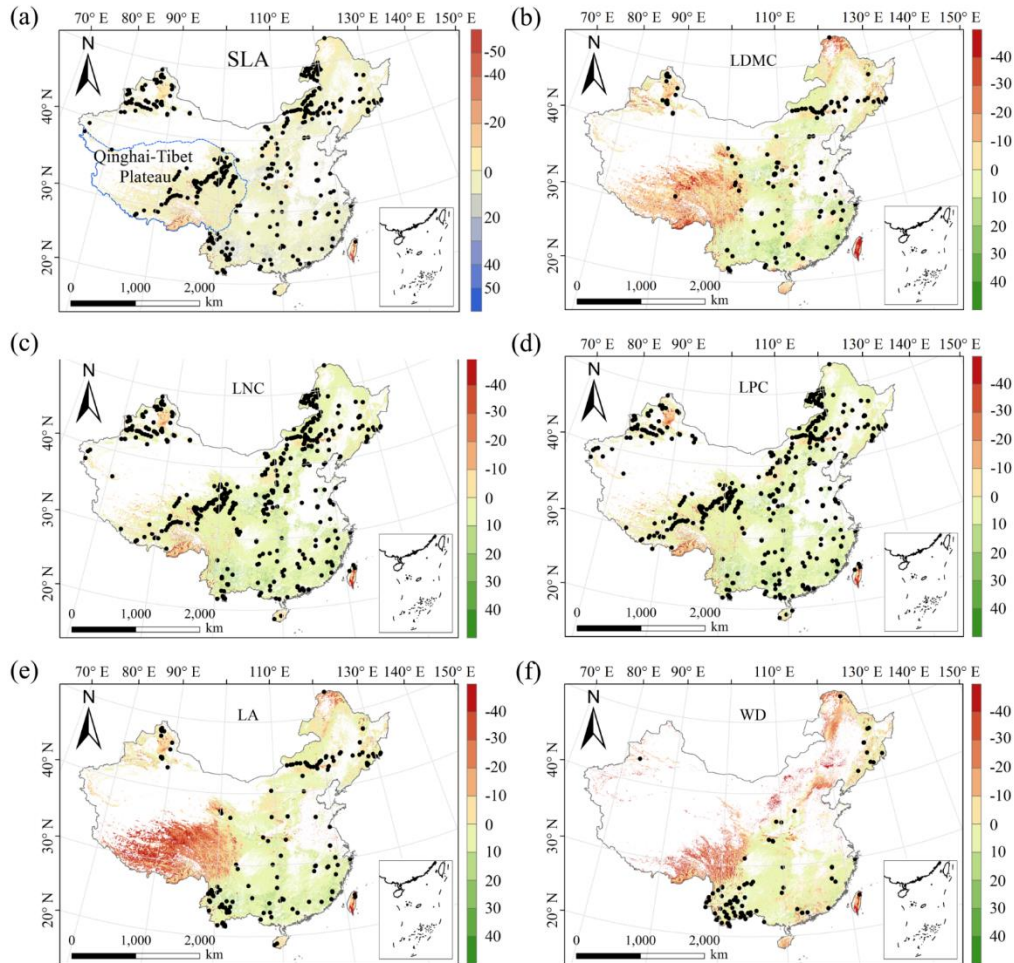
399

3.5 Uncertainty assessments

400

The MESS values of all plant functional traits were positive in most regions, indicating a wide applicability domain of our models (Fig. 6). Nevertheless, trait predictions should be interpreted carefully for northeastern China and the Qinghai-Tibet Plateau due to the sparse samplings in these regions.

403



404

405

406

407

408

409

410

Figure 6. Multivariate environmental similarity surface (MESS) assessments for the six plant functional traits. The black dots represented the locations of trait observations. More intense shades indicate greater similarity (blue) or difference (red) in environmental conditions of the location compared to the predictive factors covered by the training dataset. The white areas represent artificial land cover types. SLA, specific leaf area; LDMC, leaf dry matter content; LNC, leaf N concentration; LPC, leaf P concentration; LA, leaf area; WD, wood density.

411

4 Discussion

412

4.1 Comparison with previous work

413

414

415

416

417

418

419

Our study predicted the spatial patterns of six key plant functional traits across China using machine learning methods and identified the applicability domain of the models. WD had the highest precision with an average of R^2 of 0.66, which was higher than the global WD prediction (Boonman et al., 2020). This improvement in precision may be attributed to the large number and dense occurrence of sample sites as well as the inclusion of vegetation indices in our study. In addition, SLA and LPC also showed good accuracy with R^2 values of 0.50, which was higher than that of Boonman et al. (2020) and consistent with that of Moreno-Martínez et al. (2018). However,

420 LNC and LA showed relatively poor performance, which may be related to the reason that these
421 two traits were more influenced by phylogeny than environmental variables (Yang et al., 2017; An
422 et al., 2021).

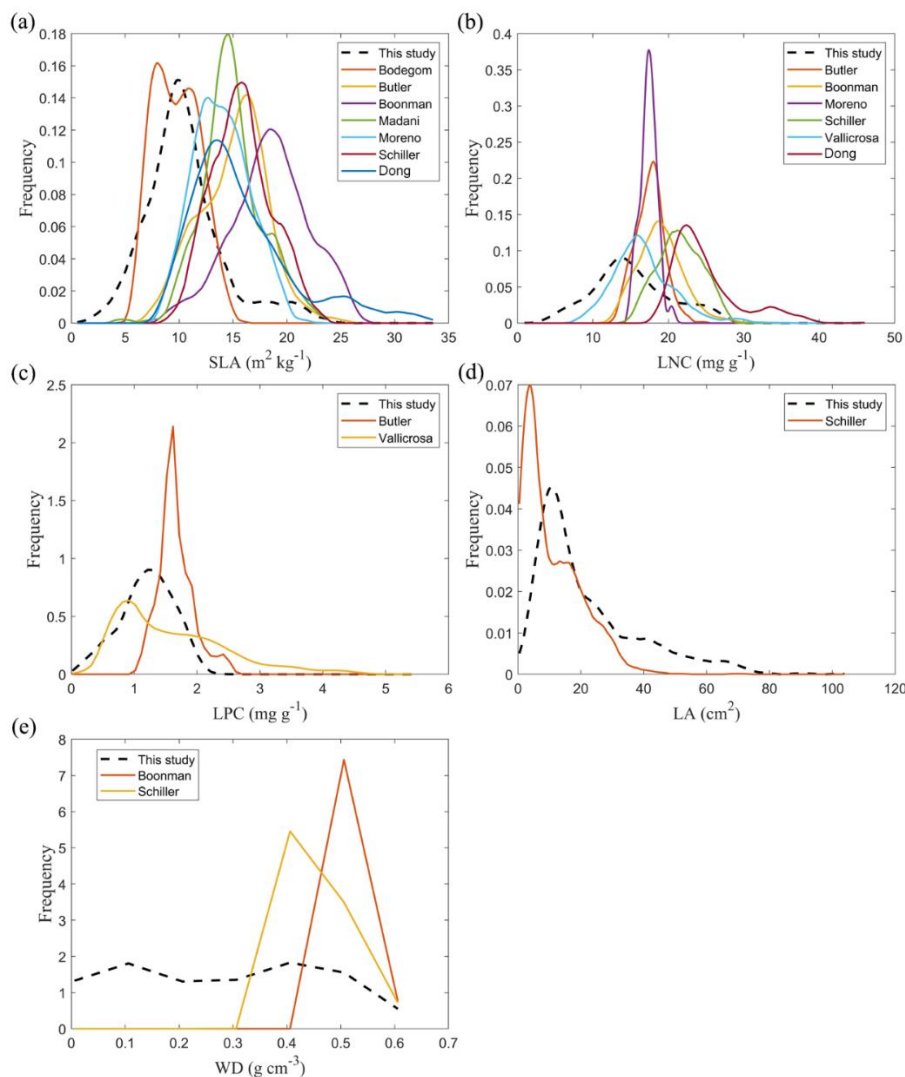
423 The frequency distribution of plant functional traits in China differed between our study and
424 previous studies (Fig. 7, Fig. F1, Table F1 in Appendix F). Given that the spatial resolution of trait
425 maps in most previous studies is 0.5° (except for Moreno-Martínez et al. (2018) and Vallicrosa et
426 al. (2022)), we resampled the data products of previous studies and our study to 0.5° spatial
427 resolution. The distribution in our study contained more predictions at lower values of SLA, LNC
428 and LPC and was broader than those for SLA and LNC in previous global studies. However, the
429 distribution of LNC in our study was consistent with that in Vallicrosa et al. (2022) at the 1 km
430 spatial resolution (Fig. F1 in Appendix F). LA in our study contained more predictions at higher
431 values and was also broader than those in previous global studies. WD did not show the lower and
432 higher predictive values [in this study](#), however, the WD values in the studies of Boonman et al.
433 (2020) and Schiller et al. (2021) had more predictions at higher values and no lower values (< 0.3
434 g cm^{-3}). Our predicted values of SLA showed the highest spatial correlation with those of Dong et
435 al. (2023), and LNC showed the strongest spatial correlation with those of Butler et al. (2017)
436 (Table 5). LA and WD showed the best spatial correlation with those of Schiller et al. (2021), but
437 LPC showed relatively weak spatial correlation with those of published studies.

438 In addition, we compared our results to the other studies focused on China. Yang et al. (2016)
439 predicted the spatial distribution of leaf mass per area ([i.e.](#), $1/\text{SLA}$) and LNC based on trait-
440 environment relationships in China and had an R^2 of 0.13-0.16. The lower predictive precision
441 may be because Yang et al. (2016) only used MAT, MAP and RAD as predictors in estimating the
442 spatial patterns of leaf mass per area and LNC, which likely led to poor performance and low
443 heterogeneity. These results also demonstrated the advantage of our methods in mapping the
444 spatial patterns of plant functional traits at a regional scale.

445 **Table 5** Spatial correlations for SLA, LNC, LPC, LA and WD between this study and other
 446 previous trait maps, labelled by the first author of the corresponding publication (see Table F1 in
 447 Appendix F for citations)

Spatial correlation	Dong	Vallicrosa	Schiller	Boonman	Moreno	Madani	Butler	Bodegom
SLA	0.398		-0.082	0.327	0.242	0.136	-0.042	0.319
LNC	0.156	0.359	0.229	0.252			0.394	
LPC		0.136					0.057	
LA			0.514					
WD			0.647	0.107				

448 The spatial correlation of leaf dry matter content (LDMC) between our study and previous studies was
 449 not included, as the LDMC maps were not available. SLA, specific leaf area ($\text{m}^2 \text{kg}^{-1}$); LNC, leaf N
 450 concentration (mg g^{-1}); LPC, leaf P concentration (mg g^{-1}); LA, leaf area (cm^2); WD, wood density (g cm^{-3}).
 451



452 **Figure 7.** Frequency distributions of plant functional traits in our study (“This study”, dashed
 453 black lines) and other trait maps, identified by the first author of the corresponding publication
 454 (see Table F1 for citations). SLA, specific leaf area ($\text{m}^2 \text{kg}^{-1}$); LNC, leaf N concentration (mg g^{-1});
 455

456 LPC, leaf P concentration (mg g^{-1}); LA, leaf area (cm^2); WD, wood density (g cm^{-3}).

457 **4.2 Spatial patterns of plant functional traits in China**

458 Our study revealed the spatial patterns of different plant functional traits across China, and the
459 variability among the two machine learning methods was relatively low. We compared the spatial
460 differences of trait maps between our study and previous studies at the global scale (Figs. F2-F6 in
461 Appendix F). For example, our study showed high SLA values in the southeastern Qinghai-Tibet
462 Plateau, which concurred with the global study of Boonman et al. (2020). The spatial difference of
463 SLA between our study and Bodegom et al. (2014) was relatively low, and the predictive values in
464 most regions were slightly lower in our study than those in Bodegom et al. (2014). The spatial
465 pattern of difference in SLA between our study and Moreno et al. (2018), Bulter et al. (2017) and
466 Bodegom et al. (2020) was consistent, and the values were higher in northeastern China and
467 southwestern Qinghai-Tibet Plateau in our study than those studies. Our study showed higher
468 LNC values in the northern Inner Mongolia-the Loess Plateau-the eastern Qinghai-Tibet Plateau
469 and northwestern China than those studies at the global studies (Butler et al., 2017; Moreno-
470 Mart ínez et al., 2018; Boonman et al., 2020; Vallicrosa et al., 2022; Dong et al., 2023), reflecting
471 the consistent spatial pattern among these studies. However, Yang et al. (2016) predicted high
472 LNC values in northeastern and northwestern China, northern Inner Mongolia and the entire
473 Qinghai-Tibet Plateau, and SLA and LNC had low heterogeneity overall. The discrepancy with
474 Yang et al. (2016) may be attributed to spatial extrapolation based on trait-climate relationships
475 with a low predictive precision. There was no consistent spatial pattern in LPC between our study
476 and previous studies. Consistent with the global pattern (Wright et al., 2017), LA was larger in
477 southern regions than in northern regions and showed a decreasing trend with latitude. In addition,
478 LA and WD values in our study were lower in most regions than those ones at the global scale.
479 These discrepancies between our study and previous studies at the global scale may be related to
480 three reasons. First, there is bias in the available in-situ field measurement data from China in
481 these global studies, with large gaps in western China for SLA and no data in China for WD
482 (Boonman et al., 2020). Second, some trait-environment relationships may be ~~scale-scale-~~
483 dependent (Bruehlheide et al., 2018), and these studies we compared are from the global scale ~~due~~
484 ~~to~~-because the trait maps in China are not available. Third, the methods used for trait mapping
485 were different among studies, including eco-evolutionary optimality models (Dong et al., 2023),
486 Convolutional Neural Networks based on RGB photographs (Schiller et al., 2021), machine
487 learning algorithms (Vallicrosa et al., 2022; Boonman et al., 2020) and multiple regression
488 analysis (Bodegom et al., 2014).

489 Moreover, our study also identified the applicability domain of our models for predicting the
490 spatial patterns of plant functional traits across China. Five leaf traits and WD appeared to have
491 poor applicability in northeastern China and the Qinghai-Tibet Plateau, primarily due to sparse
492 samplings. Future studies predicting plant functional traits across a large scale through remote

493 sensing observations or other supplementary data will be needed to re-evaluate our results.

494 **4.3 The role of predictive variables**

495 Our study indicates that environmental variables are important for predicting the spatial patterns
496 of plant functional traits, especially climate variables. Temperature variables were primary
497 predictors for SLA, LDMC, LPC and WD. The relationships between leaf traits and temperature
498 have been widely discussed in global and regional studies (Reich and Oleksyn, 2004; Bruelheide
499 et al., 2018). The positive linkage between WD and temperature may be driven by changes in ~~the~~
500 water viscosity ~~of water~~. Plants can adapt to the low water viscosity at high temperatures by
501 reducing the diameter and density of their vessels and by thickening cell walls (Roderick and
502 Berry, 2002; Thomas et al., 2004). Precipitation variables were important predictors for leaf
503 nutrient traits and LA. For example, precipitation of wettest quarter of a year was the factor that
504 most influenced LA variation, which has been confirmed by a previous study (An et al., 2021). A
505 smaller LA could be an adaptive strategy to decrease water loss via reducing the surface area for
506 transpiration under dry environmental conditions (Du et al., 2019). Although the effects of soil on
507 trait predictions were relatively weak, we found that SAP and pH played key roles in SLA and
508 LNC predictions. These results were similar with the previous studies that reported that soil pH
509 was an important driver of trait variation at the global scale and in tundra regions (Maire et al.,
510 2015; Kempainen et al., 2021). Additionally, from the perspective of cost-efficient theory, the
511 strong effects of SAP reflected that high SLA may be an adaptation for facilitating soil exploration
512 more efficiently in fertile soils (Freschet et al., 2010).

513 Vegetation indices have recently been proposed as important predictors of spatial patterns of
514 plant functional traits (Loozen et al., 2018). Our results corroborated these findings and further
515 suggested that EVI, MTCI and MIR reflectance are important predictors in models. Here, the
516 underlying mechanisms between vegetation indices and plant functional traits are not further
517 discussed due to their complexity and uncertainty. However, our results indicated that vegetation
518 indices and NIR reflectance are not key predictors of LNC estimation, which contrasts the
519 findings from global and regional studies (Wang et al., 2016; Loozen et al., 2018; Moreno-
520 Martínez et al., 2018). This may be related to the multitude of factors that influence the
521 relationship between LNC and vegetation indices and NIR reflectance, such as forest type and
522 canopy structure (Dahlin et al., 2013).

523 **4.4 Uncertainties**

524 Although our study mapped the spatial patterns of key functional traits of seed plants in China
525 through large-scale field investigations and compared the predictions with previous studies
526 performed at global and regional scales, there persists some uncertainties in the interpretation of
527 these results. First, the predictive ability of models was relatively worse for certain traits,
528 especially LDMC. Beyond the environmental effects, the variation in plant functional traits is also

529 regulated by phylogenetic structure among plant species (e.g., family, order and phylogenetic
530 clade) (Li et al., 2017). Consequently, incorporating the phylogenetic information will be a
531 promising avenue for further improving the accuracy of spatial predictions of plant functional
532 traits (Butler et al., 2017). A second potential issue is sampling bias; there were major spatial gaps
533 in field investigation in both the northeastern China and the Qinghai-Tibet Plateau. Due to the few
534 ~~lack of~~ measurements for small-shrubs and the lack of low-vegetationherbs, WD data is mainly
535 confined to eastern forests, and the overall quantity of WD data was much lower than that of leaf
536 traits, even in the TRY database. The environmental information of sampling sites was not always
537 obtained from original literature, thus using the public environmental products is a common
538 resolution in large-scale plant trait studies (Boonman et al., 2020; Vallicrosa et al., 2022). Such
539 mismatch between in-situ trait measurements and predictors should be resolved in further work.
540 Finally, additional key challenges in data availability must be resolved to scale up from the species
541 to the community levels, in particular with data surrounding species co-occurrence and their
542 relative cover or abundance in ecological communities (He et al., 2023). For example, Global
543 biodiversity data (e.g., sPlot and Global Biodiversity Information Agency databases) that contains
544 information on species occurrence or the proportion of species in a community has the potential
545 for enabling the calculation of community-weighted trait values and the re-evaluation of our
546 results in future work (Telenius, 2011; Bruelheide et al., 2019). The lack of consistent time period
547 and spatial resolution of predictors due to limitation of data availability is another key challenges
548 in the spatial mapping of plant functional traits. In addition, although WorldClim version 2.1
549 product has high spatial resolution and includes various aspects of climatic parameters, there
550 exists certain limitation and uncertainty in predicting trait maps. Therefore, integrating satellite
551 remote sensing monitoring methods with in-situ trait data collection can also provide an effective
552 way to estimate and assess the species diversity at a large scales (Cavender-Bares et al., 2022).

553 **4.5 Potential applications**

554 Maps of these key functional traits of seed plants highlighted large-scale variability in space,
555 which will significantly advance ecological analyses and future interdisciplinary research. First,
556 using the spatially continuous trait maps, one can optimize and develop trait-flexible vegetation
557 models to reduce uncertainties of conventional vegetation models based on PFTs, which allows for
558 the exploration of the community assembly rules based on how plants with different trait
559 combinations perform under a given set of environmental conditions (Berzaghi et al., 2020). When
560 trait-flexible vegetation models are available, incorporating trait maps into models will bridge the
561 gap for vegetation classifications and predictions of vegetation distribution under global change;
562 ~~which is not feasible in conventional vegetation models~~ (Van Bodegom et al., 2012; Yang et al.,
563 2019). Second, most studies focused on the effects of plant functional traits on ecosystem carbon
564 processes at individual, species and community scales, while how such effects scale up to regional
565 or larger scales remains challenging. In addition, the assessments of China's terrestrial ecosystem

566 carbon sink have had large uncertainties so far (Piao et al., 2022), ~~but~~ The spatial continuous
567 trait maps will provide an effective way to link ecosystem characteristics to ecosystem carbon sink
568 estimates in China (Madani et al., 2018; Šímová et al., 2019). These analyses will help shed light
569 on the mechanisms underlying plant functional traits and terrestrial ecosystem carbon storage at a
570 large scale.

571 **5 Data availability**

572 The original plant functional trait data collected in this study that were used for machine learning
573 models (named by Data file used for machine learning models.csv) and final maps of plant
574 functional traits in terrestrial ecosystems in a GeoTIFF format across China (named by plant
575 functional trait category) are now available for the private link
576 <https://figshare.com/s/c527c12d310cb8156ed2> (An et al., 2023). Once the article is accepted, we
577 will publicly publish these maps at the figshare website.

578 **6 Conclusions**

579 We generated a set of spatial continuous trait maps at a 1-km spatial resolution using machine
580 learning methods in combination with field measurements, environmental variables and vegetation
581 indices. Models for leaf traits (except for LDMC) and WD showed good accuracy and robustness,
582 whereas models of LDMC had relatively poor precision and robustness. Temperature variables
583 were the most important predictors for leaf traits (except for LA) and WD, and precipitation
584 variables were the most important predictors for leaf nutrient traits and LA. We caution that plant
585 functional trait predictions should be interpreted carefully for northeastern China and the Qinghai-
586 Tibet Plateau. The spatial continuous trait maps generated in our study are complementary to
587 current terrestrial in-situ observations and offer new avenues for predicting large-scale changes in
588 vegetation and ecosystem function under climate scenarios in China.

590 **Appendix A Data collection from literature**

- 591 An H. and Shangguan Z. P. Photosynthetic characteristics of dominant plant species at different succession stages
592 of vegetation on Loess Plateau. Chinese Journal of Applied Ecology, 2007, 18, 1175-1180.
- 593 Bai K. D., Jiang D. B., Wan C. X. Photosynthesis-nitrogen relationship in evergreen and deciduous tree species at
594 different altitudes on Mao'er Mountain, Guangxi. Acta Ecologica Sinica, 2013, 33, 4930-4938.
- 595 Bai W. J., Zheng F. L., Dong L. L., et al. Leaf traits of species in different habits in the water-wind erosion region
596 of the Loess Plateau. Acta Ecologica Sinica, 2010, 30, 2529-2540.
- 597 Chai Y F., Shang H. L., Zhang X. F., et al. Ecological variations of woody species along an altitudinal gradient in
598 the Qinling Mountains of Central China: area-based versus mass-based expression of leaf traits. Journal of
599 Forestry Research, 2021, 32, 599-608.
- 600 Chang Y. N., Zhong Q. L., Cheng D. L., et al. Stoichiometric characteristics of C, N, P and their distribution
601 pattern in plants of *Castanopsis carlesii* natural forest in Youxi. Journal of Plant Resources and Environment,

602 2013, 22, 1-10.

603 Chen F. Y., Luo T. X., Zhang L., et al. Comparison of leaf construction cost in dominant tree species of the
604 evergreen broadleaved forest in Jiulian Mountain, Jiangxi Province. *Acta Ecologica Sinica*, 2006, 26, 2485-
605 2493.

606 Chen H. Y., Huang Y. M., He K. J., et al. Temporal intraspecific trait variability drives responses of functional
607 diversity to interannual aridity variation in grasslands. *Ecology and Evolution*, 2018, 9, 5731-5742.

608 Chen L. X., Xiang W. H., Wu H. L., et al. Tree growth traits and social status affect the wood density of pioneer
609 species in secondary subtropical forest. *Ecology and Evolution*, 2017, 7, 5366-5377.

610 Chen L., Yang X. G., Song N. P., et al. Leaf water uptake strategy of plants in the arid-semiarid region of Ningxia.
611 *Journal of Zhejiang University*, 2013, 39, 565-574.

612 Chen Y. H., Han W. X., Tang L. Y., et al. Leaf nitrogen and phosphorus concentrations of woody plants differ in
613 responses to climate, soil and plant growth form. *Ecography*, 2011, 36, 178-184.

614 Cheng J. H., Chu P. F., Chen D. M., et al. Functional correlations between specific leaf area and specific root length
615 along a regional environmental gradient in Inner Mongolia grasslands. *Functional Ecology*, 2016, 30, 985-997.

616 Cheng W., Yu C. H., Xiong K. N., et al. Leaf functional traits of dominant species in karst plateau-canyon areas.
617 *Guihaia*, 2019, 39, 1039-1049.

618 Dong H. and Shekhar R. B. Negative relationship between interspecies spatial association and trait dissimilarity.
619 *Oikos*, 2019, 128, 659-667.

620 Dong T. F., Feng Y. L., Lei Y. B., et al. Comparison on leaf functional traits of main dominant woody species in
621 wet and dry habitats. *Chinese Journal of Ecology*, 2012, 31, 1043-1049.

622 Du H. D. Ecological responses of foliar anatomical structural & physiological characteristics of dominant plants at
623 different site conditions in north Shaanxi Loss Plateau. 2010, Graduation Thesis.

624 Fan Z. X., Zhang S. B., Hao G. Y., et al. Hydraulic conductivity traits predict growth rates and adult stature of 40
625 Asian tropical tree species better than wood density. *Journal of Ecology*, 2012, 100, 732-741.

626 Feng J. B., Fan S. X., Hou Y. F., et al. Interspecific and intraspecific variation of leaf function traits of herbaceous
627 plants in a forest-steppe zone, Hebei Province, China. *Journal of Northeast Forestry University*, 2021, 49, 23-
628 28.

629 Feng Q. H. The study on the response of foliar $\delta^{13}C$ of different life from plants to altitude in subalpine area of
630 Western Sichuan, China. 2011, Graduation Thesis.

631 Fu P. L., Zhu S. D., Zhang J. L., et al. The contrasting leaf functional traits between a karst forest and a nearby
632 non-karst forest in south-west China. *Functional Plant Biology*, 2019, 46, 907-915.

633 Gao S. P., Li J. X., Xu M. C., et al. Leaf N and P stoichiometry of common species in successional stages of the
634 evergreen broad-leaved forest in Tiantong National Forest Park, Zhejiang Province, China. *Acta Ecologica
635 Sinica*, 2007, 27, 947-952.

636 Geekiyana N., Goodale, U. M., Cao, K. F., et al. Leaf trait variations associated with habitat affinity of tropical
637 karst tree species. *Ecology and Evolution*, 2017, 8, 286-295.

638 Geng Y., Ma W. H., Wang L., et al. Linking above- and belowground traits to soil and climate variables: an
639 integrated database on China's grassland species. *Ecology*, 2017, 98, 1471.

640 Guo F. C. The photosynthetic characteristics of precious broad-leaved tree species in south subtropics and their
641 relationship with leaf functional traits. 2015, Graduation Thesis.

642 Guo W. J. Exploring the relationship between arbuscular mycorrhizal fungi and plant based on phylogeny and
643 plant traits. 2015, Graduation Thesis.

644 Hau C. H. Tree seed predation on degraded hillsides in Hong Kong. *Forest Ecology & Management*. 1997, 99,
645 215-221.

646 He J. S., Wang Z. H., Wang X. P., et al. A test of the generality of leaf trait relationships on the Tibetan Plateau.
647 New Phytologist, 2006, 170, 835-848.

648 He P. C., Wright I. J., Zhu S. D., et al. Leaf mechanical strength and photosynthetic capacity vary independently
649 across 57 subtropical forest species with contrasting light requirements. New Phytologist, 2019, 223, 607-618.

650 He Y. T. Studies on physioecological traits of 30 plant species in the Subalpine Meadow of the Qinling Mountains.
651 2007, Graduation Thesis.

652 Hou M M. Adaptive evolution of some species from sedges (*Carex Cyperaceae*) based on phylogeny and leaf
653 functional traits to habitat in the Poyang Lake Area. 2017, Graduation Thesis.

654 Hou Y., Liu M. X., Sun H. R., et al. Response of plant leaf traits to microhabitat change in a subalpine meadow on
655 the eastern edge of Qinghai-Tibetan Plateau, China. Chinese Journal of Applied Ecology, 2017, 28, 71-79.

656 Hu Z. Z., Michaletz S. T., Johnson D. J., et al. Traits drive global wood decomposition rates more than climate.
657 Global Change Biology, 2018, 24, 5259-5269.

658 Hua L., He P., Goldstein G., et al. Linking vein properties to leaf biomechanics across 58 woody species from a
659 subtropical forest. Plant Biology, 2019, 22, 212-220.

660 Huang J. J. and Wang X. H. Leaf nutrient and structural characteristics of 32 evergreen broad-leaved species.
661 Journal of East China Normal University (Natural Science), 2003, 1, 92-97.

662 Huang Y. L. The research about the turnover patterns and moisture adaptation mechanism of major species on the
663 South-North-facing slope. 2012, Graduation Thesis.

664 Iida Y., Kohyama T. S., Swenson N. G., et al. Linking functional traits and demographic rates in a subtropical tree
665 community: the importance of size dependency. Journal of Ecology, 2014, 102, 641-650.

666 Jia Q. Q. Functional traits of fine roots and their relationship with leaf traits of 50 major species in a subtropical
667 forest in Gutianshan. 2011, Graduation Thesis.

668 Jiang Y., Chen X., Ma J., et al., Interspecific and intraspecific variation in functional traits of subtropical evergreen
669 and deciduous broadleaved mixed forests in karst topography, Guilin, Southwest China. Tropical
670 Conservation Science, 2016, 9.

671 Jin Y., Wang C. K., Zhou Z. H., et al. Co-ordinated performance of leaf hydraulics and economics in 10 Chinese
672 temperate tree species. Functional Plant Biology, 2016, 43, 1082-1090.

673 Jing G. H. Responses of grassland community structure and functions to management practices on the semi-arid
674 area of Loess Plateau. 2017, Graduation Thesis.

675 Kang M. Spatial distribution pattern and its causes of woody plant functional traits in Tiantong region, Zhejiang
676 Province. 2012, Graduation Thesis.

677 Krober W., Li Y., Hardtle W., et al. Early subtropical forest growth is driven by community mean trait values and
678 functional diversity rather than the abiotic environment. Ecology and Evolution, 2015, 5, 3541-3556.

679 Krober W., Bohnke M., Welk E., et al. Leaf trait-environment relationships in a subtropical broadleaved forest in
680 south-east China. PloS One, 2012, 7, e35742.

681 Krober W., Zhang, S. R. Ehmig, M., et al. Linking xylem hydraulic conductivity and vulnerability to the leaf
682 economics spectrum-a cross-species study. PloS One, 2014, e109211.

683 Li F. Comparison of functional traits in semi-humid evergreen broad-leaved in Western Hill of Kunming. 2011,
684 Graduation Thesis.

685 Li K. and Xiang W. H. Comparison of specific leaf area, SPAD value and seed mass among subtropical tree
686 species in hilly area of Central Hunan, China. Journal of Central South University of Forestry & Technology,
687 2011, 31, 213-218.

688 Li L., McCormack M. L., Ma C.G., et al. Leaf economics and hydraulic traits are decoupled in five species-rich
689 tropical-subtropical forests. Ecology Letters, 2015, 18, 899-906.

690 Li Q. Leaf functional traits and their relationships with environmental factors in Beishan Mountain of Jinhua,
691 Zhejiang Province. 2020, Graduation Thesis.

692 Li S. J., Su P. X., Zhang H. N., et al. Characteristics and relationships of foliar water and leaf functional traits of
693 desert plants. *Plant Physiology Journal*, 2013, 49, 153-160.

694 Li W. H., Xu F. W., Zheng S. X., et al. Patterns and thresholds of grazing-induced changes in community structure
695 and ecosystem functioning: species-level responses and the critical role of species traits. *Journal of Applied
696 Ecology*, 2017, 54, 963-975.

697 Li W. Q., Xu Q., Li J., et al. Quantification of ecotone width of returned forest land from farmland based on
698 specific leaf area. *Journal of West China Forestry Science*, 2017, 46, 117-121.

699 Li X. F., Pei K. Q., Kery M., et al. Decomposing functional trait associations in a Chinese subtropical forest. *PloS
700 One*, 2017, 12, e0175727.

701 Li X. F., Schmid B., Wang F., et al. Net assimilation rate determines the growth rates of 14 species of subtropical
702 forest trees. *PloS One*, 2016, 11, e0150644.

703 Li X. L., Li X. H., Jiang D. M., et al. Leaf morphological characters of 22 compositae herbaceous species in
704 Horqin sandy land. *Chinese Journal of Ecology*, 2005, 24, 1397-1401.

705 Li Y. H., Luo T. X., Lu Q., et al. Comparisons of leaf traits among 17 major plant species in Shazhuyu Sand
706 Control Experimental Station of Qinghai Province. *Acta Ecologica Sinica*, 2005, 25, 994-999.

707 Li Y. L., Meng Q. T., Zhao X. Y., et al. Relationships of fresh leaf traits and leaf litter decomposition in Kerqin
708 Sandy Land. *Acta Ecologica Sinica*, 2008, 28, 2486-2494.

709 Li Y., Yao J., Yang S., et al. Trait differences research on leaf function of Liaodong oak forest main species in
710 Dongling mountain. *Guangdong Agricultural Sciences*, 2012, 23, 159-162, 171.

711 Liang X. Y., Ye Q., Liu H., et al. Wood density predicts mortality threshold for diverse trees. *New Phytologist*,
712 2021, 229, 3053-3057.

713 Li, R., Zhu, S., Chen, H. Y. H., et al. Are functional traits a good predictor of global change impacts on tree species
714 abundance dynamics in a subtropical forest? *Ecology Letters*, 2015, 18, 1181-1189.

715 Li Y. Y., Shi H., Shao M. A. Cavitation resistance of dominant trees and shrubs in Loess hilly region and their
716 relationship with xylem structure. *Journal of Beijing Forestry University*, 2010, 32, 8-13.

717 Lin G. G., Guo, D. L., Li, L., et al. Contrasting effects of ectomycorrhizal and arbuscular mycorrhizal tropical tree
718 species on soil nitrogen cycling: the potential mechanisms and corresponding adaptive strategies. *Oikos*, 2018,
719 127, 518-530.

720 Liu C. H. and Li Y. Y. Relationship between leaf traits and PV curve parameters in the typical deciduous woody
721 plants occurring in Southern Huanglong Mountain. *Journal of Northwest Forestry University*, 2013, 28, 1-5.

722 Liu G. F., Freschet G. T., Pan X., et al. Coordinated variation in leaf and root traits across multiple spatial scales in
723 Chinese semi-arid and arid ecosystems. *New Phytologist*, 2010, 188, 543-553.

724 Liu G. F., Wang L., Jiang L., et al. Specific leaf area predicts dryland litter decomposition via two mechanisms.
725 *Journal of Ecology*, 2017, 106, 218-229.

726 Liu J. H., Zeng D. H. and Don K. L. Leaf traits and their interrelationships of main plant species in southeast
727 Horqin sandy land. *Chinese Journal of Ecology*, 2006, 25, 921-925.

728 Liu J. X., Chen J., Jiang M. X., et al. Leaf traits and persistence of relict and endangered tree species in a rare plant
729 community. *Functional Plant Biology*, 2012, 39, 512-518.

730 Liu L. H. The traits and adaptive strategies of main herbaceous plants and lianas on micro-topographical units in
731 Huangcangyu reserves of Anhui Province. 2012, Graduation Thesis.

732 Liu M. C., Kong D. L., Lu X. R., et al. Higher photosynthesis, nutrient- and energy-use efficiencies contribute to
733 invasiveness of exotic plants in a nutrient poor habitat in northeast China. *Physiologia Plantarum*, 2017, 160,

734 373-382.

735 Liu R. H., Bai J. L., Bao H., et al. Variation and correlation in functional traits of main woody plants in the
736 *Cyclobalanopsis glauca* community in the karst hills of Guilin, southwest China. Chinese Journal of Plant
737 Ecology, 2020, 44, 828-841.

738 Liu W. D., Su J. R., Li S. F., et al. Stoichiometry study of C, N and P in plant and soil at different successional
739 stages of monsoon evergreen broad-leaved forest in Pu'er, Yunnan Province. Acta Ecologica Sinica, 2010, 30,
740 6581-6590.

741 Liu X. C., Jia H. B., Wang Q. Y. Genetic variation and correlation in wood properties of *Betula platyphlla* in
742 natural Stands. Journal of Northeast Forestry University, 2018, 36, 8-10.

743 Liu Y. Y. Spatial distribution and habitat associations of trees in a typical mixed broad-leaved Korean pine (*Pinus*
744 *koraiensis*) forest. 2014, Graduation Thesis.

745 Luo Y. H., Cadotte M. W., Burgess K. S., et al. Greater than the sum of the parts: how the species composition in
746 different forest strata influence ecosystem function. Ecology Letters, 2019, 22, 1449-1461.

747 Lv J. Z., Miao Y. M., Zhang H. F., et al. Comparisons of leaf traits among different functional types of plant from
748 Huoshan Mountain in the Shanxi Province. Plant Science Journal, 2010, 28, 460-465.

749 Ma J., Wu L. F., Wei X., et al. Habitat adaptation of two dominant tree species in a subtropical monsoon forest:
750 leaf functional traits and hydraulic properties. Guihaia, 2015, 35, 261-268.

751 Mo J. M., Zhang D. Q., Huang Z. L., et al. Distribution pattern of nutrient elements in plants of Dinghushan Lower
752 Subtropical Evergreen Broad-Leaved Forest. Journal of Tropical and Subtropical Botany, 2000, 8, 198-206.

753 Niu C. Y., Meinzer F. C. and Hao G. Y. Divergence in strategies for coping with winter embolism among co-
754 occurring temperate tree species: the role of positive xylem pressure, wood type and tree stature. Functional
755 Ecology, 2017, 31, 1550-1560.

756 Niu D. C., Li Q., Jiang S. G., et al. Seasonal variations of leaf C:N:P stoichiometry of six shrubs in desert of
757 China's Alxa Plateau. Chinese Journal of Plant Ecology, 2013, 37, 317-325.

758 Niu K. C., He J. S. and Lechowicz M. J. Grazing-induced shifts in community functional composition and soil
759 nutrient availability in Tibetan alpine meadows. Journal of Applied Ecology, 2016, 53, 1554-1564.

760 Niu K. C., Zhang S. and Lechowicz M. Harsh environmental regimes increase the functional significance of
761 intraspecific variation in plant communities. Functional Ecology, 2020, 34, 1666-1677.

762 Niu S. L. Photosynthesis research on the predominant legume species in Hunshandak Sandland. 2004, Graduation
763 Thesis.

764 Qi L. X. Response of leaf traits of *Pinus mongoliensis* and *Pinus massoniana* to elevation gradient in Daiyun
765 Mountain. 2015, Graduation Thesis.

766 Ren Q. J., Li Q. J., Bu H. Y., et al. Comparison of physiological and leaf morphological traits for photosynthesis of
767 the 51 plant species in the Maqu alpine swamp meadow. Chinese Journal of Plant Ecology, 2015, 39, 593-603.

768 Ren Y. T. The study of leaf functional traits of typical plants across the Alashan Desert. 2017, Graduation Thesis.

769 Ren Y., Wei C. G. and Guo X. Y. Comparison on leaf function traits of six kinds of plant in Ordos. Journal of Inner
770 Mongolia Forestry Science & Technology, 2019, 45, 43-46, 55.

771 Rios R. S., Salgado-Luarte C. and Gianoli E. Species divergence and phylogenetic variation of ecophysiological
772 traits in lianas and trees. PloS One, 2007, 9, e99871.

773 Shang K. K. Differentiation and maintenance of relict deciduous broad-leaved forest patterns along micro-
774 topographic gradient in subtropical area, East China. 2011, Graduation Thesis.

775 Song Y T. Study on functional plant ecology in Songnen Grassland Northeast China. 2012, Graduation Thesis.

776 Song Y T., Zhou D. W., Li Q., et al. Leaf nitrogen and phosphorus stoichiometry in 80 herbaceous plant species of
777 Songnen grassland in Northeast China. Chinese Journal of Plant Ecology, 2012, 36, 222-230.

- 778 Tan X. Y. Research on leaf functional diversity of forest communities in rainy area of south-west China. 2014,
779 Graduation Thesis.
- 780 Tang Q. Q. Variation in functional traits of plants in the Subtropical Evergreen and Deciduous Broad-leaved Mixed
781 Forest. 2016, Graduation Thesis.
- 782 Tang Y. Inter-specific variations and relationship in leaf traits of major temperate species in northern China. 2011,
783 Graduation Thesis.
- 784 Tao J. P., Zuo J., He Z., et al. Traits including leaf dry matter content and leaf pH dominate over forest soil pH as
785 drivers of litter decomposition among 60 species. *Functional Ecology*, 2019, 33, 1798-1810.
- 786 Tian M., Yu G. R., He N. P., et al. Leaf morphological and anatomical traits from tropical to temperate coniferous
787 forests: Mechanisms and influencing factors. *Scientific Reports*, 2016, 6, 19703.
- 788 Wang B. Analysis of leaf functional traits of 13 species trees in northwestern Fujian Province. 2019, Graduation
789 Thesis.
- 790 Wang B. B. A study on ecological stoichiometry of six kinds of dominant shrubs in Huangcangyu Nature Reserve.
791 2015, Graduation Thesis.
- 792 Wang G. H. Leaf trait co-variation, response and effect in a chronosequence. *Journal of Vegetation Science*, 2007,
793 18, 563-570.
- 794 Wang G. H., Liu J. L. and Meng T. T. Leaf trait variation captures climate differences but differs with species
795 irrespective of functional group. *Journal of Plant Ecology*, 2015, 8, 61-69.
- 796 Wang J. Y., Wang S. Q., Li R. L., et al. C:N:P stoichiometric characteristics of four forest types' dominant tree
797 species in China. *Chinese Journal of Plant Ecology*, 2011, 35, 587-595.
- 798 Wang K. B. Vegetation ecological features and net primary productivity simulation in Yanggou watershed in the
799 Loess hill-gully areas of China. 2011, Graduation Thesis.
- 800 Wang S. S. The traits and adaptive strategies of main herbaceous plants and lianas on micro-topographical units in
801 Longjishan reserves of Anhui Province. 2016, Graduation Thesis.
- 802 Wei L. P. Variations in functional traits of main tree species along tree-crown in broadleaved Korean Pine Forest in
803 Jiaohe, Jilin Province. 2014, Graduation Thesis.
- 804 Wei L. P., Hou J. H. and Jiang S. S. Changes of leaf functional traits of two main species along tree height in
805 broad-leaved Korean pine forest. *Guangdong Agricultural Sciences*, 2014, 12, 55-58, 71.
- 806 Wei L. Y. and Shangguan Z. P. Relation between specific leaf areas and leaf nutrient contents of plants growing on
807 slopelands with different farming-abandoned periods in the Loess Plateau. *Acta Ecologica Sinica*, 2008, 28,
808 2526-2535.
- 809 Wei L. Y., Zhou J. W., Xiao H. G., et al. Variations in leaf functional traits among plant species grouped by growth
810 and leaf types in Zhenjiang, China. *Journal of Forestry Research*, 2011, 28, 241-248.
- 811 Wu D. H., Pietsch K. A., Staab M., et al. Wood species identity alters dominant factors driving fine wood
812 decomposition along a subtropical plantation forests tree diversity gradient in subtropical plantation forests.
813 *Biotropica*, 2021, 53, 643-657.
- 814 Wu T. G., Chen B. F., Xiao Y. H., et al. Leaf stoichiometry of trees in three forest types in Pearl River Delta, South
815 China. *Chinese Journal of Plant Ecology*, 2009, 34, 58-63.
- 816 Xie Y. J. The characteristics of 20 dominant plant functional traits in evergreen broad-leaf forest in Daming
817 Mountain Nature Reserve, Guangxi. 2013, Graduation Thesis.
- 818 Xu M. F., Ke X. H., Zhang Y., et al. Wood densities of six hardwood tree species in Eastern Guangdong and
819 influencing factors. *Journal of South China Agricultural University*, 2016, 37, 100-106.
- 820 Xu M. S., Zhao Y. T., Yang X. D., et al. Geostatistical analysis of spatial variations in leaf traits of woody plants in
821 Tiantong, Zhejiang Province. *Chinese Journal of Plant Ecology*, 2016, 40, 48-59.

822 Xu Y. Z. Biomass estimate and storage mechanisms in northern subtropical forest ecosystems, central China. 2016,
823 Graduation Thesis.

824 Xun Y. H., Di X. Y. and Jin G. Z. Vertical variation and economic strategy of leaf trait of major tree species in a
825 typical mixed broadleaved-Korean pine forest. *Chinese Journal of Plant Ecology*, 2020, 44, 730-741.

826 Yan E. R., Wang X. H., Guo M., et al. C:N:P stoichiometry across evergreen broad-leaved forests, evergreen
827 coniferous forests and deciduous broad-leaved forests in the Tiantong region, Zhejiang Province, eastern
828 China. *Chinese Journal of Plant Ecology*, 2010, 34, 48-57.

829 Yang S. The adaptive strategies of main herbaceous plants traits to different micro-topographical units in
830 Dashushan Mountain, Hefei. 2017, Graduation Thesis.

831 Yang Y., Xu X., Xu M., et al. Adaptation strategies of three dominant plants in the trough-valley karst region of
832 northern Guizhou Province, Southwestern China, evidence from associated plant functional traits and
833 ecostochiometry. *Earth and Environment*, 2020, 48, 413-423.

834 Yang Z., Fan S. X., Zhou B. C., et al. Leaf function and soil nutrient differences of dominant tree species on
835 different slope aspects at the south foothills of Taihang Mountains. *Journal of Henan Agricultural University*,
836 2020, 54, 408-414.

837 Yin Q. L., Wang L., Lei, M. L., et al. The relationships between leaf economics and hydraulic traits of woody
838 plants depend on water availability. *Science of the Total Environment*, 2018, 621, 245-252.

839 Yu Y. H., Zhong X. P. and Chen W. Analysis of relationship among leaf functional traits and economics spectrum
840 of dominant species in northwestern Guizhou Province. *Journal of Forest and Environment*, 2018, 38, 196-
841 201.

842 Yuan S. Preliminary research on plant functional traits and the capability of carbon sequestration of major tree
843 species in Changbai Mountain Area. 2011, Graduation Thesis.

844 Zhang H., Chen H. Y. H., Lian J. Y., et al. Using functional trait diversity patterns to disentangle the scale-
845 dependent ecological processes in a subtropical forest. *Functional Ecology*, 2018, 32, 1379-1389.

846 Zhang J. G., Fu S. L., Wen Z. D., et al. Relationship of key leaf traits of 16 woody plant species in Low
847 Subtropical China. *Journal of Tropical and Subtropical Botany*, 2009, 17, 395-400.

848 Zhang J. L., Poorter L., Cao K. F. Productive leaf functional traits of Chinese savanna species. *Plant Ecology*, 2012,
849 213, 1449-1460.

850 Zhang J. Y. Comparative study on the different plant functional groups leaf traits at the Maoershan Region. 2008,
851 Graduation Thesis.

852 Zhang Q. W., Zhu S. D., Jansen S., et al. Topography strongly affects drought stress and xylem embolism
853 resistance in woody plants from a karst forest in Southwest China. *Functional Ecology*, 2020, 35, 566-577.

854 Zhang S. B. and Cao K. F. Stem hydraulics mediates leaf water status, carbon gain, nutrient use efficiencies and
855 plant growth rates across dipterocarp species. *Functional Ecology*, 2009, 23, 658-667.

856 Zhang S. B., Cao K. F., Fan Z. X., et al. Potential hydraulic efficiency in angiosperm trees increases with growth-
857 site temperature but has no trade-off with mechanical strength. *Global Ecology and Biogeography*, 2013, 22,
858 971-981.

859 Zhang Y., Ren Y. X., Yao J., et al. Leaf nitrogen and phosphorous stoichiometry of trees in *Pinus tabulaeformis*
860 Carr stands, North China. *Journal of Anhui Agricultural University*, 2012, 39, 247-251.

861 Zhao Y. T., Ali, A. and Yan, E. R. The plant economics spectrum is structured by leaf habits and growth forms
862 across subtropical species. *Tree Physiology*, 2016, 37, 173-185.

863 Zheng X. J., Li S. and Li Y. Leaf water uptake strategy of desert plants in the Junggar Basin, China. *Chinese*
864 *Journal of Plant Ecology*, 2011, 35, 893-905.

865 Zheng Y. M. Carbon, nitrogen and phosphorus stoichiometry of plant and soil in the sandy hills of Poyang Lake.

- 866 2014, Graduation Thesis.
- 867 Zheng Z. X. Comparison of plant leaf, height and seed functional traits in dry-hot valleys. 2010, Graduation Thesis.
- 868 Zhou J. Y., He J. J., Guo Z. Y., et al. A study on specific leaf area and leaf dry matter content of five dominant
- 869 species in Xiangshan Mountain, Huaibei City, Anhui Province. *Journal of Huaibei Normal University*
- 870 (Natural Sciences), 2013, 34, 51-54.
- 871 Zhou X., Zuo X. A., Zhao X. Y., et al. Plant functional traits and interrelationship of 34 plant species in south
- 872 central Horqin Sandy Land, China. *Journal of Desert Research*, 2015, 35, 1489-1495.
- 873 Zhu B. R., Xu B. and Zhang D. Y. Extent and sources of variation in plant functional traits in grassland. *Journal of*
- 874 Beijing Normal University (Natural Science), 2011, 47, 485-489.
- 875 Zhu S. D., Song J. J., Li R. H., et al. Plant hydraulics and photosynthesis of 34 woody species from different
- 876 successional stages of subtropical forests. *Plant Cell and Environment*, 2013, 36, 879-891.
- 877 Zhu X B, Liu Y. M. and Sun S. C. Leaf expansion of the dominant woody species of three deciduous oak forests in
- 878 Nanjing, East China. *Chinese Journal of Plant Ecology*, 2005, 29, 125-136.

879 **Appendix B**

880 **Table B1** Summary of statistics in plant functional traits, environmental variables and geographical
 881 distribution in China.

Trait	Unit	Range	Mean	CV (%)	No. of species	Entries	Sites
SLA	m ² kg ⁻¹	0.06–81.68	17.88	54.96	2463	9195	1032
LDMC	g g ⁻¹	0.06–0.95	0.34	100.00	1582	3957	193
LNC	mg g ⁻¹	3.41–66.02	21.52	37.44	2335	7407	567
LPC	mg g ⁻¹	0.09–9.70	1.83	62.19	2074	6266	515
LA	cm ²	0.0033–2553.33	36.16	259.64	1838	5976	691
WD	g cm ⁻³	0.25–1.37	0.68	33.16	768	1788	639
Altitude	m	-144–5454					1430
MAT	°C	-12.07–24.32					1430
MAP	mm	15–2982					1430
Soil total N	g kg ⁻¹	0.11–10.25					1430
Bulk density	g cm ⁻³	0.83–1.45					1430

882 SLA, specific leaf area; LDMC, leaf dry matter content; LNC, leaf N concentration; LPC, leaf P concentration; LA,
 883 leaf area; WD, wood density; MAT, mean annual temperature; MAP, mean annual precipitation.

884 **Table B2** List of all the predictors including environment and remote sensing variables used in this
 885 study.

Type of variables	Variable name	Abbreviations	Units	Time periods	Spatial resolution	Source
Climate	Mean annual temperature	MAT	°C	1970-2000	1 km	WorldClim version 2.1
	Mean diurnal range	MDR	°C	1970-2000	1 km	WorldClim version 2.1
	Temperature seasonality	TS	°C	1970-2000	1 km	WorldClim version 2.1
	Max temperature of warmest month	Tmin	°C	1970-2000	1 km	WorldClim version 2.1
	Min temperature of coldest month	Tmax	°C	1970-2000	1 km	WorldClim version 2.1
	Temperature annual range	TAR	°C	1970-2000	1 km	WorldClim version 2.1
	Isothermality	IS	%	1970-2000	1 km	WorldClim version 2.1
	Mean temperature of wettest quarter	MTEQ	°C	1970-2000	1 km	WorldClim version 2.1
	Mean temperature of driest quarter	MTDQ	°C	1970-2000	1 km	WorldClim version 2.1
	Mean temperature of warmest quarter	MTWQ	°C	1970-2000	1 km	WorldClim version 2.1
	Mean temperature of coldest quarter	MTCQ	°C	1970-2000	1 km	WorldClim version 2.1
	Mean annual precipitation	MAP	mm	1970-2000	1 km	WorldClim version 2.1
	Precipitation of wettest month	PEM	mm	1970-2000	1 km	WorldClim version 2.1
	Precipitation of driest month	PDM	mm	1970-2000	1 km	WorldClim version 2.1
	Precipitation seasonality	PS	%	1970-2000	1 km	WorldClim version 2.1
	Precipitation of wettest quarter	PEQ	mm	1970-2000	1 km	WorldClim version 2.1
	Precipitation of driest quarter	PDQ	mm	1970-2000	1 km	WorldClim version 2.1
	Precipitation of warmest quarter	PWQ	mm	1970-2000	1 km	WorldClim version 2.1
	Precipitation of coldest quarter	PCQ	mm	1970-2000	1 km	WorldClim version 2.1
	Aridity index	AI	/	1970-2000	1 km	Global CGIAR-CSI
Solar radiation	RAD	$\text{kJ m}^{-2} \text{day}^{-1}$	1970-2000	1 km	WorldClim version 2.1	
Topography	Elevation	/	m		1 km	SRTM 90m V4.1
Soil	Soil sand content	SAND	%	/	1 km	Shangguan et al. (2013)
	Soil silt content	SILT	%	/	1 km	Shangguan et al. (2013)
	Soil clay content	CLAY	%	/	1 km	Shangguan et al. (2013)
	Bulk density	BD	g cm^{-3}	/	1 km	Shangguan et al. (2013)
	Soil pH	pH	/	/	1 km	Shangguan et al. (2013)
	Soil organic matter	SOC	g kg^{-1}	/	1 km	Shangguan et al. (2013)
	Soil total N	STN	g kg^{-1}	/	1 km	Shangguan et al. (2013)
	Soil total P	STP	g kg^{-1}	/	1 km	Shangguan et al. (2013)
	Soil alkali-hydrolysable N	SAN	mg kg^{-1}	/	1 km	Shangguan et al. (2013)
	Soil available P	SAP	mg kg^{-1}	/	1 km	Shangguan et al. (2013)
	Soil available K	SAK	mg kg^{-1}	/	1 km	Shangguan et al. (2013)
	Cation exchange capacity	CEC	me kg^{-1}	/	1 km	Shangguan et al. (2013)

Continued

Type of variables	Variable name	Abbreviations	Units	Time periods	Spatial resolution	Source
EVI	MODIS EVI long-term monthly averages		/	2001-2018	1 km	MOD13A3 V006
NIR	MODIS NIR long-term monthly averages		/	2001-2018	1 km	MOD13A3 V006
MIR	MODIS MIR long-term monthly averages		/	2001-2018	1 km	MOD13A3 V006
Red	MODIS red long-term monthly averages		/	2001-2018	1 km	MOD13A3 V006
Blue	MODIS blue long-term monthly averages		/	2001-2018	1 km	MOD13A3 V006
MTCI	MTCI long-term monthly averages		/	2003-2011	4.63 km	MTCI level 3 product
Land cover	Land cover map		/	2015	100 m	Copernicus Global Land Service Collection 3

886 The remote sensing variables are calculated as long-term monthly averages from 2001 to 2018. Thus 12 variables
 887 of each remote sensing category are obtained.

888

889

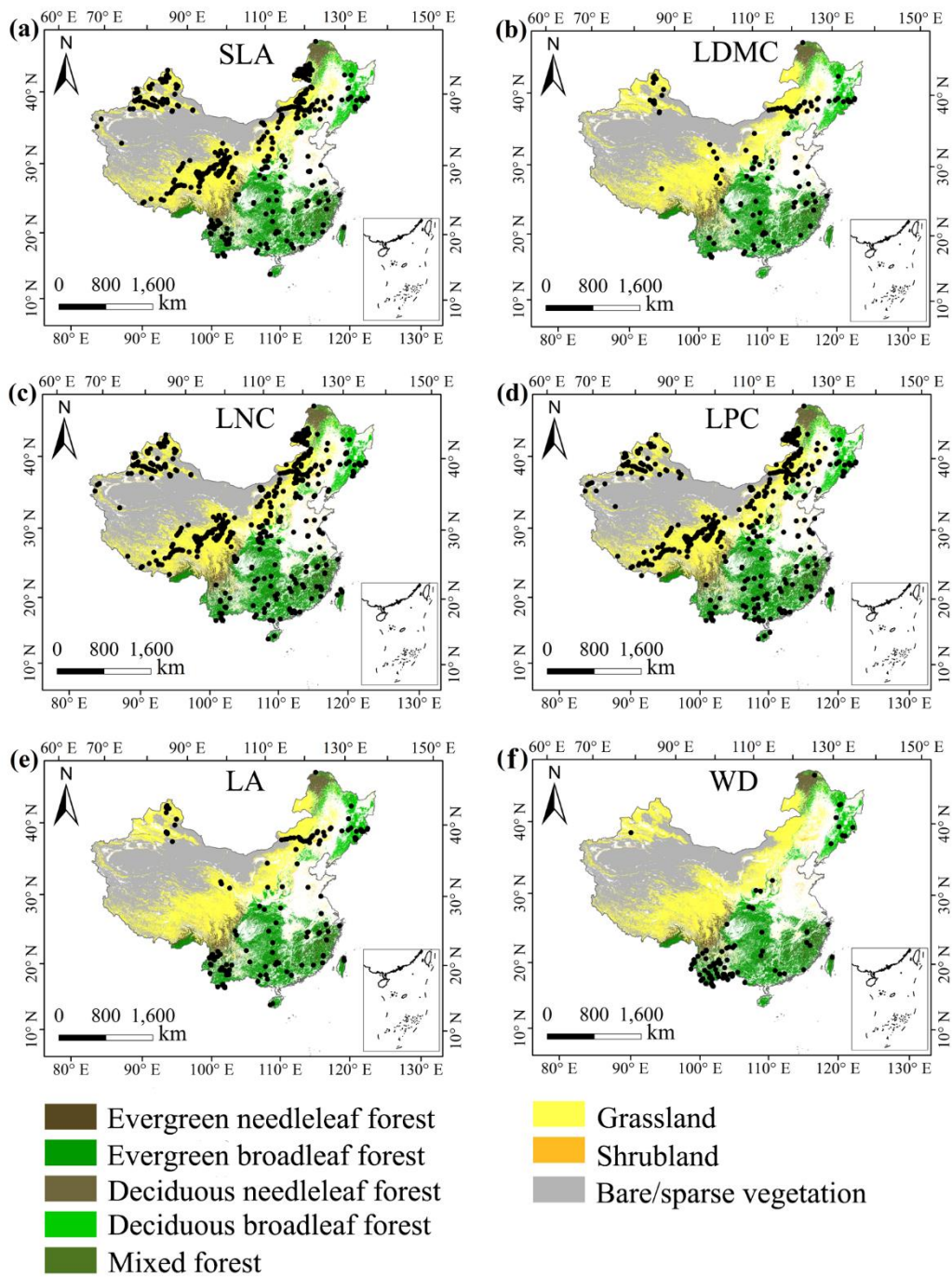
890

891

892 **Table B3** The number of samples of eight plant functional trait used for model training (80%) and
 893 validation (20%).

Traits	No. of samples	No. of samples used for model training	No. of samples used for model validation
SLA	9195	7356	1839
LDMC	3957	3166	791
LNC	7407	5926	1481
LPC	6266	5013	1253
LA	5976	4781	1195
WD	1787	1430	357

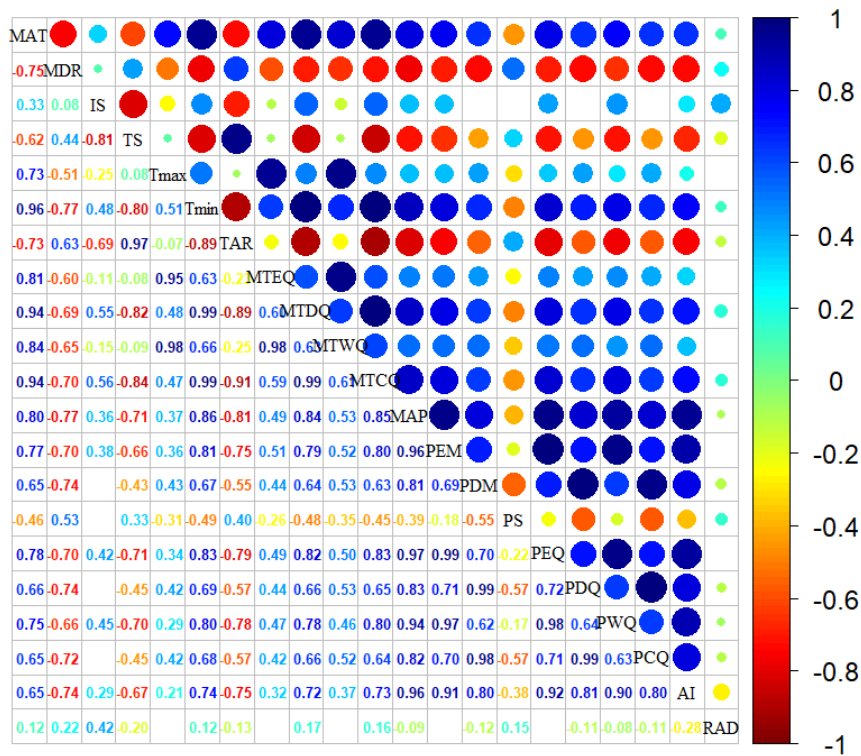
894 SLA, specific leaf area ($\text{m}^2 \text{kg}^{-1}$); LDMC, leaf dry matter content (g g^{-1}); LNC, leaf N concentration
 895 (mg g^{-1}); LPC, leaf P concentration (mg g^{-1}); LA, leaf area (cm^2); WD, wood density (g cm^{-3}).



896

897 **Figure B1.** The distribution of sampling site of each plant functional traits across China. The

898 black dots represented the locations of trait observations.



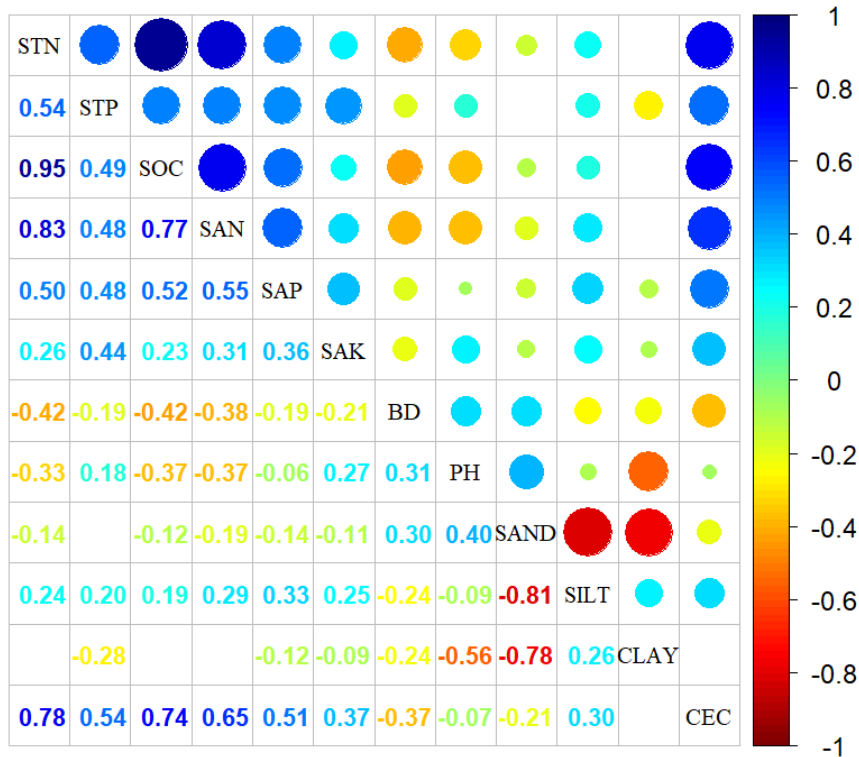
899

900

901

902

Figure B2B1. Correlations among climate variables. The blank indicates that the correlations are not significant ($P > 0.05$). The size of the circles is proportional to the correlation coefficient. The abbreviation of climate variables is seen in Table B2.



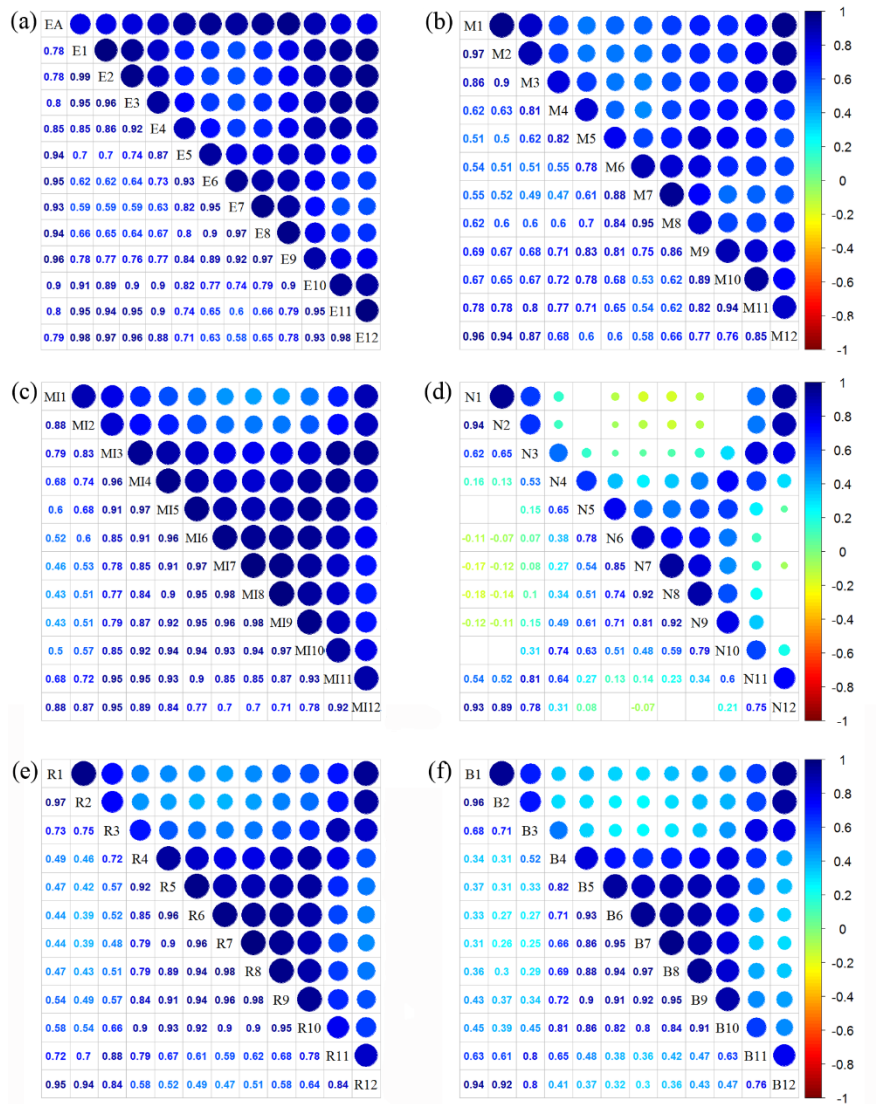
903

904

905

906

Figure B3B2. Correlations among soil variables. The blank indicates that the correlations are not significant ($P > 0.05$). The size of the circles is proportional to the correlation coefficient. The abbreviation of soil variables is seen in Table B2.



907

908

Figure B4B3. Correlations among monthly remote sensing variables. The blank indicates that the

909

correlations are not significant ($P > 0.05$). The size of the circles is proportional to the correlation

910

coefficient. (a) enhanced vegetation index (EVI); (b) MERIS terrestrial chlorophyll index (MTCI);

911

(c) MIR reflectance; (d) NIR reflectance; (e) red reflectance; (f) blue reflectance.

912 **Appendix C**

913 **Table C1** Optimal parameter combination and model performance of random forest for plant functional
 914 traits

Traits	n.tree	mtry	R ²	NRMSE	MAE
SLA	1000	24	0.476	0.22	5.134
LDMC	1000	11	0.234	0.20	0.072
LNC	1000	57	0.392	0.00	0.098
LPC	1000	20	0.587	0.05	0.129
LA	1000	18	0.278	0.48	26.622
WD	1000	9	0.531	0.02	0.072

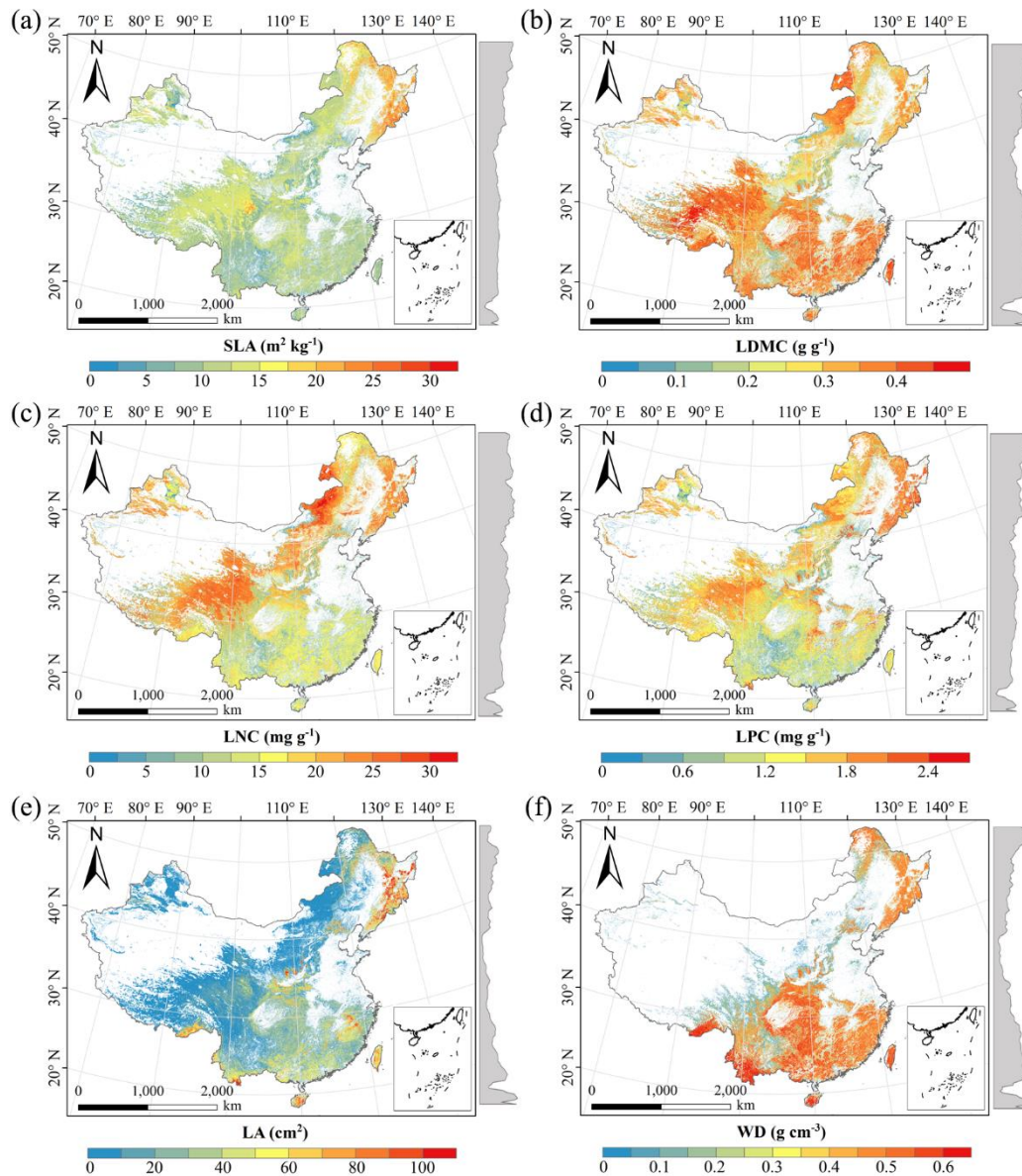
915 SLA, specific leaf area; LDMC, leaf dry matter content; LNC, leaf N concentration; LPC, leaf P
 916 concentration; LA, leaf area; WD, wood density.

917

918 **Table C2** Optimal parameter combination and model performance of boosted regression trees for plant
 919 functional traits

Traits	n.tree	interaction. depth	shrinkage	learning rate	bag fractions	R ²	NRMSE	MAE
SLA	3000	6	0.01	10	0.75	0.486	0.20	5.082
LDMC	3000	2	0.01	10	0.75	0.247	0.19	0.071
LNC	3000	6	0.01	10	0.70	0.414	0.00	0.096
LPC	3000	7	0.01	10	0.75	0.591	0.05	0.129
LA	3000	3	0.001	10	0.75	0.282	0.55	27.556
WD	3000	4	0.01	10	0.70	0.627	0.01	0.066

920 SLA, specific leaf area; LDMC, leaf dry matter content; LNC, leaf N concentration; LPC, leaf P
 921 concentration; LA, leaf area; WD, wood density.



923

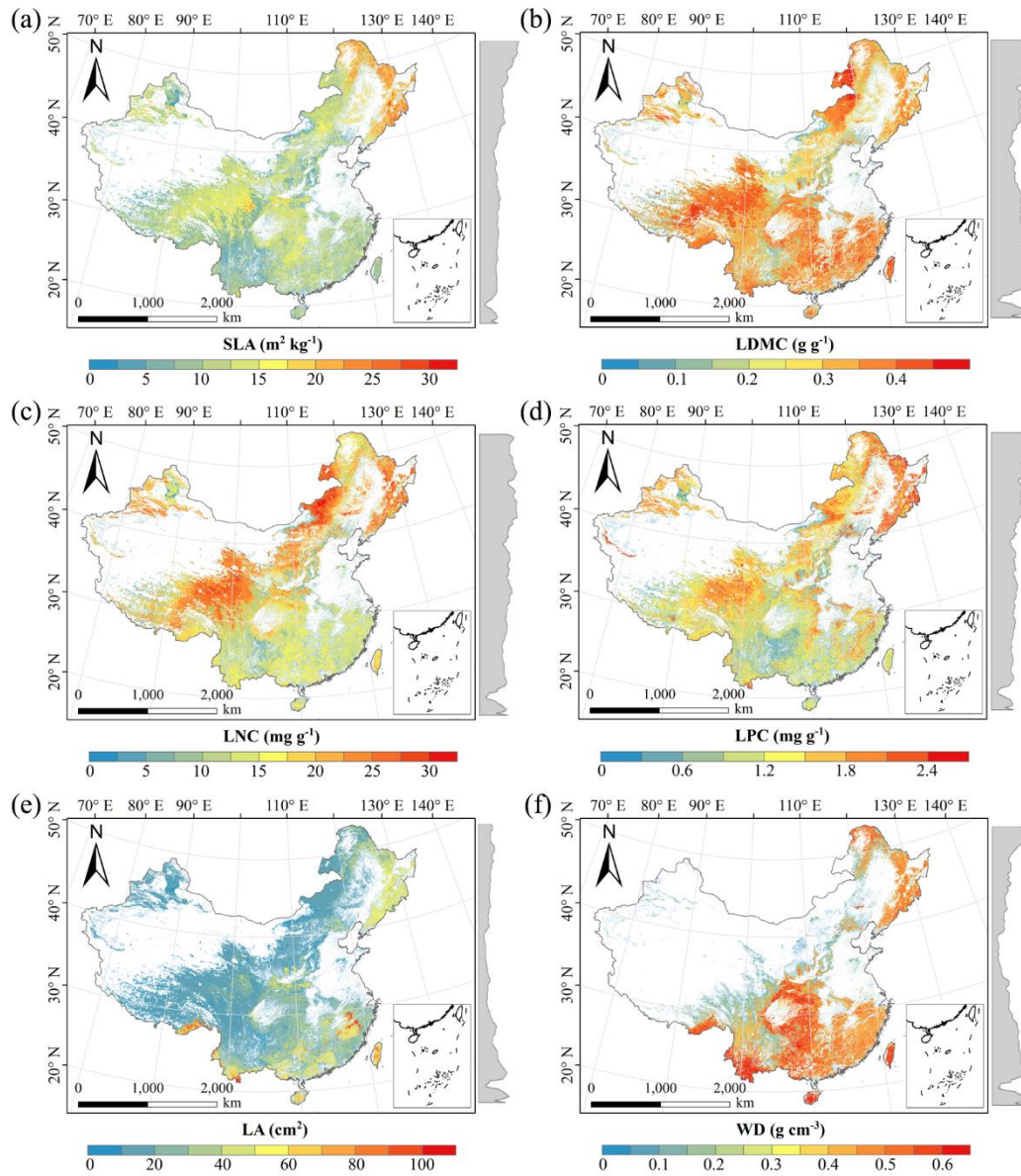
924

925

926

927

Figure D1. Spatial distribution of plant functional traits based on random forest. The grey curves on the right of maps were trait distribution along with latitude. The white areas represent artificial land cover types. SLA, specific leaf area; LDMC, leaf dry matter content; LNC, leaf N concentration; LPC, leaf P concentration; LA, leaf area; WD, wood density.



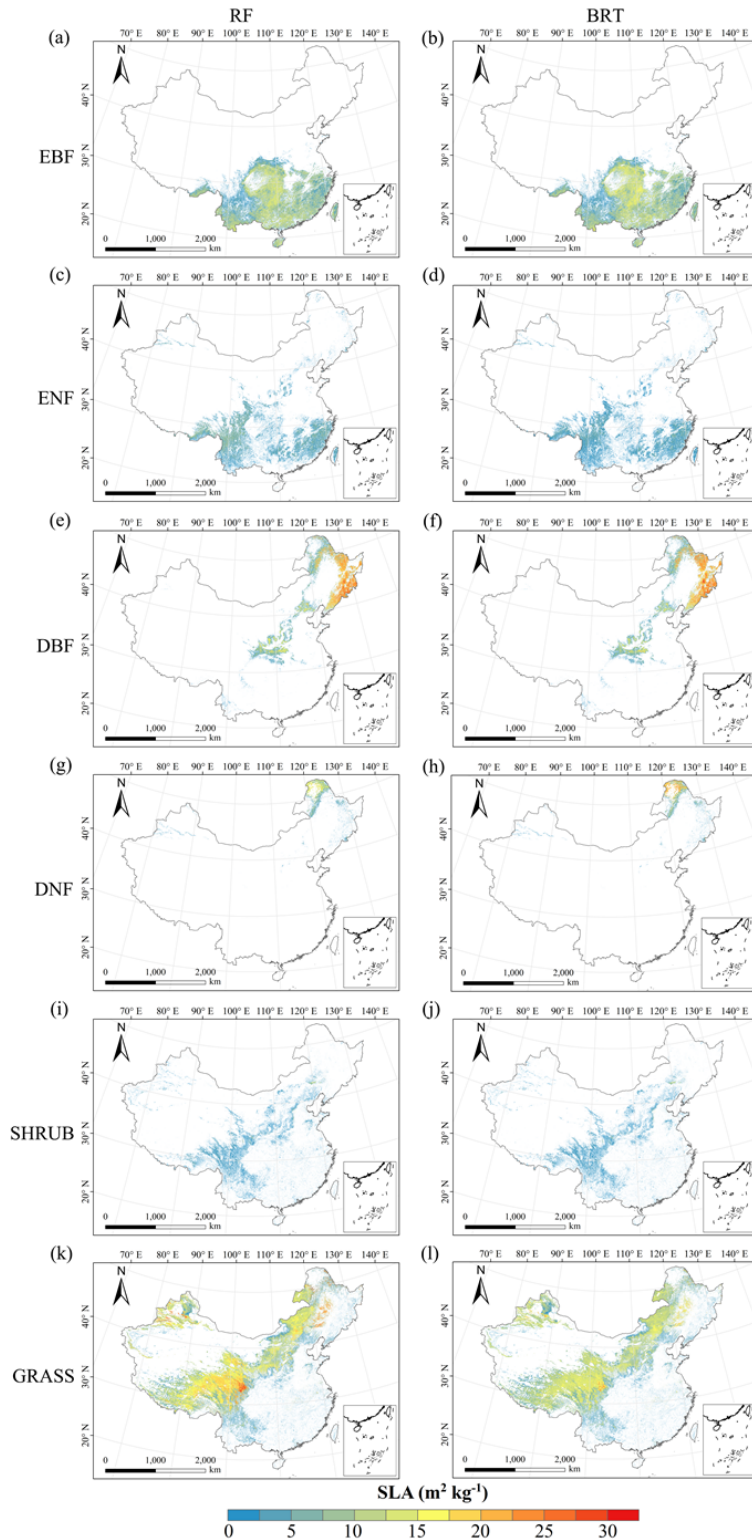
928

929 **Figure D2.** Spatial distribution of plant functional traits based on boosted regression trees. The

930 grey curves on the right of maps were trait distribution along with latitude. The white areas

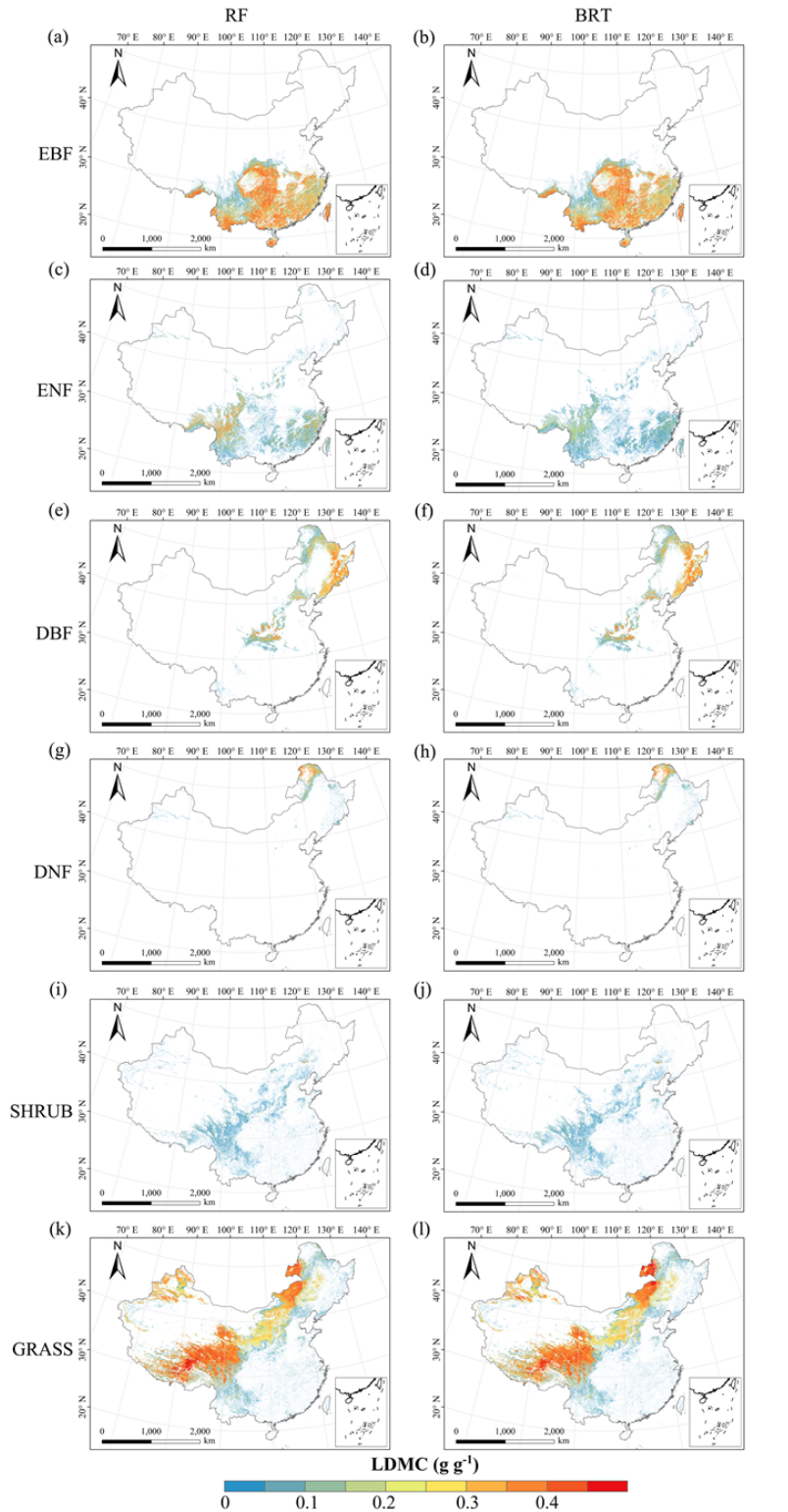
931 represent artificial land cover types. SLA, specific leaf area; LDMC, leaf dry matter content; LNC,

932 leaf N concentration; LPC, leaf P concentration; LA, leaf area; WD, wood density.



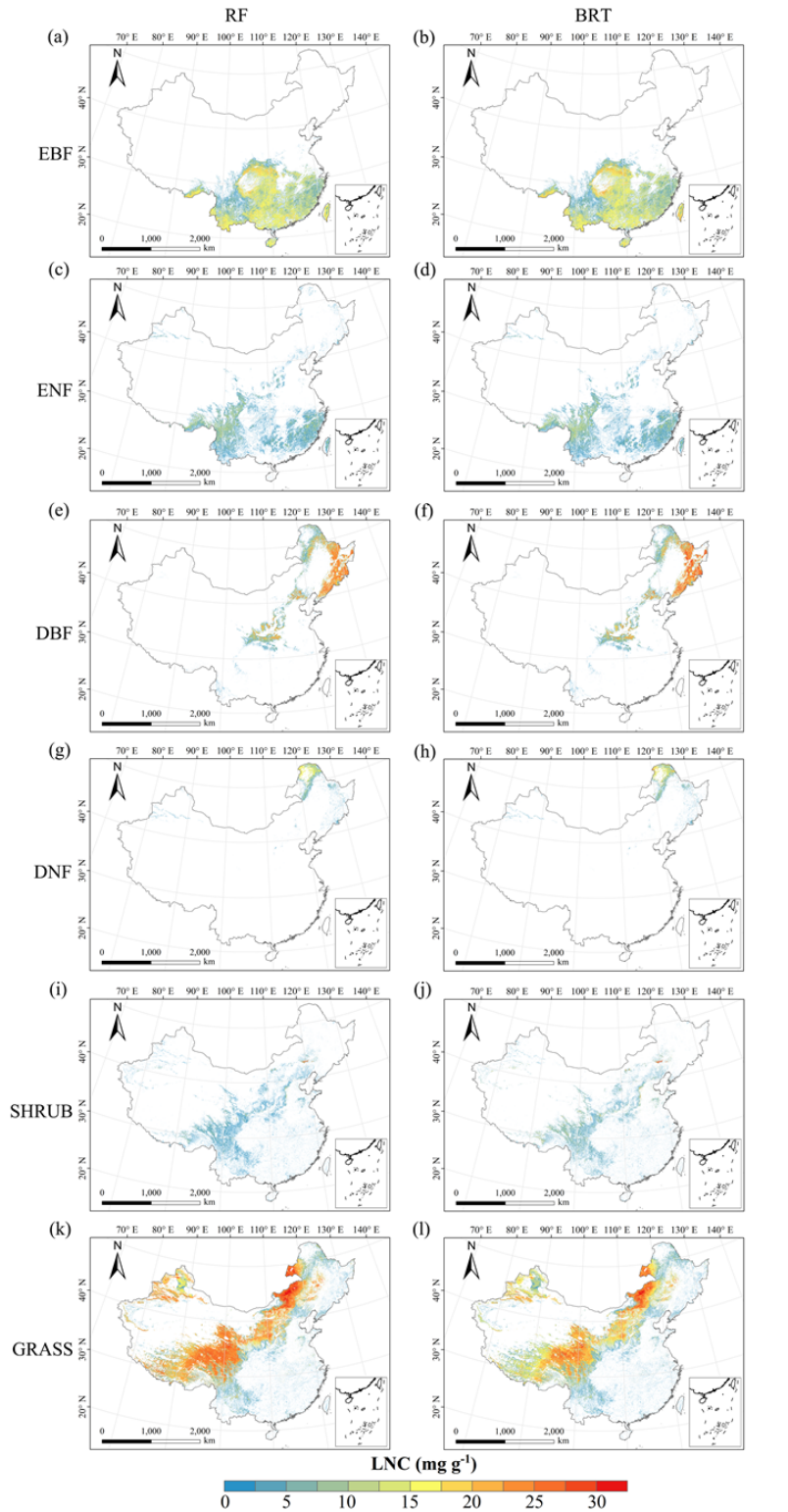
933

934 **Figure D3.** Spatial distribution of specific leaf area for each plant functional type. The left panel
 935 was obtained from RF method (random forest), the right panel was obtained from BRT method
 936 (boosted regression trees). The white areas represent other natural vegetation types and artificial
 937 land cover types. EBF, evergreen broadleaf forest; ENF, evergreen needleleaf forest; DBF,
 938 deciduous broadleaf forest; DNF, deciduous needleleaf forest; SHRUB, shrubland; GRASS,
 939 grassland.



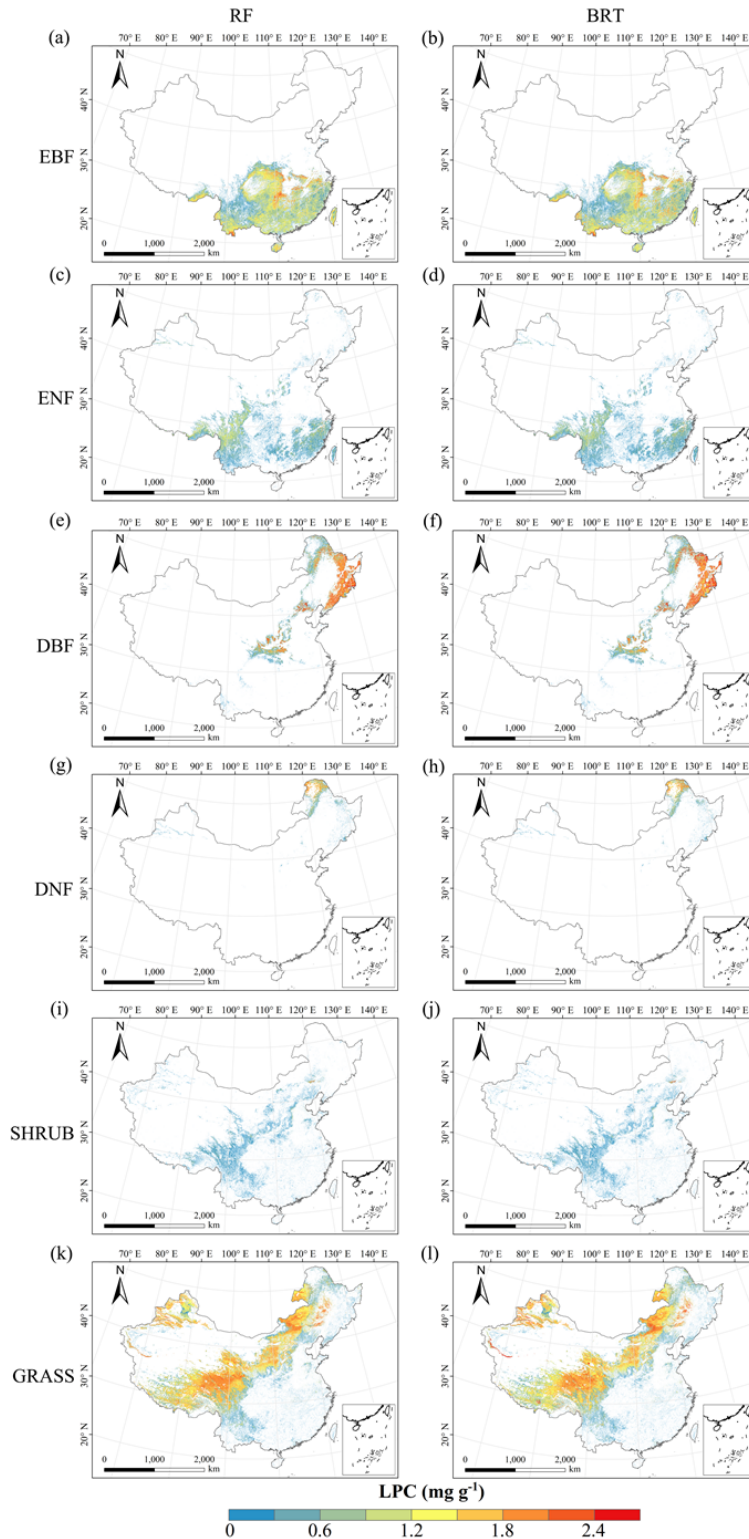
940

941 **Figure D4.** Spatial distribution of leaf dry matter content for each plant functional type. The left
 942 panel was obtained from RF method (random forest), the right panel was obtained from BRT
 943 method (boosted regression trees). The white areas represent other natural vegetation types and
 944 artificial land cover types. EBF, evergreen broadleaf forest; ENF, evergreen needleleaf forest; DBF,
 945 deciduous broadleaf forest; DNF, deciduous needleleaf forest; SHRUB, shrubland; GRASS,
 946 grassland.



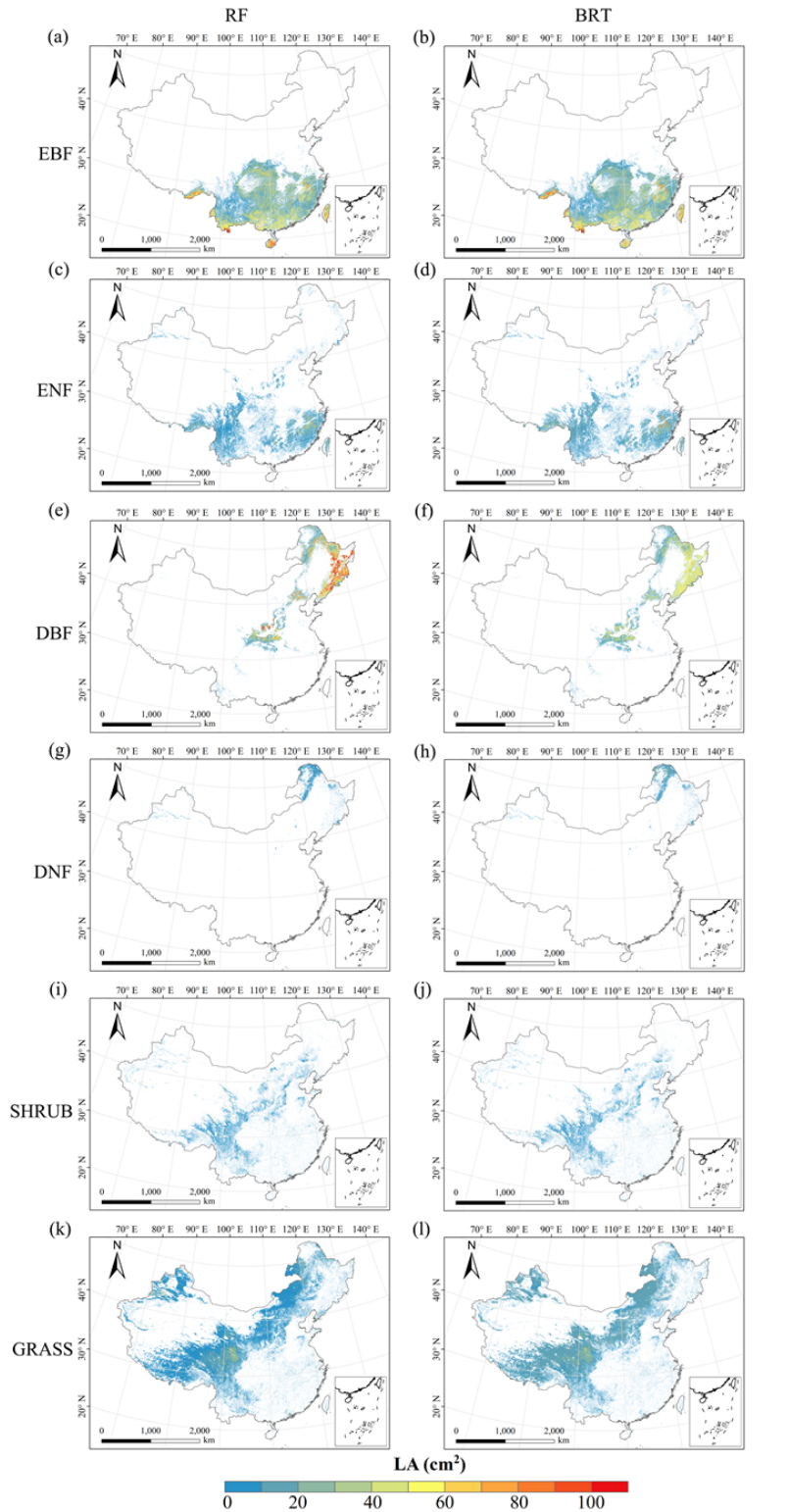
947

948 **Figure D5.** Spatial distribution of leaf N concentration for each plant functional type. The left
 949 panel was obtained from RF method (random forest), the right panel was obtained from BRT
 950 method (boosted regression trees). The white areas represent other natural vegetation types and
 951 artificial land cover types. EBF, evergreen broadleaf forest; ENF, evergreen needleleaf forest; DBF,
 952 deciduous broadleaf forest; DNF, deciduous needleleaf forest; SHRUB, shrubland; GRASS,
 953 grassland.



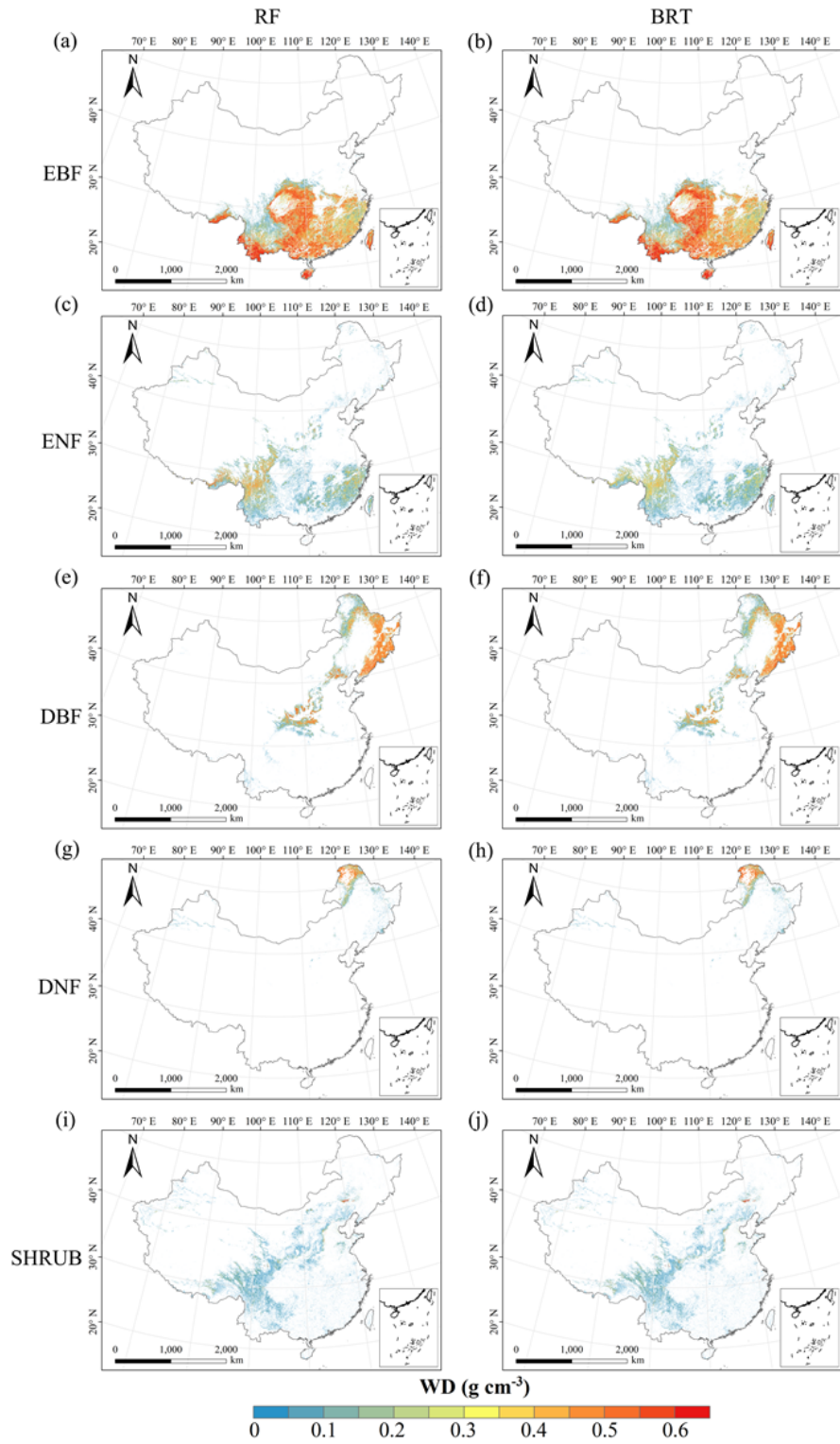
954

955 **Figure D6.** Spatial distribution of leaf P concentration for each plant functional type. The left
 956 penal was obtained from RF method (random forest), the right penal was obtained from BRT
 957 method (boosted regression trees). The white areas represent other natural vegetation types and
 958 artificial land cover types. EBF, evergreen broadleaf forest; ENF, evergreen needleleaf forest; DBF,
 959 deciduous broadleaf forest; DNF, deciduous needleleaf forest; SHRUB, shrubland; GRASS,
 960 grassland.



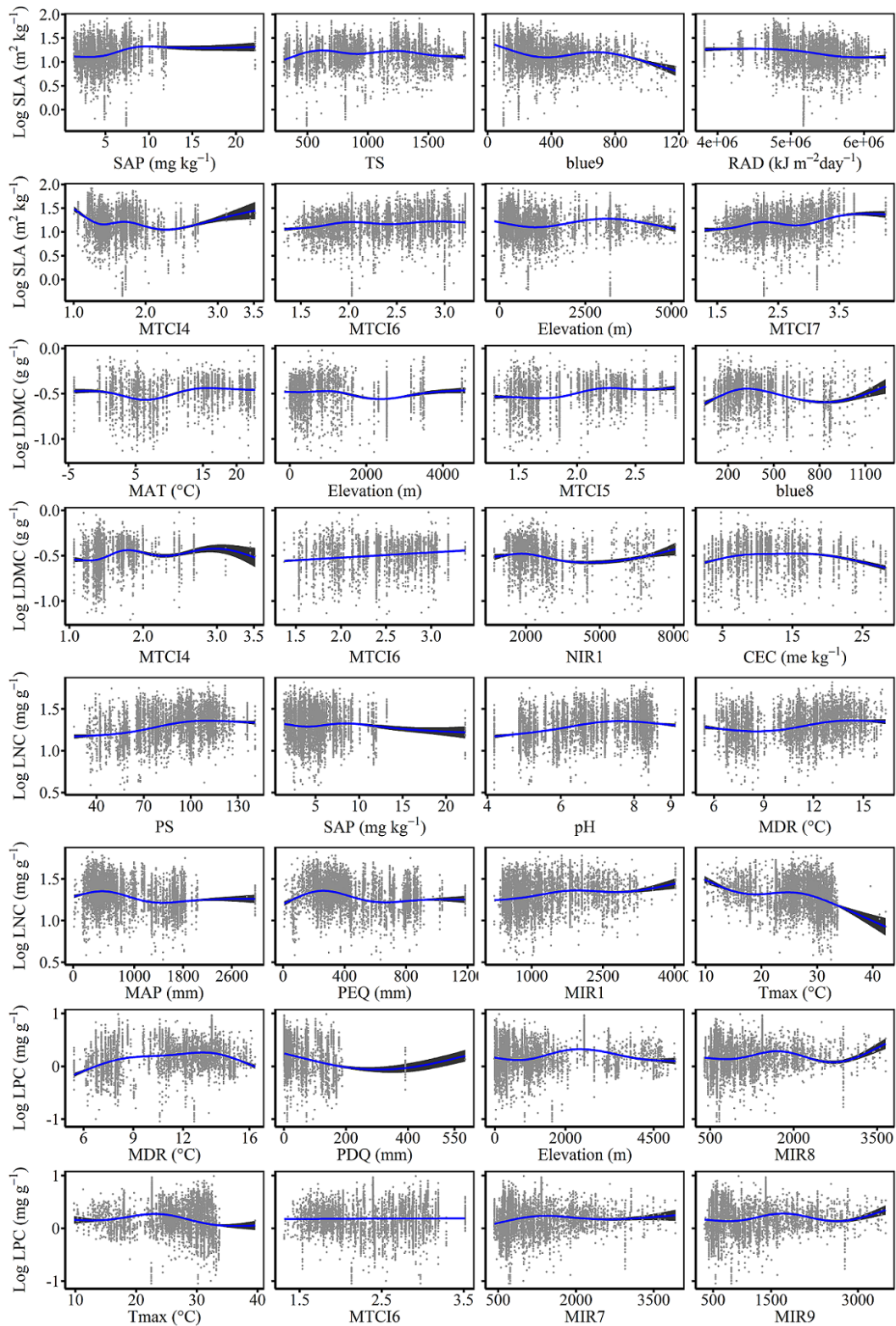
961

962 **Figure D7.** Spatial distribution of leaf area for each plant functional type. The left panel was
 963 obtained from RF method (random forest), the right panel was obtained from BRT method
 964 (boosted regression trees). The white areas represent other natural vegetation types and artificial
 965 land cover types. EBF, evergreen broadleaf forest; ENF, evergreen needleleaf forest; DBF,
 966 deciduous broadleaf forest; DNF, deciduous needleleaf forest; SHRUB, shrubland; GRASS,
 967 grassland.

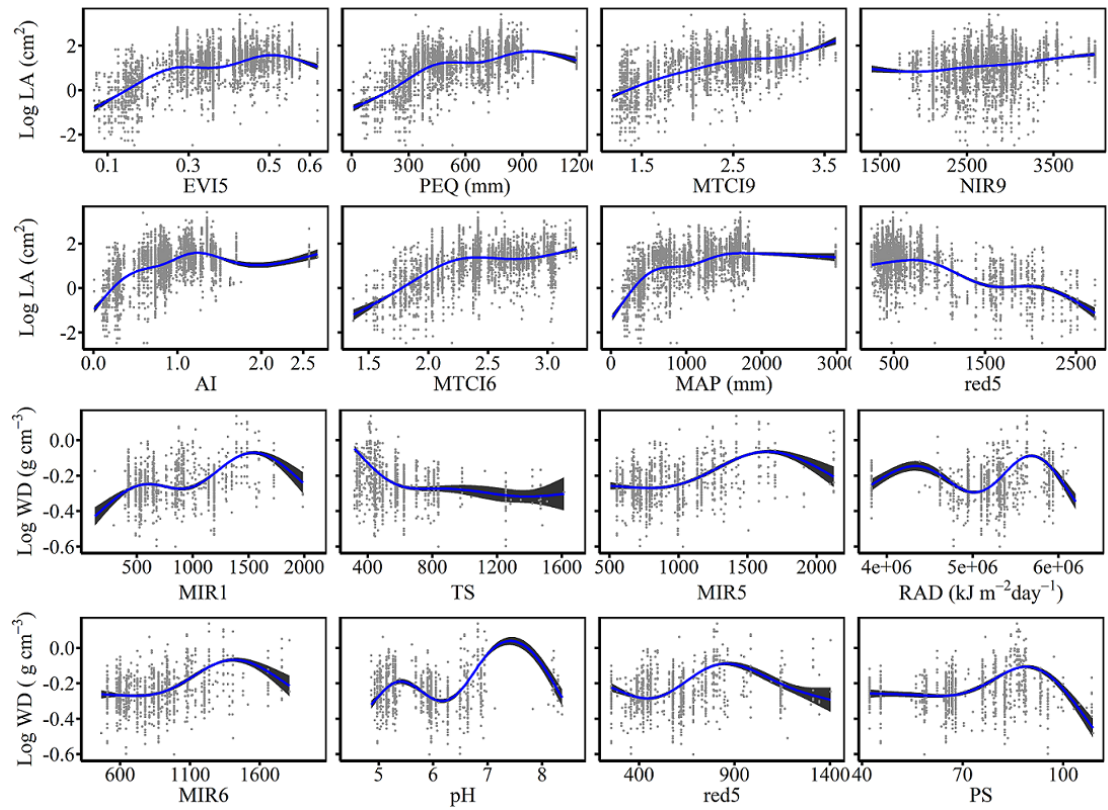


968

969 **Figure D8.** Spatial distribution of wood density for each plant functional type. The left panel was
 970 obtained from RF method (random forest), the right panel was obtained from BRT method
 971 (boosted regression trees). The white areas represent other natural vegetation types and artificial
 972 land cover types. EBF, evergreen broadleaf forest; ENF, evergreen needleleaf forest; DBF,
 973 deciduous broadleaf forest; DNF, deciduous needleleaf forest; SHRUB, shrubland.



975
 976 **Figure E1.** The relationships between SLA (specific leaf area), LDMC (leaf dry matter content),
 977 LNC (leaf N concentration), LPC (leaf P concentration) and their eight most important predictors.



978

979

980

Figure E2. The relationships between LA (leaf area), WD (wood density) and their eight most important predictors.

981 **Appendix F Comparisons between our study with trait maps from previous**
 982 **studies**

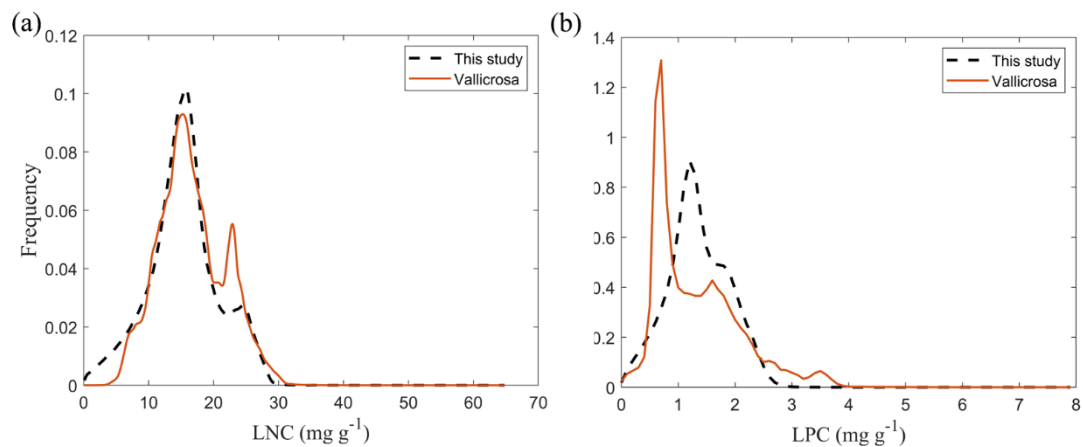
983 Given that the trait maps predicted for China were not available from the literature and
 984 authors, we compared our study with those studies performed at the global scale (see Table F1).
 985 Thus, we extracted the data in China from global trait maps. Before the quantitative comparisons
 986 with previous studies, we performed two steps to make the data products as comparable as
 987 possible and improve the consistency between different studies. First, due to different spatial
 988 resolution of global trait maps (mainly 0.5 °) and our study, we resampled the data products of
 989 previous studies and our maps to 0.5 ° spatial resolution. In addition, Vallicrosa et al. (2022)
 990 generated the global maps of LNC and LPC with a 1 km spatial resolution, we also compared the
 991 frequency distribution of Vallicrosa et al. (2022) with that of our study at a 1 km spatial resolution.
 992 Second, our study focused on natural vegetation, so the global trait maps were used to filter out
 993 non-natural vegetation (e.g., croplands). For example, Madani et al. (2018) predicted the spatial
 994 distributions of SLA that included croplands. We quantitatively compared our maps with previous
 995 studies from two perspectives. The comparisons among trait maps were made using frequency
 996 plots and spatial correlations (Figure 7 and Table 5). And the maps of spatial differences between
 997 our study and previous studies were displayed as Figs F1-F5 in Appendix F.

998 **Table F1-** Summary table of related trait maps of previous studies used in this study.

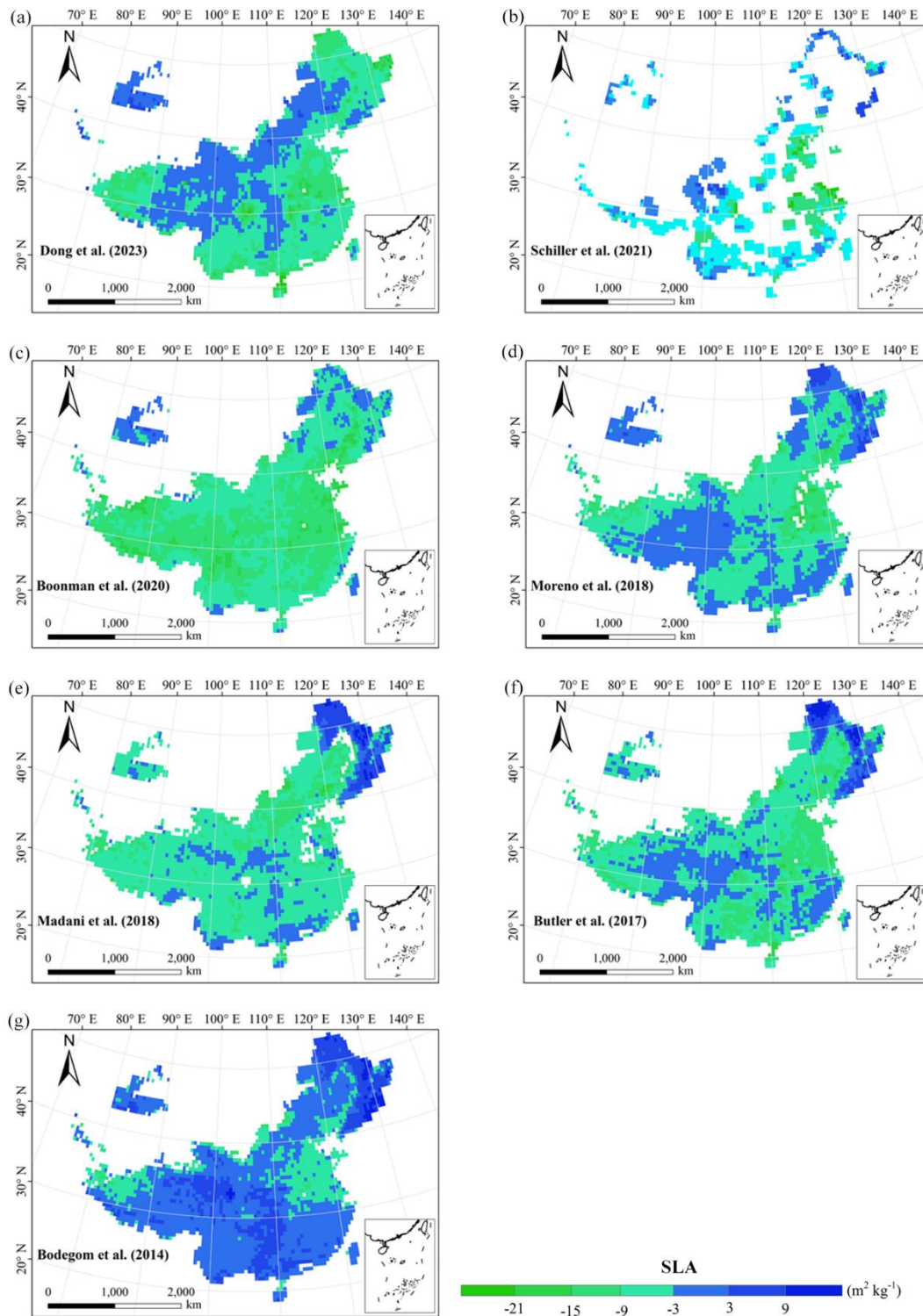
References	Related traits	Methods	Predictors	Consideration of PFT	Resolution
Dong et al. (2023)	SLA LNC	Optimality models	Climate	Yes	0.5 °
Vallicrosa et al. (2022)	LNC LPC	Neural networks	Climate Soil N and P deposition	Yes	0.0083 °
Schiller et al. (2021)	SLA LNC LA WD	Convolutional Neural Networks	Climate In-situ RGB images	No	0.5 °
Boonman et al. (2020)	SLA LNC WD	Generalized linear model, Generalized additive model, Random forest, Boosted regression trees, Ensemble model	Climate Soil	No	0.5 °
Moreno et al. (2018)	SLA LNC LPC LDMC	Regularized regression, forest, networks, Kernel networks	Climate Elevation Reflectance	Yes	0.0045 °

Madani et al. (2018)	SLA	Generalized additive model	Climate	No	0.5 °
Butler et al. (2017)	SLA LNC LPC	Bayesian model	Climate Soil	Yes	0.5 °
Bodegom et al. (2014)	SLA WD	Multiple regression analysis	Climate Soil	No	0.5 °

999 The resolutions 0.5 °, 0.0083 ° and 0.0045 ° correspond to square grid cell sizes of about 50 km, 1 km
1000 and 500 m at the equator. PFT, plant functional type; SLA, specific leaf area; LDMC, leaf dry matter
1001 content; LNC, leaf N concentration; LPC, leaf P concentration; LA, leaf area; WD, wood density.
1002

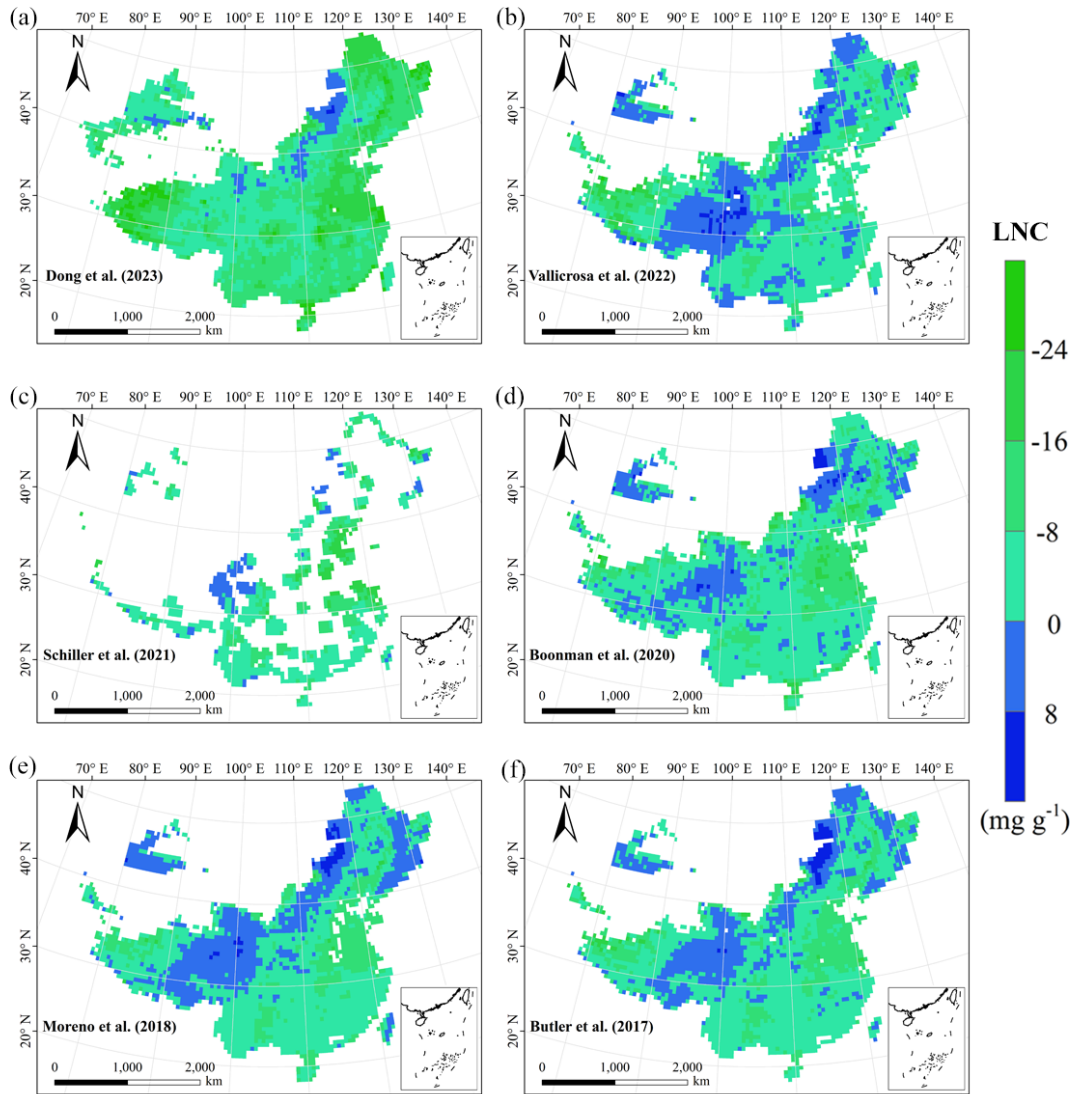


1003
1004 **Figure F1.** Frequency distributions of plant functional traits in our study (“This study”, dashed
1005 black lines) and Vallicrosa et al. (2022) at 1 km spatial resolution. (a) LNC, leaf N concentration
1006 (mg g⁻¹); (b) LPC, leaf P concentration (mg g⁻¹).



1007
1008
1009

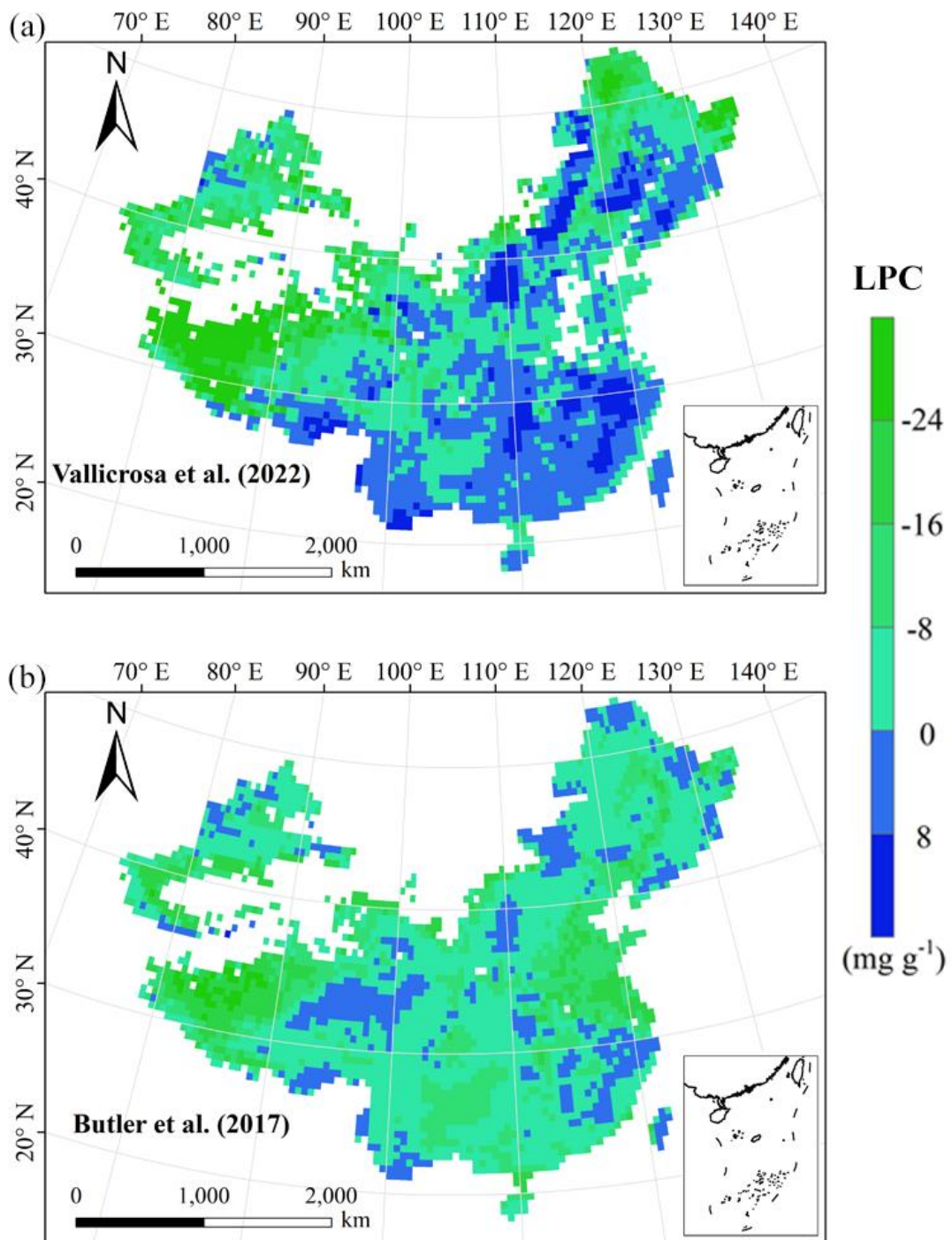
Figure F2. Spatial differences in SLA (specific leaf area, $\text{m}^2 \text{kg}^{-1}$) between our study and trait maps from previous studies (see Table F1 for citations).



1010

1011 **Figure F3.** Spatial differences in LNC (leaf N concentration, mg g^{-1}) between our study and trait maps

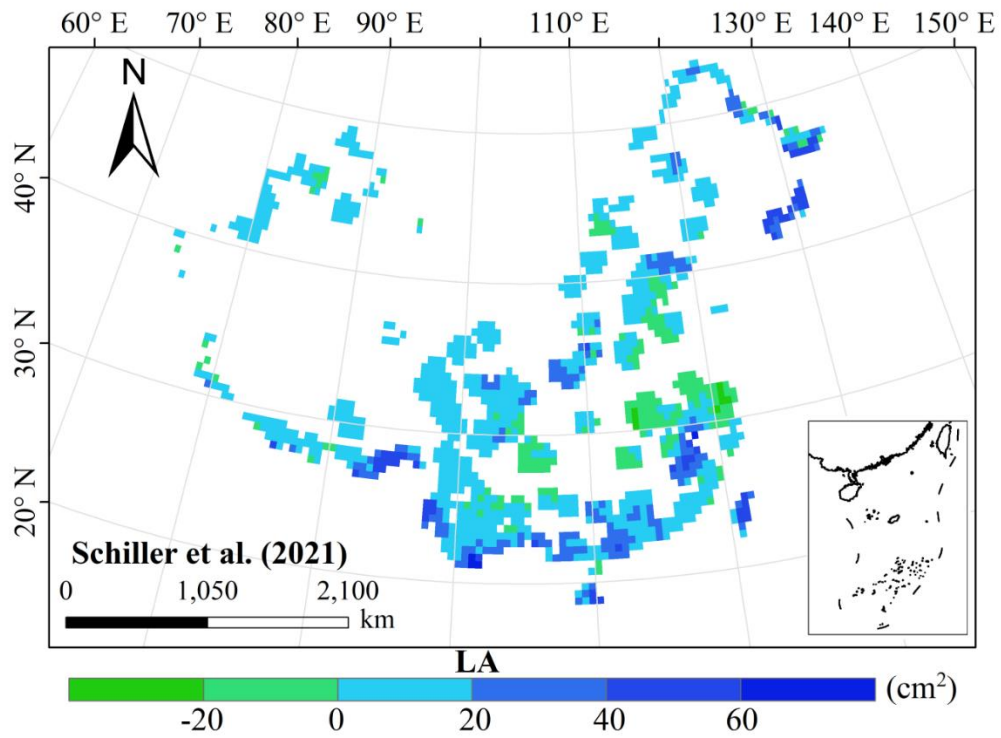
1012 from previous studies (see Table F1 for citations).



1013

1014 **Figure F4.** Spatial differences in LPC (leaf P concentration, mg g^{-1}) between our study and trait maps

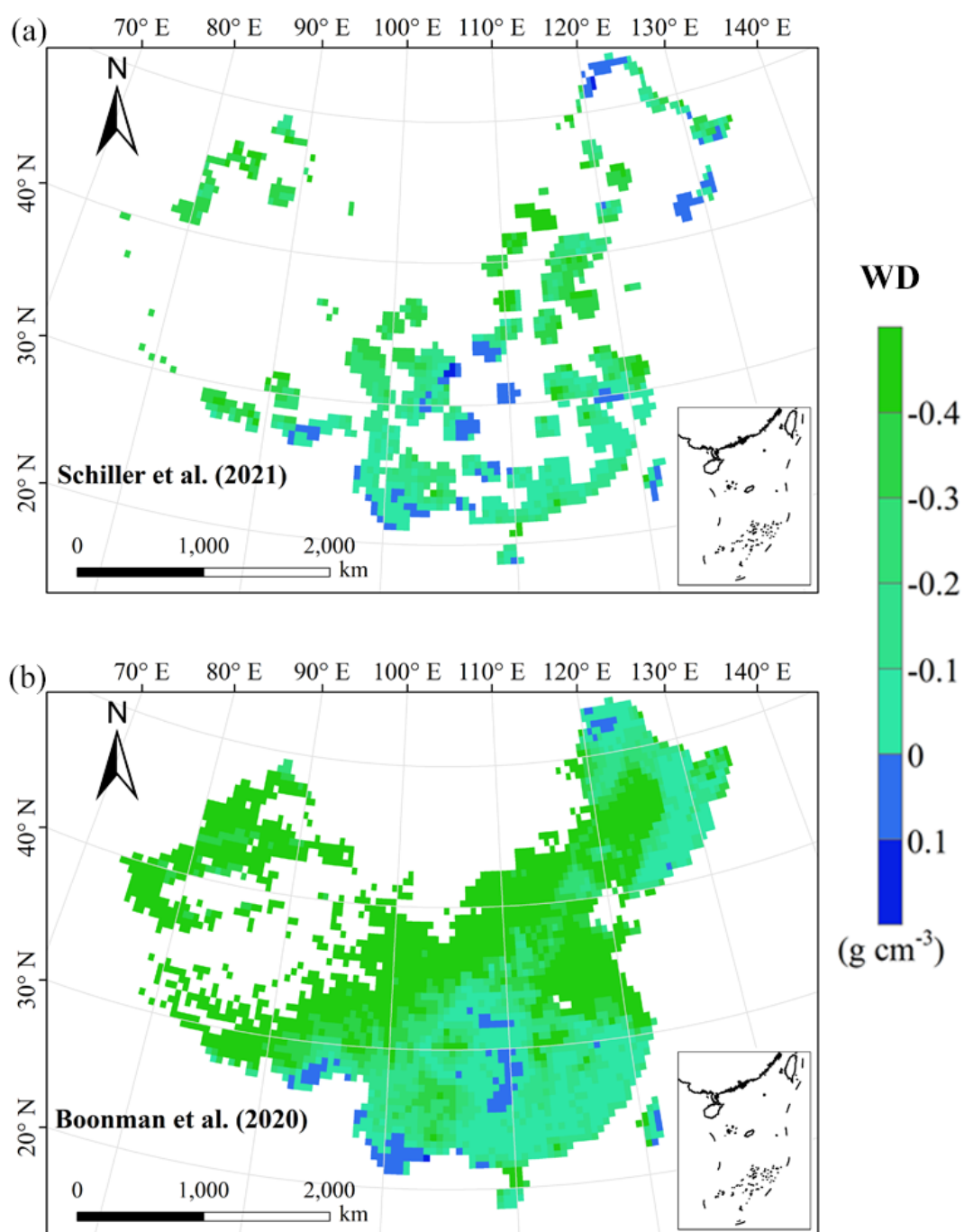
1015 from previous studies (see Table F1 for citations).



1016

1017 **Figure F5.** Spatial differences in LA (leaf area, cm²) between our study and trait maps from previous

1018 studies (see Table F1 for citations).



1019

1020

1021

Figure F6. Spatial differences in WD (wood density, g cm^{-3}) between our study and trait maps from previous studies (see Table F1 for citations).

1022 **Author contributions.** NA and NL designed the research. NA did the analysis, processed the data
1023 and wrote the draft of the paper. All co-authors commented on the manuscript and agreed upon the
1024 final version of the paper.

1025
1026 **Competing interests.** The contact author has declared that none of the authors has any competing
1027 interests.

1028
1029 **Disclaimer.** Publisher's note: Copernicus Publications remains neutral with regard to
1030 jurisdictional claims in published maps and institutional affiliations.

1031
1032 **Acknowledgement.** We acknowledge financial supports from the National Natural Science
1033 Foundation of China (41991234) and the Joint CAS-MPG Research Project (HZXM20225001MI).

1034
1035 **Financial support.** This work has been supported by the National Natural Science Foundation of
1036 China (grant no. 41991234) and the Joint CAS-MPG Research Project (grant no.
1037 HZXM20225001MI).

1038

1039 **References**

1040 Ali, A. M., Darvishzadeh, R., Skidmore, A. K., van Duren, I., Heiden, U., and Heurich, M.:
1041 Estimating leaf functional traits by inversion of PROSPECT: assessing leaf dry matter
1042 content and specific leaf area in mixed mountainous forest. *Int. J. Appl. Earth Obs. Geoinf.*,
1043 45, 66–76, <https://doi.org/10.1016/j.jag.2015.11.004>, 2016.

1044 An, N. N., Lu, N., Fu, B. J., Wang, M. Y., and He, N. P.: Distinct responses of leaf traits to
1045 environment and phylogeny between herbaceous and woody angiosperm species in China.
1046 *Front. Plant Sci.* 12, 799401, <https://doi.org/10.3389/fpls.2021.799401>, 2021.

1047 Bakker, M. A., Carreño-Rocabado, G., and Poorter, L.: Leaf economics traits predict litter
1048 decomposition of tropical plants and differ among land use types. *Funct. Ecol.*, 25, 473–483,
1049 <https://doi.org/10.1111/j.1365-2435.2010.01802.x>, 2011.

1050 Berzaghi, F., Wright, I. J., Kramer, K., Oddou-Muratorio, S., Bohn, F. J., Reyer, C. P. O., Sabate,
1051 S., Sanders, T. G. M., and Hartig, F.: Towards a new generation of trait-flexible vegetation
1052 models. *Trends Ecol. Evol.*, 35, 191–205, <https://doi.org/10.1016/j.tree.2019.11.006>, 2020.

1053 Blumenthal, D. M., Mueller, K. E., Kray, J. A., Ocheltree, T. W., Augustine, D. J., Wilcox, K. R.,
1054 and Cornelissen, H.: Traits link drought resistance with herbivore defence and plant
1055 economics in semi-arid grasslands: The central roles of phenology and leaf dry matter
1056 content. *J. Ecol.*, 108, 2336–2351, <https://doi.org/10.1111/1365-2745.13454>, 2020.

1057 Bohner, A. Soil chemical properties as indicators of plant species richness in grassland
1058 communities. Integrating efficient grassland farming and biodiversity, Proceedings of the
1059 13th International Occasional Symposium of the European Grassland Federation, Tartu,

1060 Estonia, 29–31 August, 48–51, 2005.

1061 Boonman, C. C. F., Benitez-Lopez, A., Schipper, A. M., Thuiller, W., Anand, M., Cerabolini, B. E.
1062 L., Cornelissen, J. H. C., Gonzalez-Melo, A., Hattingh, W. N., Higuchi, P., Laughlin, D. C.,
1063 Onipchenko, V. G., Penuelas, J., Poorter, L., Soudzilovskaia, N. A., Huijbregts, M. A. J., and
1064 Santini, L.: Assessing the reliability of predicted plant trait distributions at the global scale.
1065 *Glob. Ecol. Biogeogr.*, 29, 1034–1051, <https://doi.org/10.1111/geb.13086>, 2020.

1066 Breiman, L.: Random forests. *Mach. Learn.*, 45, 5–32, <https://doi.org/10.1023/a:1010933404324>,
1067 2001.

1068 Bruelheide, H., Dengler, J., Purschke, O., Lenoir, J., Jimenez-Alfaro, B., Hennekens, S. M., Botta-
1069 Dukat, Z., Chytrý, M., Field, R., Jansen, F., Kattge, J., Pillar, V. D., Schrodte, F., Mahecha, M.
1070 D., Peet, R. K., Sandel, B., van Bodegom, P., Altman, J., Alvarez-Davila, E., Arfin Khan, M.
1071 A. S., et al.: Global trait-environment relationships of plant communities. *Nat. Ecol. Evol.*, 2,
1072 1906–1917, <https://doi.org/10.1038/s41559-018-0699-8>, 2018.

1073 Bruelheide, H., Dengler, J., Jiménez-Alfaro, B., Purschke, O., Hennekens, S. M., Chytrý, M.,
1074 Pillar, V. D., Jansen, F., Kattge, J., Sandel, B., Aubin, I., Biurrun, I., Field, R., Haider, S.,
1075 Jandt, U., Lenoir, J., Peet, R. K., Peyre, G., Sabatini, F. M., Schmidt, M., et al.: sPlot – A new
1076 tool for global vegetation analyses. *J. Veg. Sci.*, 30, 161–186,
1077 <https://doi.org/10.1111/jvs.12710>, 2019.

1078 Buchhorn, M., Bertels, L., Smets, B., De Roo, B., Lesiv, M., Tsendbazar, N. E., Masiliunas, D.,
1079 and Linlin, L.: Copernicus Global Land Service: Land Cover 100m: Version 3 Globe 2015-
1080 2019: Algorithm Theoretical Basis Document. <https://doi.org/10.5281/zenodo.3938968>, 2020.

1081 Butler, E. E., Datta, A., Flores-Moreno, H., Chen, M., Wythers, K. R., Fazayeli, F., Banerjee, A.,
1082 Atkin, O. K., Kattge, J., Amiaud, B., Blonder, B., Boenisch, G., Bond-Lamberty, B., Brown,
1083 K. A., Byun, C., Campetella, G., Cerabolini, B. E. L., Cornelissen, J. H. C., Craine, J. M.,
1084 Craven, D., de Vries, F. T., Diaz, S., Domingues, T. F., Forey, E., Gonzalez-Melo, A., Gross,
1085 N., Han, W., Hattingh, W. N., Hickler, T., Jansen, S., Kramer, K., Kraft, N. J. B., Kurokawa,
1086 H., Laughlin, D. C., Meir, P., Minden, V., Niinemets, U., Onoda, Y., Penuelas, J., Read, Q.,
1087 Sack, L., Schamp, B., Soudzilovskaia, N. A., Spasojevic, M. J., Sosinski, E., Thornton, P. E.,
1088 Valladares, F., van Bodegom, P. M., Williams, M., Wirth, C., and Reich, P. B.: Mapping local
1089 and global variability in plant trait distributions. *P. Nat. Acad. Sci. USA*, 114, 10937–10946,
1090 <https://doi.org/10.1073/pnas.1708984114>, 2017.

1091 Cavender-Bares, J., Schneider, F. D., Santos, M. J., Armstrong, A., Carnaval, A., Dahlin, K. M.,
1092 Fatoyinbo, L., Hurr, G. C., Schimel, D., Townsend, P. A., Ustin, S. L., Wang, Z. H., and
1093 Wilson, A. M.: Integrating remote sensing with ecology and evolution to advance
1094 biodiversity conservation. *Nat. Ecol. Evol.*, 6, 506–519, <https://doi.org/10.1038/s41559-022-01702-5>, 2022.

1096 Clevers, J. G. P. W., and Gitelson, A. A.: Remote estimation of crop and grass chlorophyll and
1097 nitrogen content using red-edge bands on Sentinel-2 and -3. *Int. J. Appl. Earth Obs. Geoinf.*,

1098 23, 344–351, <https://doi.org/10.1016/j.jag.2012.10.008>, 2013.

1099 Dahlin, K. M., Asner, G. P., and Field, C. B.: Environmental and community controls on plant
1100 canopy chemistry in a Mediterranean-type ecosystem. *P. Nat. Acad. Sci. USA*, 110, 6895–
1101 6900, <https://doi.org/10.1073/pnas.1215513110>, 2013.

1102 Darvishzadeh, R., Skidmore, A., Schlerf, M., and Atzberger, C.: Inversion of a radiative transfer
1103 model for estimating vegetation LAI and chlorophyll in a heterogeneous grassland. *Remote
1104 Sens. Environ.*, 112, 2592–2604, <https://doi.org/10.1016/j.rse.2007.12.003>, 2008.

1105 Diaz, S., Kattge, J., Cornelissen, J. H., Wright, I. J., Lavorel, S., Dray, S., Reu, B., Kleyer, M.,
1106 Wirth, C., Prentice, I. C., Garnier, E., Bonisch, G., Westoby, M., Poorter, H., Reich, P. B.,
1107 Moles, A. T., Dickie, J., Gillison, A. N., Zanne, A. E., Chave, J., Wright, S. J., Sheremet'ev, S.
1108 N., Jactel, H., Baraloto, C., Cerabolini, B., Pierce, S., Shipley, B., Kirkup, D., Casanoves, F.,
1109 Joswig, J. S., Gunther, A., Falczuk, V., Ruger, N., Mahecha, M. D., and Gorne, L. D.: The
1110 global spectrum of plant form and function. *Nature*, 529, 167–171,
1111 <https://doi.org/10.1038/nature16489>, 2016.

1112 Diaz, S., Hodgson, J. G., Thompson, K., Cabido, M., Cornelissen, J. H. C., Jalili, A., Montserrat-
1113 Marti, G., Grime, J. P., Zarrinkamar, F., Asri, Y., Band, S. R., Basconcelo, S., Castro-Diez, P.,
1114 Funes, G., Hamzehee, B., Khoshnevi, M., Perez-Harguindeguy, N., Perez-Rontome, M. C.,
1115 Shirvany, F. A., Vendramini, F., Yazdani, S., Abbas-Azimi, R., Bogaard, A., Boustani, S.,
1116 Charles, M., Dehghan, M., de Torres-Espuny, L., Falczuk, V., Guerrero-Campo, J., Hynd, A.,
1117 Jones, G., Kowsary, E., Kazemi-Saeed, F., Maestro-Martinez, M., Romo-Diez, A., Shaw, S.,
1118 Siavash, B., Villar-Salvador, P., and Zak, M. R.: The plant traits that drive ecosystems:
1119 evidence from three continents. *J. Veg. Sci.*, 15, 295–304, <https://doi.org/10.1111/j.1654-1103.2004.tb02266.x>, 2004.

1121 Dong, N., Dechant, B., Wang, H., Wright, I. J., and Prentice, IC.: Global leaf-trait mapping based
1122 on optimality theory. *Glob. Ecol. Biogeogr.*, <https://doi.org/10.1111/geb.13680>, 2023.

1123 Du, L., Liu, H., Guan, W., Li, J., and Li, J.: Drought affects the coordination of belowground and
1124 aboveground resource-related traits in *Solidago canadensis* in China. *Ecol. Evol.*, 9, 9948–
1125 9960, <https://doi.org/10.1002/ece3.5536>, 2019.

1126 Elith, J., Leathwick, J. R., and Hastie, T.: A working guide to boosted regression trees. *J. Anim.
1127 Ecol.*, 77, 802–813, <https://doi.org/10.1111/j.1365-2656.2008.01390.x>, 2008.

1128 Elith, J., Kearney, M., and Phillips, S.: The art of modelling range-shifting species. *Methods Ecol.
1129 Evol.*, 1, 330–342, <https://doi.org/10.1111/j.2041-210X.2010.00036.x>, 2010.

1130 Elith, J., Graham, C. H., Anderson, R. P., Dudik, M., Ferrier, S., Guisan, A., Hijmans, R. J.,
1131 Huettmann, F., Leathwick, J. R., Lehmann, A., Li, J., Lohmann, L. G., Loiselle, B. A.,
1132 Manion, G., Moritz, C., Nakamura, M., Nakazawa, Y., Overton, J. M., Peterson, A. T.,
1133 Phillips, S. J., Richardson, K., Scachetti-Pereira, R., Schapire, R. E., Soberon, J., Williams, S.,
1134 Wisz, M. S., and Zimmermann, N. E.: Novel methods improve prediction of species'
1135 distributions from occurrence data. *Ecography*, 29, 129–151,

1136 <https://doi.org/10.1111/j.2006.0906-7590.04596.x>, 2006.

1137 Finzi, A. C., Austin, A. T., Cleland, E. E., Frey, S. D., Houlton, B. Z., and Wallenstein, M. D.:
1138 Responses and feedbacks of coupled biogeochemical cycles to climate change: examples
1139 from terrestrial ecosystems. *Front. Ecol. Environ.*, 9, 61–67, <https://doi.org/10.1890/100001>,
1140 2011.

1141 Foley, J. A., Prentice, I. C., Ramankutty, N., Levis, S., Pollard, D., Sitch, S., and Haxeltine, A.: An
1142 integrated biosphere model of land surface processes, terrestrial carbon balance, and
1143 vegetation dynamics. *Global Biogeochem. Cy.*, 10, 603–628,
1144 <https://doi.org/10.1029/96gb02692>, 1996.

1145 Freschet, G. T., Cornelissen, J. H. C., van Logtestijn, R. S. P., and Aerts, R.: Evidence of the ‘plant
1146 economics spectrum’ in a subarctic flora. *J. Ecol.*, 98, 362–373,
1147 <https://doi.org/10.1111/j.1365-2745.2009.01615.x>, 2010.

1148 Grime, J. P.: Benefits of plant diversity to ecosystems: immediate, filter and founder effects. *J.*
1149 *Ecol.*, 86, 902–910, <https://doi.org/10.1046/j.1365-2745.1998.00306.x>, 1998.

1150 He, N., Yan, P., Liu, C., Xu, L., Li, M., Van Meerbeek, K., Zhou, G., Zhou, G., Liu, S., Zhou, X.,
1151 Li, S., Niu, S., Han, X., Buckley, T. N., Sack, L., and Yu, G.: Predicting ecosystem
1152 productivity based on plant community traits. *Trends Plant Sci.*, 28, 43–53,
1153 <https://doi.org/10.1016/j.tplants.2022.08.015>, 2023.

1154 Hodgson, J. G., Montserrat-Marti, G., Charles, M., Jones, G., Wilson, P., Shipley, B., Sharafi, M.,
1155 Cerabolini, B. E. L., Cornelissen, J. H. C., Band, S. R., Bogard, A., Castro-Diez, P., Guerrero-
1156 Campo, J., Palmer, C., Perez-Rontome, M. C., Carter, G., Hynd, A., Romo-Diez, A., Espuny,
1157 L. D., and Pla, F. R.: Is leaf dry matter content a better predictor of soil fertility than specific
1158 leaf area? *Ann. Bot.*, 108, 1337–1345, <https://doi.org/10.1093/aob/mcr225>, 2011.

1159 Hoeber, S., Leuschner, C., Köhler, L., Arias-Aguilar, D., and Schuldt, B.: The importance of
1160 hydraulic conductivity and wood density to growth performance in eight tree species from a
1161 tropical semi-dry climate. *Forest Ecol. Manag.*, 330, 126–136,
1162 <https://doi.org/10.1016/j.foreco.2014.06.039>, 2014.

1163 Jónsdóttir, I. S., Halbritter, A. H., Christiansen, C. T., Althuizen, I. H. J., Haugum, S. V., Henn, J. J.,
1164 Björnsdóttir, K., Maitner, B. S., Malhi, Y., Michaletz, S. T., Roos, R. E., Klanderud, K., Lee,
1165 H., Enquist, B. J., and Vandvik, V.: Intraspecific trait variability is a key feature underlying
1166 high Arctic plant community resistance to climate warming. *Ecol. Monogr.*, 93,
1167 <https://doi.org/10.1002/ecm.1555>, 2022.

1168 Jung, V., Violle, C., Mondy, C., Hoffmann, L., and Muller, S.: Intraspecific variability and trait-
1169 based community assembly. *J. Ecol.*, 98, 1134–1140, <https://doi.org/10.1111/j.1365-2745.2010.01687.x>, 2010.

1171 Kattge, J., Diaz, S., Lavorel, S., Prentice, C., Leadley, P., Bonisch, G., Garnier, E., Westoby, M.,
1172 Reich, P. B., Wright, I. J., Cornelissen, J. H. C., Violle, C., Harrison, S. P., van Bodegom, P.
1173 M., Reichstein, M., Enquist, B. J., Soudzilovskaia, N. A., Ackerly, D. D., Anand, M., Atkin,

1174 O., et al.: TRY - a global database of plant traits. *Glob. Change Biol.*, 17, 2905–2935,
1175 <https://doi.org/10.1111/j.1365-2486.2011.02451.x>, 2011.

1176 Kattge, J., Bonisch, G., Diaz, S., Lavorel, S., Prentice, I. C., Leadley, P., Tautenhahn, S., Werner, G.
1177 D. A., Aakala, T., Abedi, M., Acosta, A. T. R., Adamidis, G. C., Adamson, K., Aiba, M.,
1178 Albert, C. H., Alcantara, J. M., Alcazar, C. C., Aleixo, I., Ali, H., Amiaud, B., et al.: TRY
1179 plant trait database - enhanced coverage and open access. *Global Change Biol.*, 26, 119–188,
1180 <https://doi.org/10.1111/gcb.14904>, 2020.

1181 King, D. A., Davies, S. J., Tan, S., and Noor, N. S. M.: The role of wood density and stem support
1182 costs in the growth and mortality of tropical trees. *J. Ecol.*, 94, 670–680,
1183 <https://doi.org/10.1111/j.1365-2745.2006.01112.x>, 2006.

1184 Kirilenko, A. P., Belotelov, N. V., and Bogatyrev, B. G.: Global model of vegetation migration:
1185 incorporation of climatic variability. *Ecol. Model.*, 132, 125–133,
1186 [https://doi.org/10.1016/S0304-3800\(00\)00310-0](https://doi.org/10.1016/S0304-3800(00)00310-0), 2000.

1187 LeBauer, D. S., and Treseder, K. K.: Nitrogen limitation of net primary productivity in terrestrial
1188 ecosystems is globally distributed. *Ecology*, 89, 371–379, <https://doi.org/10.1890/06-2057.1>,
1189 2008.

1190 Li, C. X., Wulf, H., Schmid, B., He, J. S., and Schaepman, M. E.: Estimating plant traits of alpine
1191 grasslands on the Qinghai-Tibetan Plateau using remote sensing. *IEEE J. Sel. Top. Appl.*
1192 *Earth Obs. Remote Sens.*, 11, 2263–2275, <https://doi.org/10.1109/jstars.2018.2824901>, 2018.

1193 Li, D. J., Ives, A. R., and Waller, D. M.: Can functional traits account for phylogenetic signal in
1194 community composition? *New Phytol.*, 214, 607–618, <https://doi.org/10.1111/nph.14397>,
1195 2017.

1196 Li, Y. Q., Reich, P. B., Schmid, B., Shrestha, N., Feng, X., Lyu, T., Maitner, B. S., Xu, X., Li, Y. C.,
1197 Zou, D. T., Tan, Z. H., Su, X. Y., Tang, Z. Y., Guo, Q. H., Feng, X. J., Enquist, B. J., and
1198 Wang, Z. H.: Leaf size of woody dicots predicts ecosystem primary productivity. *Ecol. Lett.*,
1199 23, 1003–1013, <https://doi.org/10.1111/ele.13503>, 2020.

1200 Liang, X. Y., Ye, Q., Liu, H., and Brodribb, T. J.: Wood density predicts mortality threshold for
1201 diverse trees. *New Phytol.*, 229, <https://doi.org/10.1111/nph.17117>, 2021.

1202 Liaw, A., and Wiener, M.: Classification and Regression by randomForest. *R News*, 2, 18–22,
1203 2002.

1204 Liu, H. Y., and Yin, Y.: Response of forest distribution to past climate change: an insight into
1205 future predictions. *Chinese Science Bulletin*, 58, 4426–4436, [https://doi.org/10.1007/s11434-](https://doi.org/10.1007/s11434-013-6032-7)
1206 [013-6032-7](https://doi.org/10.1007/s11434-013-6032-7), 2013.

1207 Loozen, Y., Rebel, K. T., Karssenber, D., Wassen, M. J., Sardans, J., Peñuelas, J., and De Jong, S.
1208 M.: Remote sensing of canopy nitrogen at regional scale in Mediterranean forests using the
1209 spaceborne MERIS Terrestrial Chlorophyll Index. *Biogeosciences*, 15, 2723–2742,
1210 <https://doi.org/10.5194/bg-15-2723-2018>, 2018.

1211 Loozen, Y., Rebel, K. T., de Jong, S. M., Lu, M., Ollinger, S. V., Wassen, M. J., and Karssenber,

1212 D.: Mapping canopy nitrogen in European forests using remote sensing and environmental
1213 variables with the random forests method. *Remote Sens. Environ.*, 247, 111933,
1214 <https://doi.org/10.1016/j.rse.2020.111933>, 2020.

1215 Madani, N., Kimball, J. S., Ballantyne, A. P., Affleck, D. L. R., van Bodegom, P. M., Reich, P. B.,
1216 Kattge, J., Sala, A., Nazeri, M., Jones, M. O., Zhao, M., and Running, S. W.: Future global
1217 productivity will be affected by plant trait response to climate. *Sci. Rep.*, 8, 1–10,
1218 <https://doi.org/10.1038/s41598-018-21172-9>, 2018.

1219 Martínez-Vilalta, J., Mencuccini, M., Vayreda, J., and Retana, J.: Interspecific variation in
1220 functional traits, not climatic differences among species ranges, determines demographic
1221 rates across 44 temperate and Mediterranean tree species. *J. Ecol.*, 98, 1462–1475,
1222 <https://doi.org/10.1111/j.1365-2745.2010.01718.x>, 2010.

1223 Matheny, A. M., Mirfenderesgi, G., and Bohrer, G.: Trait-based representation of hydrological
1224 functional properties of plants in weather and ecosystem models. *Plant Divers*, 39, 1–12,
1225 <https://doi.org/10.1016/j.pld.2016.10.001>, 2017.

1226 Moles, A. T., Warton, D. I., Warman, L., Swenson, N. G., Laffan, S. W., Zanne, A. E., Pitman, A.,
1227 Hemmings, F. A., and Leishman, M. R.: Global patterns in plant height. *J. Ecol.*, 97, 923–932,
1228 <https://doi.org/10.1111/j.1365-2745.2009.01526.x>, 2009.

1229 Moreno-Martínez, Á., Camps-Valls, G., Kattge, J., Robinson, N., Reichstein, M., van Bodegom, P.,
1230 Kramer, K., Cornelissen, J. H. C., Reich, P., Bahn, M., Niinemets, Ü., Peñuelas, J., Craine, J.
1231 M., Cerabolini, B. E. L., Minden, V., Laughlin, D. C., Sack, L., Allred, B., Baraloto, C., Byun,
1232 C., Soudzilovskaia, N. A., and Running, S. W.: A methodology to derive global maps of leaf
1233 traits using remote sensing and climate data. *Remote Sens. Environ.*, 218, 69–88,
1234 <https://doi.org/10.1016/j.rse.2018.09.006>, 2018.

1235 Myers-Smith, I. H., Thomas, H. J. D., and Björkman, A. D.: Plant traits inform predictions of
1236 tundra responses to global change. *New Phytol.*, 221, 1742–1748,
1237 <https://doi.org/10.1111/nph.15592>, 2019.

1238 NEODC, 2015. NEODC - NERC Earth Observation Data Centre. Natural Environment Research
1239 Council. <http://neodc.nerc.ac.uk/>.

1240 Peng, C. H.: From static biogeographical model to dynamic global vegetation model: a global
1241 perspective on modelling vegetation dynamics. *Ecol. Model.*, 135, 33–54,
1242 [https://doi.org/10.1016/S0304-3800\(00\)00348-3](https://doi.org/10.1016/S0304-3800(00)00348-3), 2000.

1243 Perez-Harguindeguy, N., Diaz, S., Garnier, E., Lavorel, S., Poorter, H., Jaureguiberry, P., Bret-
1244 Harte, M. S., Cornwell, W. K., Craine, J. M., Gurvich, D. E., Urcelay, C., Veneklaas, E. J.,
1245 Reich, P. B., Poorter, L., Wright, I. J., Ray, P., Enrico, L., Pausas, J. G., de Vos, A. C.,
1246 Buchmann, N., Funes, G., Quétier, F., Hodgson, J. G., Thompson, K., Morgan, H. D., ter
1247 Steege, H., van der Heijden, M. G. A., Sack, L., Blonder, B., Poschlod, P., Vaieretti, M. V.,
1248 Conti, G., Staver, A. C., Aquino, S., and Cornelissen, J. H. C.: New handbook for
1249 standardised measurement of plant functional traits worldwide. *Aust. Bot.*, 61, 167–234,

1250 <https://doi.org/10.1071/bt12225>, 2013.

1251 Piao, S. L., He, Y., Wang, X. H., and Chen, F. H.: Estimation of China's terrestrial ecosystem
1252 carbon sink: Methods, progress and prospects. *Science China Earth Sciences*, 65, 641–651,
1253 <https://doi.org/10.1007/s11430-021-9892-6>, 2022.

1254 Potapov, P., Li, X. Y., Hernandez-Serna, A., Tyukavina, A., Hansen, M. C., Kommareddy, A.,
1255 Pickens, A., Turubanova, S., Tang, H., Silva, C. E., Armston, J., Dubayah, R., Blair, J. B.,
1256 Hofton, M.: Mapping global forest canopy height through integration of GEDI and Landsat
1257 data, *Remote Sens. Environ.*, 253, 112165, <https://doi.org/10.1016/j.rse.2020.112165>, 2021.

1258 Qiao, J. J., Zuo, X. A., Yue, P., Wang, S. K., Hu, Y., Guo, X. X., Li, X. Y., Lv, P., Guo, A. X., and
1259 Sun, S. S.: High nitrogen addition induces functional trait divergence of plant community in a
1260 temperate desert steppe. *Plant and Soil*, <https://doi.org/10.1007/s11104-023-05910-1>, 2023.

1261 Reich, P. B., and Oleksyn, J.: Global patterns of plant leaf N and P in relation to temperature and
1262 latitude. *Proc. Natl. Acad. Sci. U. S. A.*, 101, 11001–11006,
1263 https://doi.org/10.1073/pnas.0403588101_2004.

1264 Reich, P. B., and Cornelissen, H.: The world-wide ‘fast-slow’ plant economics spectrum: a traits
1265 manifesto. *Journal of Ecology*, 102, 275–301, <https://doi.org/10.1111/1365-2745.12211>, 2014.

1266 Reich, P. B., Uhl, C., Walters, M. B., and Ellsworth, D. S.: Leaf lifespan as a determinant of leaf
1267 structure and function among 23 Amazonian tree species. *Oecologia*, 86, 16–24,
1268 <https://doi.org/10.1007/BF00317383>, 1991.

1269 Ridgeway, G.: Gbm: generalized boosted regression models. R package version 1.5-6, Available at:
1270 <http://cran.r-project.org/web/packages/gbm/index.html>, accessed 11/02/20092006.

1271 Roderick, M. L., and Berry, S. L.: Linking wood density with tree growth and environment: a
1272 theoretical analysis based on the motion of water. *New Phytol.*, 149, 473–485,
1273 <https://doi.org/10.1046/j.1469-8137.2001.00054.x>, 2002.

1274 Romero, A., Aguado, I., and Yebra, M.: Estimation of dry matter content in leaves using
1275 normalized indexes and PROSPECT model inversion. *Int. J. Remote Sens.*, 33, 396–414,
1276 <https://doi.org/10.1080/01431161.2010.532819>, 2012.

1277 Sakschewski, B., von Bloh, W., Boit, A., Rammig, A., Kattge, J., Poorter, L., Penuelas, J., and
1278 Thonicke, K.: Leaf and stem economics spectra drive diversity of functional plant traits in a
1279 dynamic global vegetation model. *Global Change Biol.*, 21, 2711–2725,
1280 https://doi.org/10.1111/gcb.12870_2015.

1281 Scheiter, S., Langan, L., and Higgins, S. I.: Next-generation dynamic global vegetation models:
1282 learning from community ecology. *New Phytol.*, 198, 957–969,
1283 <https://doi.org/10.1111/nph.12210>, 2013.

1284 Schiller, C., Schmidtlein, S., Boonman, C., Moreno-Martinez, A., and Kattenborn, T.: Deep
1285 learning and citizen science enable automated plant trait predictions from photographs. *Sci.*
1286 *Rep.*, 11, <https://doi.org/10.1038/s41598-021-95616-0>, 2022.

1287 Shangguan, W., Dai, Y. J., Liu, B. Y., Zhu, A. X., Duan, Q. Y., Wu, L. Z., Ji, D. Y., Ye, A. Z., Yuan,

1288 H., Zhang, Q., Chen, D. D., Chen, M., Chu, J. T., Dou, Y. J., Guo, J. X., Li, H. Q., Li, J. J.,
1289 Liang, L., Liang, X., Liu, H. P., Liu, S. Y., Miao, C. Y., and Zhang, Y. Z.: A China data set of
1290 soil properties for land surface modeling. *J. Adv. Model. Earth Syst.*, 5, 212–224,
1291 <https://doi.org/10.1002/jame.20026>, 2013.

1292 Siefert, A., Violle, C., Chalmandrier, L., Albert, C. H., Taudiere, A., Fajardo, A., Aarssen, L. W.,
1293 Baraloto, C., Carlucci, M. B., Cianciaruso, M. V., de, L. D. V., de Bello, F., Duarte, L. D.,
1294 Fonseca, C. R., Freschet, G. T., Gaucherand, S., Gross, N., Hikosaka, K., Jackson, B., Jung,
1295 V., Kamiyama, C., Katabuchi, M., Kembel, S. W., Kichenin, E., Kraft, N. J., Lagerstrom, A.,
1296 Bagousse-Pinguet, Y. L., Li, Y., Mason, N., Messier, J., Nakashizuka, T., Overton, J. M.,
1297 Peltzer, D. A., Perez-Ramos, I. M., Pillar, V. D., Prentice, H. C., Richardson, S., Sasaki, T.,
1298 Schamp, B. S., Schob, C., Shipley, B., Sundqvist, M., Sykes, M. T., Vandewalle, M., and
1299 Wardle, D. A.: A global meta-analysis of the relative extent of intraspecific trait variation in
1300 plant communities. *Ecol. Lett.*, 18, 1406–1419, <https://doi.org/10.1111/ele.12508>, 2015.

1301 Šímová I., Sandel, B., Enquist, B. J., Michaletz, S. T., Kattge, J., Violle, C., McGill, B. J., Blonder,
1302 B., Engemann, K., Peet, R. K., Wisser, S. K., Morueta-Holme, N., Boyle, B., Kraft, N. J. B.,
1303 Svenning, J. C., and Hector, A.: The relationship of woody plant size and leaf nutrient content
1304 to large-scale productivity for forests across the Americas. *J. Ecol.*, 107, 2278–2290,
1305 <https://doi.org/10.1111/1365-2745.13163>, 2019.

1306 Sitch, S., Huntingford, C., Gedney, N., Levy, P. E., Lomas, M., Piao, S. L., Betts, R., Ciais, P., Cox,
1307 P., Friedlingstein, P., Jones, C. D., Prentice, I. C., and Woodward, F. I.: Evaluation of the
1308 terrestrial carbon cycle, future plant geography and climate-carbon cycle feedbacks using five
1309 Dynamic Global Vegetation Models (DGVMs). *Global Change Biol.*, 14, 2015–2039,
1310 <https://doi.org/10.1111/j.1365-2486.2008.01626.x>, 2008.

1311 Smart, S. M., Glanville, H. C., Blanes, M. d. C., Mercado, L. M., Emmett, B. A., Jones, D. L.,
1312 Cosby, B. J., Marrs, R. H., Butler, A., Marshall, M. R., Reinsch, S., Herrero-Járegui, C.,
1313 Hodgson, J. G., and Field, K.: Leaf dry matter content is better at predicting above-ground
1314 net primary production than specific leaf area. *Funct. Ecol.*, 31, 1336–1344,
1315 <https://doi.org/10.1111/1365-2435.12832>, 2017.

1316 Telenius, A.: Biodiversity information goes public: GBIF at your service. *Nord. J. Bot.*, 29, 378–
1317 381, <https://doi.org/10.1111/j.1756-1051.2011.01167.x>, 2011.

1318 Thomas, D. S., Montagu, K. D., and Conroy, J. P.: Changes in wood density of *Eucalyptus*
1319 *camaldulensis* due to temperature—the physiological link between water viscosity and wood
1320 anatomy. *Forest Ecol. Manag.*, 193, 157–165, <https://doi.org/10.1016/j.foreco.2004.01.028>,
1321 2004.

1322 Thomas, S. C.: Photosynthetic capacity peaks at intermediate size in temperate deciduous trees.
1323 *Tree Physiol.*, 30, 555–573, <https://doi.org/10.1093/treephys/tpq005>, 2010.

1324 Thuiller, W., Lafourcade, B., Engler, R., and Araújo, M. B.: BIOMOD – A platform for ensemble
1325 forecasting of species distributions. *Ecography*, 32, 369–373, [63](https://doi.org/10.1111/j.1600-</p>
</div>
<div data-bbox=)

1326 0587.2008.05742.x, 2009.

1327 Trabucco, A., and Zomer, R. J.: Global Aridity Index and Potential Evapo-Transpiration (ET0)
1328 Climate Database v2. CGIAR Consortium for Spatial Information (CGIAR-CSI),
1329 <https://cgiarcsi.community>, 2018.

1330 Vallicrosa, H., Sardans, J., Maspons, J., Zuccarini, P., Fernández-Martínez, M., Bauters, M., Goll,
1331 D. S., Ciais, P., Obersteiner, M., Janssens, I. A., and Peñuelas, J.: Global maps and factors
1332 driving forest foliar elemental composition: the importance of evolutionary history. *New*
1333 *Phytol.*, 233, 169–181, <https://doi.org/10.1111/nph.17771>, 2022.

1334 Van Bodegom, P. M., Douma, J. C., Witte, J. P. M., Ordoñez, J. C., Bartholomeus, R. P., and Aerts,
1335 R.: Going beyond limitations of plant functional types when predicting global ecosystem-
1336 atmosphere fluxes: exploring the merits of traits-based approaches. *Glob. Ecol. Biogeogr.*, 21,
1337 625–636, <https://doi.org/10.1111/j.1466-8238.2011.00717.x>, 2012.

1338 van Bodegom, P. M., Douma, J. C., and Verheijen, L. M. A fully traits-based approach to modeling
1339 global vegetation distribution. *P. Nat. Acad. Sci. USA*, 111, 13733–13738,
1340 <https://doi.org/10.1073/pnas.1304551110>, 2014.

1341 Verheijen, L. M., Aerts, R., Bonisch, G., Kattge, J., and Van Bodegom, P. M.: Variation in trait
1342 trade-offs allows differentiation among predefined plant functional types: implications for
1343 predictive ecology. *New Phytol.*, 209, 563–575, <https://doi.org/10.1111/nph.13623>, 2016.

1344 Wang, H., Harrison, S. P., Prentice, I. C., Yang, Y. Z., Bai, F., Togashi, H. F., Wang, M., Zhou, S.
1345 X., and Ni, J.: The China Plant Trait Database: toward a comprehensive regional compilation
1346 of functional traits for land plants. *Ecology*, 99, 500, <https://doi.org/10.1002/ecy.2091>, 2018.

1347 Webb, C. T., Hoeting, J. A., Ames, G. M., Pyne, M. I., and LeRoy Poff, N.: A structured and
1348 dynamic framework to advance traits-based theory and prediction in ecology. *Ecol. Lett.*, 13,
1349 267–283, <https://doi.org/10.1111/j.1461-0248.2010.01444.x>, 2010.

1350 Wright, I. J., Dong, N., Maire, V., Prentice, I. C., Westoby, M., Diaz, S., Gallagher, R. V., Jacobs,
1351 B. F., Kooyman, R., Law, E. A., Leishman, M. R., Niinemets, U., Reich, P. B., Sack, L., Villar,
1352 R., Wang, H., and Wilf, P.: Global climatic drivers of leaf size. *Science*, 357, 917–921,
1353 <https://doi.org/10.1126/science.aal4760>, 2017.

1354 Wright, I. J., Reich, P. B., Westoby, M., Ackerly, D. D., Baruch, Z., Bongers, F., Cavender-Bares,
1355 J., Chapin, T., Cornelissen, J. H. C., Diemer, M., Flexas, J., Garnier, E., Groom, P. K., Gulias,
1356 J., Hikosaka, K., Lamont, B. B., Lee, T., Lee, W., Lusk, C., Midgley, J. J., Navas, M. L.,
1357 Niinemets, U., Oleksyn, J., Osada, N., Poorter, H., Poot, P., Prior, L., Pyankov, V. I., Roumet,
1358 C., Thomas, S. C., Tjoelker, M. G., Veneklaas, E. J., and Villar, R.: The worldwide leaf
1359 economics spectrum. *Nature*, 428, 821–827, <https://doi.org/10.1038/nature02403>, 2004.

1360 Wullschleger, S. D., Epstein, H. E., Box, E. O., Euskirchen, E. S., Goswami, S., Iversen, C. M.,
1361 Kattge, J., Norby, R. J., van Bodegom, P. M., and Xu, X.: Plant functional types in earth
1362 system models: past experiences and future directions for application of dynamic vegetation
1363 models in high-latitude ecosystems. *Ann. Bot.*, 114, 1–16,

1364 <https://doi.org/10.1093/aob/mcu077>, 2014.

1365 Yan, P., He, N. P., Yu, K. L., Xu, L., and Van Meerbeek, K.: Integrating multiple plant functional
1366 traits to predict ecosystem productivity. *Commun Biol*, 6, 239,
1367 <https://doi.org/10.1038/s42003-023-04626-3>, 2023.

1368 Yang, Y. Z., Zhu, Q. A., Peng, C. H., Wang, H., Xue, W., Lin, G. H., Wen, Z. M., Chang, J., Wang,
1369 M., Liu, G. B., and Li, S. Q.: A novel approach for modelling vegetation distributions and
1370 analysing vegetation sensitivity through trait-climate relationships in China. *Sci. Rep.*, 6,
1371 24110, <https://doi.org/10.1038/srep24110>, 2016.

1372 Yang, Y. Z., Wang, H., Harrison, S. P., Prentice, I. C., Wright, I. J., Peng, C. H., and Lin, G. H.:
1373 Quantifying leaf-trait covariation and its controls across climates and biomes. *New Phytol.*,
1374 221, 155-168, <https://doi.org/10.1111/nph.15422>, 2018.

1375 Yang, Y. Z., Zhao, J., Zhao, P. X., Wang, H., Wang, B. H., Su, S. F., Li, M. X., Wang, L. M., Zhu,
1376 Q. A., Pang, Z. Y., and Peng, C. H.: Trait-Based Climate Change Predictions of Vegetation
1377 Sensitivity and Distribution in China. *Front. Plant Sci.*, 10, 908,
1378 <https://doi.org/10.3389/fpls.2019.00908>, 2019.

1379 Yurova, A. Y., and Volodin, E. M.: Coupled simulation of climate and vegetation dynamics. *Izv.*,
1380 *Atmos. . Ocean. Phy.*, 47, 531-539, <https://doi.org/10.1134/s0001433811050124>, 2011.

1381 Zaehle, S., and Friend, A. D.: Carbon and nitrogen cycle dynamics in the O-CN land surface
1382 model: 1. Model description, site-scale evaluation, and sensitivity to parameter estimates.
1383 *Global Biogeochem. Cy.*, 24, n/a-n/a, <https://doi.org/10.1029/2009gb003521>, 2010.